



**Università della Calabria**

**Dottorato di Ricerca in Ingegneria Chimica e dei Materiali**  
*SCUOLA DI DOTTORATO " PITAGORA " IN SCIENZE INGEGNERISTICHE*

**Tesi**

**Membrane crystallization for recovery of valuable compounds  
from waste streams**

**Settore Scientifico Disciplinare CHIM07 – Fondamenti chimici delle tecnologie**

*Supervisori*

Ch.mo Prof. Enrico DRIOLI

Eng. Francesca MACEDONIO

*Il Coordinatore del Corso di Dottorato*

Ch.mo Prof. Raffaele MOLINARI

*Candidato*

Cejna Anna QUIST-JENSEN

Ciclo XXVIII

---

*A.A. 2014-2015*





---

# ACKNOWLEDGEMENT

---

I wish to express my deepest gratitude to **Prof. Enrico Drioli**, who has served as my main supervisor. Prof. Drioli believed in me during my master study and gave me the possibility to come and work under his supervision during this PhD study. Despite his extraordinary busy schedule, there has always been time for guidance, suggestions and encouragement.

I am also thankful to **Francesca Macedonio**, who has been my co-supervisor during these three years of PhD studies. Not only did she help and support on a professional level, but also at personal level whenever needed.

The possibility to work at ITM-CNR has given me the opportunity to work at an institute devoted only to membrane technology. I would like to thank the director of ITM-CNR, **Dr. Lidietta Giorno** and all my colleagues (Researchers, postdocs, PhD students, master students and visitors who have been at the institute) for providing excellent research environment. Moreover, I would like to thank **Prof. Molinari** who has been the coordinator of this Ph.D.

I would also like to acknowledge, The King Abdulaziz City for Science and Technology (**KACST**) Kingdom of Saudi Arabia, for partly funding this work through the project: “Direct-Contact Membrane Distillation, Osmotic Distillation and Membrane Crystallization”.

Thanks to all my friends and colleagues who has made the stay in Italy an easier task. Special thanks to **Aamir**, who, since the beginning, has always been a support.

Last but not least, I would like to say thanks to my parents (**Lene** and **Vesih**), sisters (**Nalin** and **Emina**), grandparents, aunts, uncles and cousins, who has always supported me. I know four years abroad is a long time. Now I am looking forward not to miss out any birthdays or other important occasions (e.g. The National Show in Herning).

Rende, November 2015  
Cejna Anna Quist-Jensen





---

# ABSTRACT

---

**Sustainable development** and **Process intensification strategy** are guidelines for industrial processes in perspective. It is becoming more and more common that industry wants to fully exploit their resources due to environmental regulations, economic gain, sustainable standpoint, etc. In this perspective, waste streams have to be turned into resources in the most environmental friendly, economic and sustainable way. **Membrane Engineering** is already a key-figure to realize this objective. Novel membrane technologies such as membrane distillation (MD), membrane crystallization (MCr), pressure retarded osmosis (PRO), reverse electrodialysis (RED) and forward osmosis (FO), are evolving and are being suggested for a better exploitation of waste streams.

This Ph.D. study focusses, particular, on **Membrane crystallization (MCr)**, which is a novel technology for simultaneously production of water and minerals. It has several advantages with respect to conventional crystallizers in terms of purity, controlled kinetics and crystal morphology. Moreover, MCr is able to treat high concentration solutions, which are challenging for other traditional membrane operations. The current Ph.D. work emphasizes on various aspects of membrane crystallization for approaching zero-liquid discharge in industrial processes.

Improved membranes, specifically developed for MCr applications, have to be manufactured. In this study, preliminary suggestions on membrane features are given for the requirements in MCr. Lab-made PVDF membranes with different characteristics have been tested and evaluated for their performance in MCr. This study, suggests that membranes with symmetric sponge layer structure and low thickness are favorable. Membrane of asymmetric structure with many macrovoids seems more pronounced to suffer from wetting. Moreover, it has been shown that, membrane crystallization is able to treat several kinds of feed solutions including RO brine, produced water and wastewater containing high amounts of sodium sulfate. The recovered crystals exhibit high purity, good size distribution and controlled growth.  $\text{Na}_2\text{SO}_4$  can be recovered as different polymorphs and in this study it has been crystallized in the anhydrous form (Thenardite). Moreover, the process has shown excellent stability in terms of trans-membrane flux and maintenance of hydrophobicity of the membrane. In some cases the treatment has been continued for more than 90 hours by only slight cleaning with distillate water.

Membrane crystallization, in the direct-contact membrane distillation configuration, can normally treat solutions with very high concentrations. However, its limitations in the recovery of lithium from single salt solutions have been highlighted in this study. Vapor pressure, due to increase in concentration, is reduced significant, that it is not possible to reach LiCl saturation by this configuration. Likewise, combined direct-contact and osmotic distillation configuration have not been able to increase the driving force enough in order to exceed saturation. Instead vacuum membrane distillation has been introduced to eliminate the osmotic phenomena. This configuration has been able to recover LiCl in two different polymorph structures depending on the utilized operative conditions.

Furthermore, integrated membrane system, including membrane crystallization, has shown excellent capability to treat orange juice. The quality of the juice has been maintained through ultrafiltration, membrane distillation and membrane crystallization treatment. In this study, the MD/MCr feed temperature is kept below 30 °C causing a relatively low flux. However, it has still been possible to

reach from a concentration of 9 °brix to 65 °brix using MD/MCr. The advantages of MD/MCr with respect to isothermal osmotic membrane distillation configuration, is the elimination of the re-concentration stages of the draw solution.

All the carried out case studies show that MD/MCr is able to reduce the volume of the waste stream significantly. The obtained results might be used as guidelines for practical application. Moreover, the low temperatures and atmospheric pressures utilized, makes it possible in real industrial processes to use waste or low-grade heat. Unlike other processes, MCr is able to produce two high quality products (i.e. water and salts) and will therefore not produce any additional waste. Hereby, the extended treatment by means of MCr will only positively influence the overall “sustainability” of the entire industrial process.



---

# TABLE OF CONTENT

---

CHAPTER 1: MEMBRANE ENGINEERING TO ADDRESS SUSTAINABLE DEVELOPMENT ..	1
1.1 INTRODUCTION .....	1
1.1.1 MEMBRANE BASED DESALINATION .....	3
1.1.2 MINERAL RECOVERY FROM SEA .....	5
1.2 MEMBRANE DISTILLATION AND CRYSTALLIZATION .....	6
CHAPTER 2: THESIS STATEMENT .....	11
CHAPTER 3: MEMBRANE CRYSTALLIZATION – AN OVERVIEW OF APPLICATIONS .....	13
3.1 DESALINATION .....	14
3.2 INDUSTRIAL WASTEWATER TREATMENT .....	16
3.3 CRYSTALLIZATION OF BIOMOLECULES .....	19
3.4 SUMMARY .....	21
CHAPTER 4: MEMBRANE FEATURES FOR TREATMENT OF CONCENTRATED SOLUTIONS .....	27
4.1 INTRODUCTION .....	27
4.2 MATERIALS AND METHODS .....	30
4.2.1 MEMBRANE CHARACTERISTICS.....	30
4.2.2 EXPERIMENTAL SETUP .....	31
4.2.3 UTILIZED FEED SOLUTIONS.....	32
4.2.4 CHARACTERIZATION OF ACHIEVED CRYSTALS.....	33
4.3 RESULTS AND DISCUSSION.....	33
4.3.1 DIRECT CONTACT MEMBRANE DISTILLATION .....	33
4.3.2 MEMBRANE CRYSTALLIZATION OF NaCl.....	35
4.3.3 MEMBRANE CRYSTALLIZATION OF EPSOMITE.....	35
4.3.4 MEMBRANE CRYSTALLIZATION OF NaCl FROM RO BRINE.....	37
4.4 SUMMARY .....	41

CHAPTER 5: RECOVERY OF SODIUM SULFATE FROM WASTEWATER.....	43
5.1 INTRODUCTION.....	43
5.2 MATERIALS AND METHODS .....	44
5.2.1 MD SETUP AND MEMBRANE USED .....	44
5.2.2 WASTEWATER CHARACTERISTICS.....	45
5.2.3 MD AND MCr EXPERIMENTS .....	45
5.2.4 CRYSTAL CHARACTERISTICS .....	45
5.3 RESULTS AND DISCUSSION.....	46
5.3.1 POTENTIAL SCALING STUDIES .....	48
5.3.2 CRYSTALLIZATION OF SODIUM SULFATE.....	48
5.3.3 SEM AND EDX ANALYSIS .....	51
5.3.4 UNTREATED WASTEWATER VS. PRETREATED WASTEWATER.....	52
5.4 SUMMARY .....	53
CHAPTER 6: RECOVERY OF NaCl FROM PRODUCED WATER.....	55
6.1 INTRODUCTION.....	55
6.2 MATERIALS AND METHODS .....	56
6.2.1 FEED COMPOSITION.....	56
6.2.2 MEMBRANE CRYSTALLIZATION TESTS .....	56
6.3 RESULTS AND DISCUSSION.....	57
6.3.1 CHARATERIZATION OF RECOVERED CRYSTALS .....	58
6.3.2 EVALUATION OF NEW METRICS.....	62
6.4 SUMMARY .....	63
CHAPTER 7: TREATMENT OF HIGH CONCENTRATED LiCl SOLUTIONS.....	65
7.1 INTRODUCTION.....	65
7.2 MATERIALS AND METHODS .....	67
7.2.1 APPLIED MEMBRANES .....	67
7.2.2 MEMBRANE DISTILLATION TESTS.....	67
7.3 RESULTS AND DISCUSSION.....	69
7.3.1 DIRECT CONTACT MEMBRANE DISTILLATION .....	69
7.3.2 OSMOTIC MEMBRANE DISTILLATION .....	71
7.3.3 VACUUM MEMBRANE DISTILLATION.....	73
7.3.4 CHARACTERIZATION OF CRYSTALLIZES PRODUCT .....	74
7.4 SUMMARY .....	75



CHAPTER 8: TREATMENT OF AGRO FOOD .....	79
8.1 INTRODUCTION.....	79
8.2 MATERIALS AND METHODS .....	80
8.2.1 CLARIFICATION OF ORANGE JUICE.....	80
8.2.2 MD AND MCr EXPERIMENTAL SETUP.....	81
8.3 RESULTS AND DISCUSSION.....	81
8.3.1 CLARIFICATION OF ORANGE JUICE.....	81
8.4 MEMBRANE DISTILLATION .....	83
8.5 MEMBRANE CRYSTALLIZATION .....	84
8.6 EVALUATION OF NEW METRICS.....	87
8.7 SUMMARY .....	88
CHAPTER 9: CONCLUSION AND FUTURE PERSPECTIVES.....	91
PUBLICATIONS AND COMMUNICATIONS .....	95
ARTICLES IN JOURNALS .....	95
CONFERENCE PROCEEDINGS (ORAL).....	96
CONFERENCE PROCEEDINGS (POSTER).....	96
PARTICIPATION IN SCHOOLS AND CONFERENCES .....	97



---

## LIST OF FIGURES

---

Figure 1.1: Illustration of waste turned into resources .....	1
Figure 1.2: MEDINA (2006-2010), European project – Sixth framework program.....	4
Figure 1.3: 3rd generation desalination plants developed by the Global MVP project (Korea). .....	4
Figure 1.4: Potential profitable minerals to recover from RO brine .....	5
Figure 1.5: Membrane distillation configurations.....	6
Figure 1.6: Comparison of trans-membrane flux in reverse osmosis and membrane distillation. ....	7
Figure 3.1: Timeline on the development of membrane crystallization.....	13
Figure 3.2: Crystal images obtained in the study by Drioli et al.....	15
Figure 3.3: Na <sub>2</sub> SO <sub>4</sub> ·10H <sub>2</sub> O crystals obtained in the study by Li et al.....	17
Figure 3.4: Struvite crystals obtained in the study by Xie et al.....	18
Figure 3.5: Ammonium salts obtained during MCr in VMD configuration .....	18
Figure 3.6: Hen egg-white lysozyme crystallization by means of MCr.....	20
Figure 3.7: Tunable polymorph structure of Glycine by changing operative conditions in MCr .....	20
Figure 3.8: Trypsin crystallized on microporous membrane by means of MCr.....	21
Figure 4.1: Membrane distillation concept with heat and mass transfer resistance. ....	29
Figure 4.2: SEM images of membrane M1. ....	31
Figure 4.3: SEM images of M3 .....	31
Figure 4.4: SEM images of M4.....	31
Figure 4.5: Schematic representation of the lab-scale membrane distillation plant used for evaluating the membrane performance.....	32
Figure 4.6: Average flux of DCMD tests using distillate water as feed solution.....	33
Figure 4.7: Average flux of DCMD tests utilizing synthetic seawater and brine as feed solution.....	34
Figure 4.8: Permeate quality of DCMD tests utilizing synthetic seawater and brine as feed solution..	34
Figure 4.9: Trans-membrane flux of MCr tests in the crystallization of NaCl .....	35
Figure 4.10: Permeate quality of MCr tests in the crystallization of NaCl. ....	35
Figure 4.11: Trans-membrane flux and MgSO <sub>4</sub> concentration for MCr treatment of MgSO <sub>4</sub> solution	36
Figure 4.12: Epsomite crystals produced by means of MCr. ....	36
Figure 4.13: Trans-membrane flux and concentration factor for MCr tests.....	38
Figure 4.14: Permeate conductivity for MCr treatment of saline solutions .....	38
Figure 4.15: Crystal size distribution for membrane crystallization at different feed flow rates. ....	39
Figure 4.16: Length to width ratio for membrane crystallization at different flow rates. ....	40
Figure 4.17: Scanning electron microscopy images of NaCl crystallized from RO brine .....	40
Figure 4.18: Energy-dispersive X-ray (EDX) spectra of NaCl crystallized from RO brine. ....	41

Figure 5.1: Solubility of sodium sulfate with temperature.....	43
Figure 5.2: Phase diagram of sodium sulfate: dependence on relative humidity and temperature .....	44
Figure 5.3: Schematic diagram of the set-up used for MCr .....	44
Figure 5.4: Trans-membrane flux vs. time for different experimental conditions. ....	46
Figure 5.5: Driving force vs. time for different experimental conditions. ....	47
Figure 5.6: Normalized flux vs. time for different experimental conditions.....	48
Figure 5.7: Na <sub>2</sub> SO <sub>4</sub> concentration for different test conditions.....	49
Figure 5.8. Sodium sulfate produced from "wastewater solution # 2".....	49
Figure 5.9. Crystal size distribution achieved during crystallization of "wastewater solution # 2".....	50
Figure 5.10. SEM images of (a) Na <sub>2</sub> SO <sub>4</sub> from solution # 1 (b) Na <sub>2</sub> SO <sub>4</sub> from solution # 1, (c) Na <sub>2</sub> SO <sub>4</sub> from solution # 2 and (d) Na <sub>2</sub> SO <sub>4</sub> from solution # 2 .....	51
Figure 5.11. SEM images of (a) Na <sub>2</sub> SO <sub>4</sub> from solution # 3, (b) Na <sub>2</sub> SO <sub>4</sub> from solution # 1, (c) Na <sub>2</sub> SO <sub>4</sub> from solution # 4 and (d) Na <sub>2</sub> SO <sub>4</sub> from solution # 4 .....	51
Figure 5.12. EDX analysis of Na <sub>2</sub> SO <sub>4</sub> recovered through MCr. ....	52
Figure 5.13: Recovery factor of the four wastewater solutions.....	52
Figure 6.1: Trans-membrane flux of PP and PVDF membranes in MCr tests of produced water. ....	57
Figure 6.2: Trans-membrane flux of commercial PP module in MCr tests of produced water. ....	57
Figure 6.3: SEM images of the crystals precipitated from produced water .....	58
Figure 6.4: Example of EDX spectra obtained for the crystals precipitated from produced water.....	58
Figure 6.5: XRD spectra obtained from the recovered crystals from produced water. ....	59
Figure 6.6: Mean diameter of the produced crystals at different feed temperatures and feed flow rates. ....	60
Figure 6.7: Growth rate of the produced crystals at different feed temperatures and feed flow rates... ..	60
Figure 6.8: Coefficient of variation (CV) of the produced crystals at different feed temperatures and feed flow rates.....	61
Figure 6.9: Diameter, coefficient of variation and growth rate for crystals recovered from semi-pilot plant at different time intervals .....	61
Figure 6.10: Percentages of analyzed crystals with length to width ratio below 1.4. ....	62
Figure 6.11: Mass and waste intensities and overall water recovery factor with duration of treatment. ....	62
Figure 6.12: Productivity/Size, Productivity/Weight ratio and overall water recovery factor with duration of treatment .....	63
Figure 7.1: Illustration of the decrease in brine volume and increase in recovery factor for obtaining lithium recovery. ....	66
Figure 7.3: Schematic representation of set-up applied for (a) DCMD and OMD, (b) VMD. ....	68
Figure 7.4: Flux for DCMD with single solute lithium chloride solution starting from 6M.....	69
Figure 7.5 : Theoretical evaluation of trans-membrane flux at increasing LiCl concentration for several feed temperatures in the DCMD configuration. Permeate bulk temperature: 25°C.....	70
Figure 7.6: Close-up of Figure 7.5 for evaluation of negative flux.....	71
Figure 7.7: Flux for OMD with single solute lithium chloride solution starting from 7M. Draw solution: 4.5 M CaCl <sub>2</sub> ·2H <sub>2</sub> O. ....	71
Figure 7.8: Theoretical evaluation of trans-membrane flux at increasing LiCl concentration for several feed temperatures in combined OMD and DCMD configuration. Draw solution: 4.5 M CaCl <sub>2</sub> ·2H <sub>2</sub> O (Continuously kept at 4.5 M), Permeate bulk temperature: 25°C. ....	72
Figure 7.9: Close-up of Figure 7.8 for evaluation of negative flux.....	72
Figure 7.10: Flux for VMD with single solute lithium chloride solution starting from 8M. ....	73



Figure 7.11: Theoretical evaluation of flux vs vapor pressure of feed solution for DCMD, VMD and OMD.....	74
Figure 7.12: Phase diagram of LiCl-H <sub>2</sub> O. (Lix: LiCl·xH <sub>2</sub> O) .....	74
Figure 7.13: Morphology of LiCl obtained in membrane crystallization, (a) the orthorhombic polymorphic form (b) the cubic polymorphic form .....	75
Figure 7.14: Distribution between cubic structures and orthorhombic structures at different feed temperatures and feed flow rates.....	75
Figure 8.1: Flow sheet of orange juice processing. ....	80
Figure 8.2: Permeability of ultrafiltration experiments. ....	81
Figure 8.3: Images of UF feed before and after centrifugation. ....	82
Figure 8.4: Images of UF retentate before and after centrifugation. ....	82
Figure 8.5: Average flux with standard deviation for membrane distillation experiments. ....	83
Figure 8.6: Concentration (° Brix) of membrane distillation experiments.....	84
Figure 8.7: Trans-membrane flux for membrane crystallization experiment.....	84
Figure 8.8: Distillate water flux before and after juice treatment. . ....	85
Figure 8.9: Concentration (° Brix) of membrane crystallization experiment.....	85
Figure 8.10: Viscosity of membrane crystallization experiment.....	86
Figure 8.11: Analytical evaluations on samples of orange juice coming from the different steps of the UF/MD/MCr treatment.....	86
Figure 8.12: Crystal images obtained by optical microscope.....	87
Figure 8.13: Crystal size distribution of the crystal produced by MCr. ....	87
Figure 8.14: Mass reduction of the different treatment stages of juice processing .....	88



---

## LIST OF TABLES

---

Table 3.1: Economic analysis of various integrated membrane systems. ....	15
Table 3.2: Water production cost of several integrated membrane systems when the sale of the produced salt is considered. ....	16
Table 4.1: Characteristics of the prepared membranes.....	30
Table 4.2: Composition of synthetic seawater and brine .....	32
Table 4.3: Crystal characteristics obtained with membrane M1 at different flow rates.....	37
Table 4.4: Crystal characteristics for membrane crystallization of RO brine at feed flow rate = 100 ml/min. ....	38
Table 4.5: Crystal characteristics for membrane crystallization of RO brine at feed flow rate = 140 ml/min. ....	39
Table 4.6: Energy-dispersive X-ray (EDX) analysis of NaCl crystallized from RO brine. ....	40
Table 5.1: Detailed description of membrane modules from Microdyn-Nadir (MD020CP2N) .....	45
Table 5.2: Characteristics of the utilized wastewater. ....	45
Table 5.3: DCMD and MCr experiments for the treatment of wastewater. ....	45
Table 5.4: Crystal characteristics achieved in the crystallization of "wastewater solution # 2". ....	50
Table 6.1: Main properties of produced water used .....	56
Table 6.2: Membrane characteristics used in MCr treatment of produced water.....	56
Table 7.1: Properties of PP membrane applied in DCMD, OMD and VMD.....	67
Table 7.2: Concentration of LiCl solutions used in the different configurations. ....	69
Table 8.1: Ultrafiltration membrane characteristics.....	80
Table 8.2: Operative conditions in ultrafiltration experiments.....	80
Table 8.3: Operative conditions in membrane distillation experiments.....	81
Table 8.4: Determination of suspended solids. ....	82



---

# CHAPTER 1:

## MEMBRANE ENGINEERING TO ADDRESS SUSTAINABLE DEVELOPMENT

---

### 1.1 INTRODUCTION

Population increase, climate changes and ongoing industrialization are putting pressure on water, energy and minerals, which are crucial resources for sustainability and development of future society. These resources are, moreover, limited and cannot be used without any concern. Fresh water resources are sufficient only in limited parts of the world. It is estimated that 50% of the world population will live in water stressed regions in 2025, which highlights the importance of adequate water management and treatment [1]. Energy consumptions also grew rapidly in the last decades and is projected to increase further in the following years [2]. Furthermore, mineral deficiency is also becoming a threat to future development. As a consequence, efficient technologies able to minimize utilization of water, energy and minerals are being developed. In this logic sustainable development has become important for industrial processes, and is defined as:

*"Meeting the needs of the present without compromising the ability of future generations to meet their needs"* Brundtland commission 1987 [3].

Some unintended negative consequences of non-sustainable practices are that large amounts of material inputs are lost to landfill or incinerator (around 50% in Europe) equivalent to a value of €5 billion per year [4], [5]. To improve sustainability, waste has to be turned into resources. A well-known example of such kind of process is found in nature as the O<sub>2</sub>-CO<sub>2</sub> circle. Nevertheless, the increased industrialization has promoted the extensive production of CO<sub>2</sub> where only a small part is recycled. The same trend is observed for various other industrial processes. Today, many waste streams are not fully explored, but by technological development waste can be turned into resources to sustain limited resources (Figure 1.1).

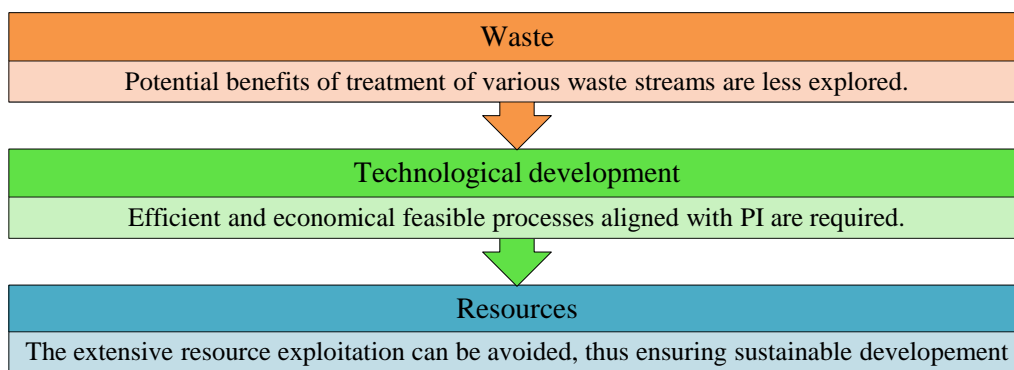


Figure 1.1: Illustration of waste turned into resources

Lack of a precise definition of sustainable development has evolved specific guidelines such as the process intensification strategy (PIS) helping to meet the requirements of sustainable development. Process intensification as defined by Stankiewicz and Moulijn [6], [7] is the development of novel equipment and techniques that, compared to those commonly used, dramatically improves manufacturing and processing, by decreasing substantially equipment size, improving raw material to production ratio, decreasing energy consumption and waste production, and ultimately results in

cheaper, sustainable technologies. Membrane engineering, through the process intensification strategy, can redesign conventional process engineering with applications in several industrial processes e.g. pharmaceutical production, gas separation, energy production, tissue engineering and bio-artificial organs, food applications, wastewater treatment, potable water production and many other applications where separations is needed for the manufacture of chemicals, electronics, etc. [8]. For this reason, membrane engineering improves the conventional processes in achieving the required technological development for obtaining sustainable development. Membrane engineering, is highly aligned with PIS due to several reasons including high selectivity and permeability for transport of specific components, easy to integrate with other processes or other membrane operations, less energy intensive, high efficiency, low capital costs, small footprints, high safety, operational simplicity and flexibility [9]–[12]. To easier compare the conventional unit operations with membrane technology, Criscuoli and Drioli [13] have proposed the terms of new metrics. New metrics allow monitoring the progress and improvement of membrane operations in the logic of process intensification taking into account plant size, weight, flexibility, modularity etc. Overall assessment of sustainable processes should also consider existing metrics (mass and waste intensity), environmental factors, economic, and society indicators. Mass and waste intensities (Eq. 1.1 and Eq. 1.2) are used to quantify the amount of product which is produced from the particular process with respect to amount of input materials or waste produced from the process. Reduction in mass and waste intensities is preferred for an improvement of the process. Membrane operations have small footprints and, therefore, Eq. 1.3 and Eq. 1.4 can be used to quantify how productivity is influenced by plant size or weight (Eq. 1.3 and Eq. 1.4 should be higher than 1 to be in favor of a membrane plant.) The productivity to weight ratio is of particular interest if the plant is constructed off-shore or in remote areas. Taking into account the entire lifetime of the plant, it is important it has flexibility and modularity (Eq. 1.5 and Eq. 1.6), so it can be adjusted according to changes in the productivity, variation in pressure, temperature, feed compositions or other process related parameters. The modularity equation considers changes in increase/decrease in plant size compared to the productivity. These metrics should also be higher than 1 for a membrane plant to be preferred [13].

$$\text{Mass Intensity} = \frac{\text{Total Mass [kg]}}{\text{Mass of Product [kg]}} \quad (\text{Eq. 1.1})$$

$$\text{Waste Intensity} = \frac{\text{Total Waste [kg]}}{\text{Mass of Product [kg]}} \quad (\text{Eq. 1.2})$$

$$\text{Productivity/Size ratio} = \frac{\frac{\text{Productivity}}{\text{Size}} (\text{Membranes})}{\frac{\text{Productivity}}{\text{Size}} (\text{Tradional process})} \quad (\text{Eq. 1.3})$$

$$\text{Productivity/Weight ratio} = \frac{\frac{\text{Productivity}}{\text{Weight}} (\text{Membranes})}{\frac{\text{Productivity}}{\text{Weight}} (\text{Tradional process})} \quad (\text{Eq. 1.4})$$

$$\text{Flexibility} = \frac{\text{Variations}_{\text{handled}} (\text{Membranes})}{\text{Variations}_{\text{handled}} (\text{Tradional process})} \quad (\text{Eq. 1.5})$$

$$\text{Modularity} = \frac{\left| \frac{\text{area}_2}{\text{area}_1} - \frac{\text{productivity}_2}{\text{productivity}_1} \right| (\text{Membranes})}{\left| \frac{\text{area}_2}{\text{area}_1} - \frac{\text{productivity}_2}{\text{productivity}_1} \right| (\text{Traditional process})} \quad (\text{Eq. 1.6})$$

Today, membrane operations have gained many accomplishments. In fact membrane operations are already the most used technologies within water production and are also increasing in numbers within wastewater handling. Some examples are found in wastewater treatment, where membrane bioreactors (MBR) are the best available technology (BAT) [14], [15]. Another example of the success of membrane engineering is in desalination, where reverse osmosis (RO) is already the most widely used process with more than 60 % of the total desalination capacity [16]. However, membrane technology in wastewater treatment and in membrane based desalination continues to develop and to improve.

### 1.1.1 MEMBRANE BASED DESALINATION

Desalination has the capability to decrease water scarcity and to achieve food security by producing water for domestic, industrial and agricultural sectors [17]. There have been many developments over the last three decades, which have contributed to a reduction in unit water cost of RO desalination, particularly: membrane performance and decrease of membrane cost, reduction in energy consumption caused by improvement of pumping systems and the recourse to efficient energy recovery systems, improvements in pretreatment processes, development of high boron rejection membranes, reduction in usage of chemicals with improved membrane performance, increases in plant capacity, the use of the so called build, own, operate, transfer (BOOT) contracts [18]. Despite the success of RO, the process is still associated to some drawbacks including:

- Needs to increase water recovery factor (today, only around 50 %);
- To reduce energy consumptions (mainly electrical energy);
- Environmental concern regarding brine disposal, which will only increase further with increase in desalination capacity.

Integrated membrane systems might be the solution to these concerns. Already today, desalination can partly be taken place as an integrated membrane system, since pre-treatment can also be carried out by pressure driven membrane operations such as microfiltration (MF), ultrafiltration (UF) and nanofiltration (NF) [19], [20]. However, in order to minimize the associated drawbacks in RO desalination more attention has to be given to the post-treatment. Novel membrane operations for improvement of desalination are forward osmosis (FO) and membrane distillation (MD) for water production, pressure retarded osmosis (PRO) and reverse electrodialysis (RED) for energy production and membrane crystallization (MCr) for minerals recovery. Each of these processes is still in the development stage. Nevertheless, several international projects aim to develop these novel membrane operations in particular for desalination applications. Some projects to mention are MEDINA (Membrane-based desalination, an integrated approach, 2006-2010, EU), MEGATON (2009-2014, Japan), SEAHERO (Seawater engineering & architecture of high efficiency reverse osmosis 2007-2012, 2013-2018, S. Korea), Global MVP (2013-2018, S. Korea). The objective of MEDINA (Figure 1.2) has been to improve the overall performance of membrane-based desalination processes through integration of different membrane operations in RO pre-treatment (i.e. ultrafiltration, microfiltration, nanofiltration and MBR) and RO post-treatment stages (i.e. MD and MCr).



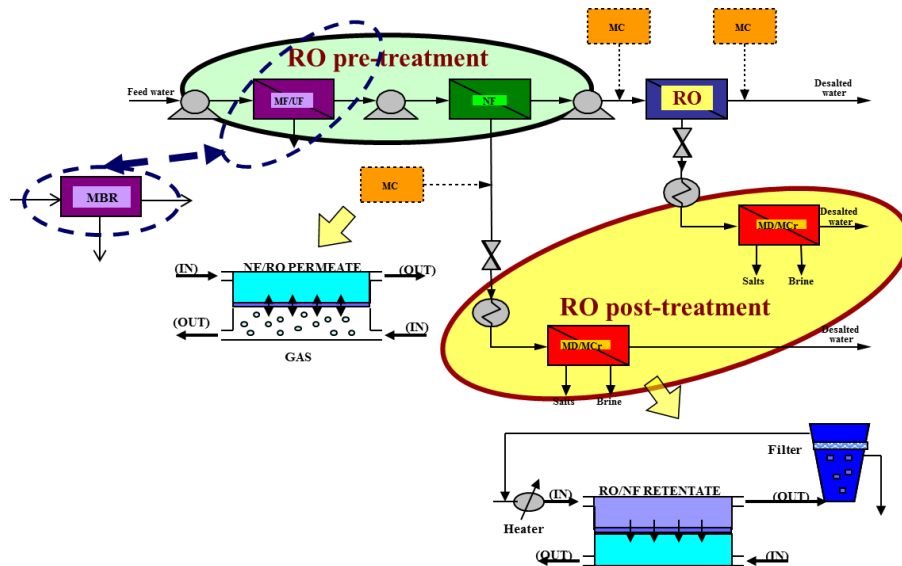


Figure 1.2: MEDINA (2006-2010), European project – Sixth framework program - Priority 1.1.6.3 - Global Change and Ecosystems

SeaHERO focusses on large scale plants, low energy consumptions and low fouling by improvement of all the desalination phases [21]. The 2<sup>nd</sup> stage of the project aims to develop hybrid systems for improving water production and concentrate management by integrating membrane distillation (MD) with pressure retarded osmosis (PRO) and forward osmosis (FO) with RO. MEGATON has similar fields of interests as SeaHERO with the particular goal of reaching fresh water capacity of 1,000,000 m<sup>3</sup>/d. MEGATON is also exploring the use of low pressure RO for reducing energy while using PRO for energy production [22], [23]. Furthermore, the project intends to minimize chemical treatment. The latest launched project; the Global MVP aims to develop further the so-called 3<sup>rd</sup> generation desalination plant, by also introducing PRO for energy production, MD for enhancing water production and as an additional step, a valuable resource recovery stage (Figure 1.3). The project emphasizes on lithium and strontium recovery from the discharged RO brine [23], but in fact, several other compounds might be recovered from RO brine in perspective.

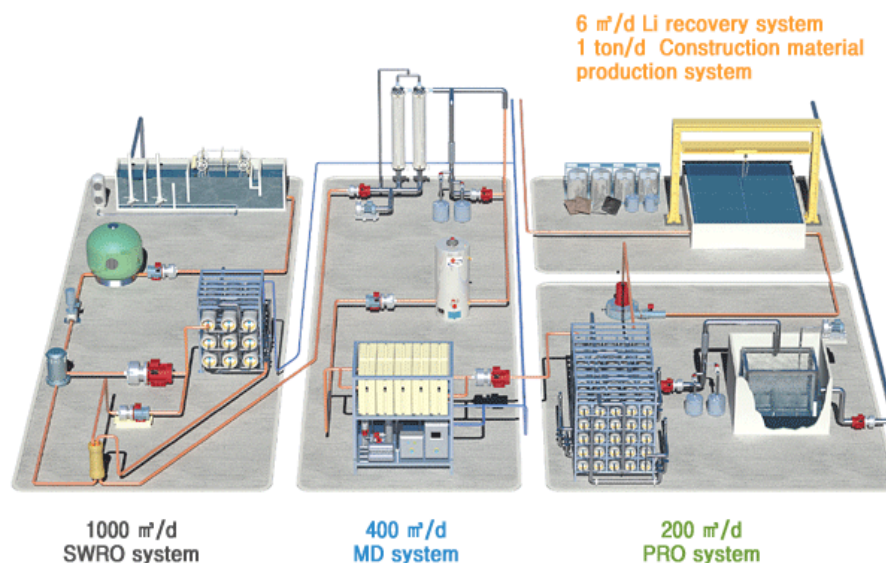


Figure 1.3: Overview of 3<sup>rd</sup> generation desalination plants developed by the Global MVP project (Korea) [24].

### 1.1.2 MINERAL RECOVERY FROM SEA

The interesting objective of recovering minerals from the sea might actually partly aim to reduce brine disposal. Moreover, as an interesting and positive side effect, it can contribute to the conventional mining industry and hereby reduce mineral depletion. The continued extraction of minerals from mining leads to degradation of the high concentrated ores, thus less concentrated ores have to be deployed. Low concentrated ores are more difficult to extract and at higher associated costs [25].

Seawater is an additional source for mineral extraction. The most part of the ions present in the periodic table might be recovered from seawater in the logic of “*mining from the sea*”. Today some minerals are already being extracted such as  $\text{Na}^+$ ,  $\text{Mg}^{2+}$ ,  $\text{Ca}^{2+}$ ,  $\text{K}^+$  [26]. Several research activities have been carried out to extend the number of ions to be recovered from seawater [26]. The ocean has in general much greater content in comparison to mineral resources on land [26], [27]. Although, one can argue that the resources in ocean are present in lower concentrations which reduces the possibility of recovery. In 2010 Bardi stated that extraction from low concentrated resources, for many ions, is too expensive in terms of the required energy. Besides the highest concentrated ions in seawater (Na, Mg, Ca, K) already being extracted, Bardi, however, have also mentioned lithium as a potential economically feasible component to recover depending on the future use of lithium ion batteries [26]. Nevertheless, mineral recovery might be too expensive and energy intensive with respect to extraction directly from seawater only with this objective in mind. However, systems producing energy and water and, moreover, extracting minerals can be developed similar to the integrated desalination system from global MVP. This integration can minimize many of the drawbacks associated with the production methods of today and, furthermore, in the logic of sustainable development, RO brine can be turned from waste streams to mineral resources. Shahmansouri et al. have highlighted some of the potential profitable elements which can be recovered from RO brine (Figure 1.4) [28]. The results obtained by Shahmansouri et al. [28] correspond well with feasible economic components found by others [29]. In prospective rubidium, cesium, lithium, strontium etc. could also add significant value to the desalination process. However, technological development is required to be able to recover minerals from such kind of solutions. In particular, because RO brine and other high concentrated industrial wastewaters are difficult to treat due to the complex solutions and high concentrations. Nevertheless, emerging membrane operations including membrane distillation (MD) and membrane crystallization (MCR) can be the answer to the request of technological development, where water production and minerals recovery is combined in a single unit operation.

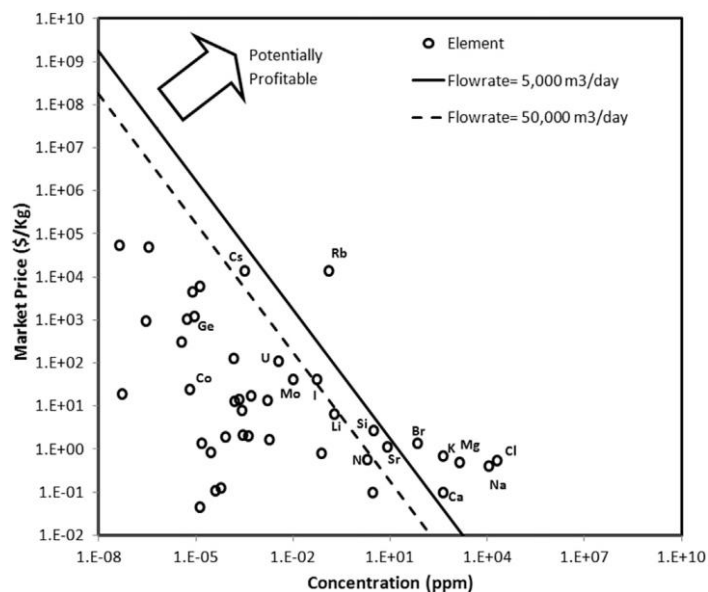


Figure 1.4: Potential profitable minerals to recover from RO brine [28].

## 1.2 MEMBRANE DISTILLATION AND CRYSTALLIZATION

MD is a membrane contactor technology patented first time in 1963 by Bodell [31]. MD operations is based on vapor pressure gradient created across a microporous hydrophobic membrane [30]. The driving force is mainly temperature implied and can be estimated through the Antoine equation (Eq. 1.7).

$$P_{H_2O} = \left[ A - \frac{B}{C + T} \right] \quad (\text{Eq. 1.7})$$

$P_{H_2O}$  is the vapor pressure of pure water in [Pa] and  $A$ ,  $B$  and  $C$  are constants, which depends on the component. For water the constants are  $A = 23.1965$ ,  $B = 3816.44$ ,  $C = -46.13$ . [22].  $T$  is the temperature in Kelvin [K].

The hydrophobic nature of the membrane prevents liquid intrusion into the pores. Therefore, only volatile components is transported through the membrane and condensed on permeate site. MD can be carried out in various configurations differing in mass and heat transfer mechanisms, in different driving force and in how the volatile components are condensed and collected. Four well known configurations of membrane distillation exist: direct contact membrane distillation (DCMD), vacuum membrane distillation (VMD), sweep gas membrane distillation (SGMD) and air gap membrane distillation (AGMD) (Figure 1.5) [32].

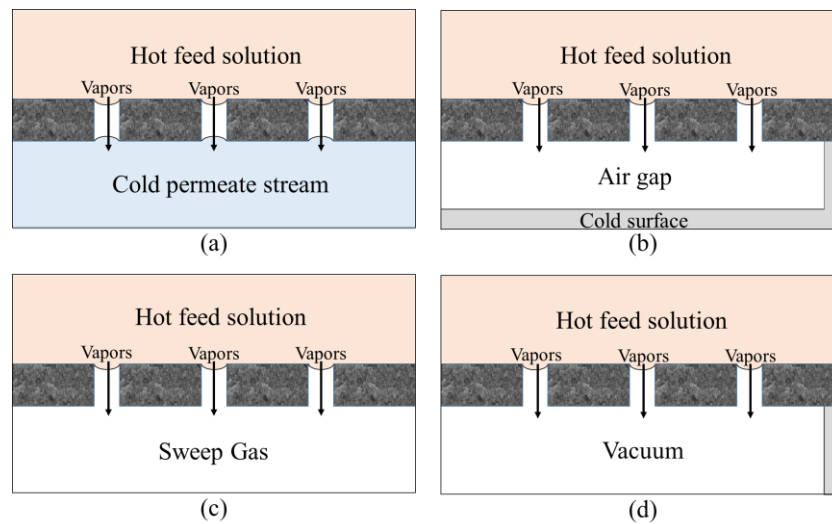


Figure 1.5: Membrane distillation configurations. (a) DCMD, (b) AMD, (c) SGMD and (d) VMD. [32]

MCr is an extension of the MD process, where the mass transfer of volatile solvents allows to concentrate feed solution above their saturation limit, thus attaining a supersaturated environment where crystals may nucleate and grow. The advantages of using MD and MCr are the very low temperatures and pressures, high permeate quality independent of feed characteristics (theoretical 100 % rejection of non-volatile components), simple configuration and treatment of highly concentrated solutions [30]. Unlike pressure driven membrane operations, the impact of concentration in MD and MCr is very small [33]. As an example, the flux in reverse osmosis decreases drastically at increasing concentration and constant applied pressure (Figure 1.6). RO is only able to reach concentration around 85 g/L. In contrast, MD shows almost constant flux justifying the low impact of concentration on trans-membrane flux. Moreover, flux can be improved by applying a relative small feed temperature increase [34], due to exponential relationship between temperature and vapor pressure (Eq. 1.7).

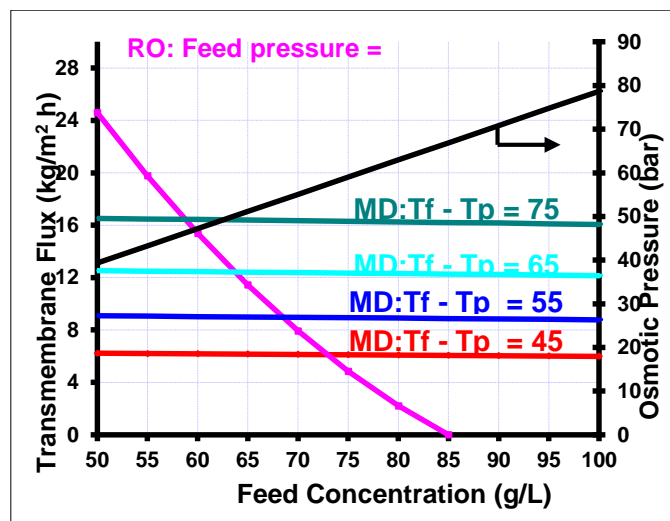


Figure 1.6: Comparison of trans-membrane flux in reverse osmosis and membrane distillation [34].

Furthermore, MCr has some important advantages with respect to traditional crystallization processes such as well-controlled nucleation and growth kinetics, faster crystallization rates and reduced induction time, control of super-saturation level and rate. Therefore, it is possible to target the crystal polymorph form, obtain crystals with narrow size distribution and of high purity [35]. For the application in membrane crystallization, DCMD is the most widely used methodology [36] because no additional separation and purification is needed if i.e. aqueous solutions are treated (water vapor is transferred through the membrane and condensed by cold liquid water stream). Therefore DCMD is more simple and economical than other configurations (such as SGMD and AGMD where a condenser has to be used for the compression of the achieved permeate [37]).

Despite the great potential of MD and MCr, neither has been fully commercialized due to some drawbacks not yet defeated. Like in other membrane operations, optimization and development of appropriate membranes is crucial to reach commercial scale. In general, commercial membranes available for MD and MCr are manufactured for ultrafiltration or microfiltration. The determining parameters, such as porosity, pore size, thickness, hydrophobicity etc. have not been improved according to MD/MCr application. Therefore, many times only one parameter can be chosen as the best and, therefore, at the impairment of the others when selecting commercial membranes. Nevertheless, during the last 5-10 years numerous studies have been conducted in membrane preparation, mostly to be used in MD, and have achieved better development of the membranes. Relative low flux is also characterizing MD and MCr, although significantly improved due to membrane development has occurred. Moreover, resistance towards wetting is also one of the crucial parameter for long duration treatment and final commercialization. Continued development of MD and MCr reduces the gap between lab-scale testing and large-scale applications. MD has been suggested in desalination to treat the concentrated solutions not able to be treated by RO. Today several desalination projects are projecting MD in pilot-scale with the final aim of full-scale integrated membrane based desalination. In this regard MCr is still some steps behind MD in commercialization potential, although the processes are so interrelated that development of MD positively influences MCr. The major difference of MD and MCr is for example, that the membranes for MCr applications need to be optimized for concentrations near saturations. Process parameters can not only be optimized for enhancing flux, but also crystal quality and characteristics have to be considered. In MD, there is mainly a single product, i.e. fresh water, whereas in MCr several salts can be the product besides water. Studies on MCr have to consider the nature of the present salts, which again should be optimized according to operative conditions, temperature polarization, scaling mechanisms etc.

## REFERENCES

- [1] WHO, “World Health Organization - Water,” *Fact sheet 391*, 2014. [Online]. Available: <http://www.who.int/mediacentre/factsheets/fs391/en/>.
- [2] C. Rühl, P. Appleby, J. Fennema, A. Naumov, and M. Schaffer, “Economic development and the demand for energy: A historical perspective on the next 20 years,” *Energy Policy*, vol. 50, pp. 109–116, Nov. 2012.
- [3] World Commission on Environment and Development (United Nations), “Our common future,” 1987.
- [4] R. Tansey, “Preventing waste - Recycling isn’t enough for a circular economy,” Friends of the Earth Europe 2015.
- [5] European Environment Agency, *Material resources and waste (2012 updated) - The european environment state and outlook 2010*. 2012.
- [6] A. I. Stankiewicz and J. A. Moulijn, “Process Intensification: Transforming Chemical Engineering,” *Chem. Eng. Prog.*, pp. 22–34, 2000.
- [7] A. Stankiewicz, “Reactive separations for process intensification: An industrial perspective,” *Chem. Eng. Process.*, vol. 42, pp. 137–144, 2003.
- [8] E. Drioli and L. Giorno, Eds., *Comprehensive membrane science and engineering*. Elsevier Ltd, 2010.
- [9] J.-C. Charpentier, “Among the trends for a modern chemical engineering, the third paradigm: The time and length multiscale approach as an efficient tool for process intensification and product design and engineering,” *Chem. Eng. Res. Des.*, vol. 88, no. 3, pp. 248–254, Mar. 2010.
- [10] E. Drioli, A. I. Stankiewicz, and F. Macedonio, “Membrane engineering in process intensification — An overview,” *J. Memb. Sci.*, vol. 380, pp. 1–8, 2011.
- [11] F. Macedonio, E. Drioli, a. a. Gusev, a. Bardow, R. Semiat, and M. Kurihara, “Efficient technologies for worldwide clean water supply,” *Chem. Eng. Process. Process Intensif.*, vol. 51, pp. 2–17, Jan. 2012.
- [12] E. Drioli, A. Brunetti, G. Di Profio, and G. Barbieri, “Process intensification strategies and membrane engineering,” *Green Chem.*, vol. 14, p. 1561, 2012.
- [13] A. Criscuoli and E. Drioli, “New Metrics for Evaluating the Performance of Membrane Operations in the Logic of Process Intensification,” *Ind. Eng. Chem. Res.*, vol. 46, pp. 2268–2271, 2007.
- [14] Simon Judd, *The MBR book - Principles and Applications of Membrane Bioreactors in Water and Wastewater Treatment*, 2nd Editio. Butterworth-Heinemann Elsevier, 2010.
- [15] M. Kraume and A. Drews, “Membrane Bioreactors in Waste Water Treatment - Status and Trends,” *Chem. Eng. Technol.*, vol. 33, pp. 1251–1259, 2010.
- [16] Global Water Intelligence, *IDA desalination yearbook 2011-2012*. Media Analytics Ltd.
- [17] C. A. Quist-Jensen, F. Macedonio, and E. Drioli, “Membrane technology for water production in agriculture: Desalination and wastewater reuse,” *Desalination*, vol. 364, pp. 17–32, May 2015.
- [18] UNESCO Centre for Membrane Science and Technology University of New South Wales, *Emerging trends in desalination: A review*. National Water Commission, 2008.
- [19] S. Jamaly, N. N. Darwish, L. Ahmed, and S. W. Hasan, “A short review on reverse osmosis pretreatment technologies,” *Desa*, vol. 354, pp. 30–38, 2014.
- [20] L. Henthorne and B. Boysen, “State-of-the-art of reverse osmosis desalination pretreatment,” *Desalination*, vol. 356, pp. 129–139, 2015.
- [21] S. Kim, B. S. Oh, M.-H. Hwang, S. Hong, J. H. Kim, S. Lee, and I. S. Kim, “An ambitious step to the future desalination technology: SEAHERO R&D program (2007–2012),” *Appl. Water Sci.*, vol. 1, no. 1–2, pp. 11–17, May 2011.
- [22] M. Kurihara and M. Hanakawa, “Mega-ton Water System: Japanese national research and development project on seawater desalination and wastewater reclamation,” *Desalination*, vol. 308, pp. 131–137, Jan. 2013.
- [23] S.-H. Kim and D.-I. Kim, “Scaling-up and piloting of pressure-retarded osmosis,” *Desalin. Water Reuse*, vol. 24, no. 3, pp. 36–38, 2014.
- [24] “Global MVP.” [Online]. Available: <http://www.globalmvp.org/>.
- [25] U. Bardi, “World Mineral resources and the Limits to Economic Growth,” *E3S Web of*

- Conferences*, vol. 2, 2014.
- [26] U. Bardi, “Extracting Minerals from Seawater: An Energy Analysis,” *Sustainability*, vol. 2, pp. 980–992, Apr. 2010.
- [27] F. Macedonio, C. A. Quist-Jensen, and E. Drioli, “Raw materials recovery from seawater for zero liquid discharge,” in *The International Desalination Association World Congress on Desalination and Water Reuse 2015/San Diego, CA, USA*, 2015.
- [28] A. Shahmansouri, J. Min, L. Jin, and C. Bellona, “Feasibility of extracting valuable minerals from desalination concentrate: a comprehensive literature review,” *J. Clean. Prod.*, vol. 100, pp. 4–16, Aug. 2015.
- [29] T. Jeppesen, L. Shu, G. Keir, and V. Jegatheesan, “Metal recovery from reverse osmosis concentrate,” *J. Clean. Prod.*, vol. 17, pp. 703–707, 2009.
- [30] E. Drioli, A. Ali, and F. Macedonio, “Membrane distillation: Recent developments and perspectives,” *Desalination*, vol. 356, pp. 56–84, 2015.
- [31] B. R. Bodell, Silicone rubber vapor diffusion in saline water distillation, US Patent No 285,032, 1963.
- [32] K. W. Lawson and D. R. Lloyd, “Membrane distillation,” *J. Memb. Sci.*, vol. 124, no. 1, pp. 1–25, Feb. 1997.
- [33] A. Ali, F. Macedonio, E. Drioli, S. Aljlil, and O. A. Alharbi, “Experimental and theoretical evaluation of temperature polarization phenomenon in direct contact membrane distillation,” *Chem. Eng. Res. Des.*, vol. 91, no. 10, pp. 1966–1977, Oct. 2013.
- [34] F. Macedonio, “Membrane contactors for water purification and recovery factor increase in desalination plants,” Ph.D. Dissertation, University of Calabria, 2009.
- [35] E. Curcio and E. Drioli, “Membrane Distillation and Related Operations — A Review,” *Separat.*, no. May 2004, pp. 35–86, 2005.
- [36] C. Charcosset, R. Kieffer, D. Mangin, D. Lyon, “Coupling between Membrane Processes and Crystallization Operations,” *Ind. Eng. Chem. Res.* 49, pp. 5489–5495, 2010.
- [37] E. Curcio, A. Criscuoli, and E. Drioli, “Membrane Crystallizers,” *Ind. Eng. Chem. Res.*, vol. 40, no. 12, pp. 2679–2684, Jun. 2001.





---

## CHAPTER 2:

# THESIS STATEMENT

---

Sustainable development and process intensification are guidelines for future industrial processes. In this logic, treatment of waste streams can be of particular importance. However, existing commercial processes can have difficulties in the treatment of these normal high concentrated solutions. For this reason, novel membrane technologies such as membrane distillation and membrane crystallization are emerging.

The aim of this Ph.D. thesis is to enhance the understanding of fundamentals essential of membrane distillation and membrane crystallization to address successful and widespread applications of these processes. Several feed solutions and wastewater streams using different membranes and operative conditions have been tested to identify positive and negative aspect of membrane crystallization. The qualitative application of the conclusions drawn is believed to be applicable for practical applications of membrane crystallizers, though the carried out research and mentioned results are based on laboratory work and theoretical evaluations.

A brief overview of each chapter included into the thesis has been described below:

In **Chapter 3** state-of-the-art in membrane crystallizers has been described. Its utilization in treatment of desalinated brine, different kinds of wastewater and in crystallization of biomolecules has been highlighted.

In **Chapter 4** lab-made PVDF membranes have been tested using several feed solutions and operative conditions. This chapter aims to help in selection of appropriate membranes for the various MCr applications from RO brine to real wastewater, to produced water, to highly concentrated solutions, to agro food.

In **Chapter 5**, sodium sulfate has been recovered from wastewater utilizing DCMD configuration. Sodium sulfate has been recovered as the Thenardite polymorph structure. The MCr setup has shown good stability in terms of trans-membrane flux with operation for more than 90 h.

In **Chapter 6**, sodium chloride has been recovered from produced water. Lab-made and commercial membranes at different operative conditions have been tested. Despite the complex solutions, no or less impurities have been incorporated into the crystal lattice.

In **Chapter 7**, the potential to recover different compounds from reverse osmosis brine has been discussed. In particular, the attention has been focused on the possibility to recover lithium. In order to reach this aim and due to the high solubility of LiCl, single salt solution, have been considered and crystallized. DCMD, OMD and VMD configurations have been evaluated and two polymorph structures of LiCl have been obtained.

In **Chapter 8**, the possibility to treat agro food by means of MD and MCr has been demonstrated. Regardless of the long duration of the experiments, the quality of juice has been maintained. Some crystallized compounds have been detected at very high concentrations.

**Chapter 9** concludes the work performed in this Ph.D. study and highlights the future perspectives on membrane crystallization.



---

## CHAPTER 3:

# MEMBRANE CRYSTALLIZATION – AN OVERVIEW OF APPLICATIONS

---

Crystallization is a common application for separation, purification and production of various species in the chemical industry. Membrane crystallization is a relative new membrane operation. The first study dates back to 1986, where calcium oxalate was precipitated by means of reverse osmosis [1]. In 1987 the first study suggested to use membrane distillation (MD) and in 1991 Taurine was crystallized from pharmaceutical wastewater using MD [2]. Later Sluys et al. [3] report membrane assisted seeded crystallization using microfiltration in the crystallization of  $\text{CaCO}_3$ . The authors states that around 98 % of the calcium ions can be removed from the feed solution. However, initial feed concentration was relatively low (only 0.0025 M). TNO has patented similar processes using MF for the separating solutes from solutions [4]. RO has also been applied in membrane assisted crystallization for adipic acid [5], [6] and  $(\text{NH}_4)_2\text{SO}_4$  [5]. Other membrane operations integrated with crystallization is electro dialysis (ED) and RO for l-tryptophan recovery from its crystallization wastewater [7], silver particles from an emulsion liquid membrane-crystallization process [8], and organic solvent nanofiltration (OSN) for the crystallization of the pharmaceutical compound griseofulvin [9]. However, the limitations of applied pressure for reaching saturation and the problem of concentration polarization in pressure driven membrane operations might result in the further use of MD. In 2001 Curcio et al. [10], for the first time reported the currently known membrane crystallizers using direct-contact MD or osmotic membrane distillation (OMD). This study proved that MD was able to concentrate NaCl solution from below saturation to supersaturation and produce NaCl crystals. In the following years the membrane crystallizer concept was developed and has today proved its applications in wide range of fields such as in the chemical and pharmaceutical industry, desalination, wastewater treatment etc.

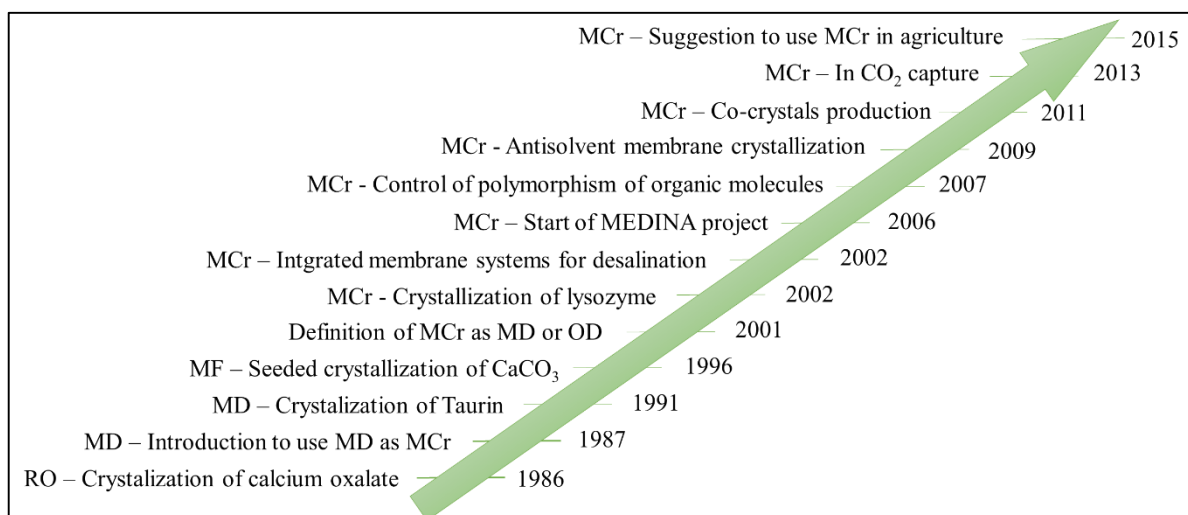


Figure 3.1: Timeline on the development of membrane crystallization.

The reason for the increasing popularity and usage of membrane crystallizer is basically due to the fact of the several advantages of MCr with respect to conventional crystallizers. High control of the crystallization process is required for a high quality product in terms of purity, polymorph, shape, narrow size distribution and desired size. Nevertheless, in conventional crystallization processes perfect control of these features are difficult to obtain. In MCr mass transfer through the membrane is used to reach saturation levels of the desirable salts to be crystallized. Membrane crystallization compared to conventional crystallization techniques has a well-controlled pathway of crystallization [10]. An

additional advantage of membrane crystallization is in the crystallization of macromolecular solutions in which altered polymorphs (thermodynamic and kinetic products) can be obtained by changing hydrodynamic conditions and degree of saturation [11]. In MCr homogeneous solutions are obtained whereas in conventional crystallizers, such as mixed-suspension mixed-product-removal crystallizer, control of evaporation rate is achieved by temperature and mixing regulation [12]. Nevertheless, perfect mixing and temperature gradient is difficult to obtain and conventional crystallizer is often difficult to model, causing the process to be based on several trials. The purity of the produced crystals in membrane crystallizer is superior to conventional methodologies. In fact Weckesser and König [13] have compared membrane based crystallization and vacuum evaporation crystallization for NaCl/KCl solution. They found that vacuum evaporation crystallization provides a higher growth rate compared to membrane crystallization, however the incorporation of potassium into NaCl crystals is depressed in membrane crystallization, thus membrane crystallization is suggested as a gentle crystallization process for which higher purity crystals can be obtained [13]. The two main steps of a crystallization process (evaporation and crystallization) are separated in MCr causing a well-controlled pathway of crystallization and uniform crystal product. Evaporation occurs inside the membrane module for the realization of saturation while crystal growth takes place in a crystallization tank. Thanks to the microporous membrane, evaporations occurs at the interface of each pore mouth leading to a uniform saturation gradient, hence the driving force towards crystallization is similar throughout the membrane module [10]. The uniformity of crystals is proved by low values of coefficient of variation (CV), a parameter describing distribution of the crystal size according to the mean. In MCr CV values as low as 15 % has been reported [14].

Several advantages associated with membrane crystallizers have made it widely studied in the field of desalination, industrial wastewater and in crystallization of organic molecules, which will be highlighted in the next section.

### 3.1 DESALINATION

Emerging membrane technologies (for instance forward osmosis, electrodialysis and membrane distillation integrated with crystallization) are being investigated to solve the brine disposal issues [15]. In the desalination industry, membrane distillation and membrane crystallization, in particular, can add a positive effect on the process by increasing the overall water production and recovering valuable salts from the brine thus approaching zero-liquid-discharge and the goals of process intensification strategy. In 2002, Drioli and co-workers [16] suggested for the first time membrane crystallizers for seawater desalination in an integrated approach with RO. In this study real seawater from the Tirrenian coast has first been treated by NF and RO followed by MCr treatment of the RO concentrate with production of NaCl [16]. The prospects of introducing MCr on RO brine is to increase the fresh water recovery factor from around 50 % to above 90% in combination with salts recovery. In the subsequent years of this first study, several research activities have been focalized on integrated membrane systems in desalination. In 2004, a MCr unit was applied on synthetic NF retentate. That resulted in recovery of NaCl and magnesium sulfate in form of Epsomite ( $\text{MgSO}_4 \cdot 7\text{H}_2\text{O}$ ) (Figure 3.2 a and b) [14]. In this study it was also proposed to separate  $\text{CaCO}_3$  from seawater by gas-liquid membrane contactor technology to avoid scaling (Figure 3.2c) [14].

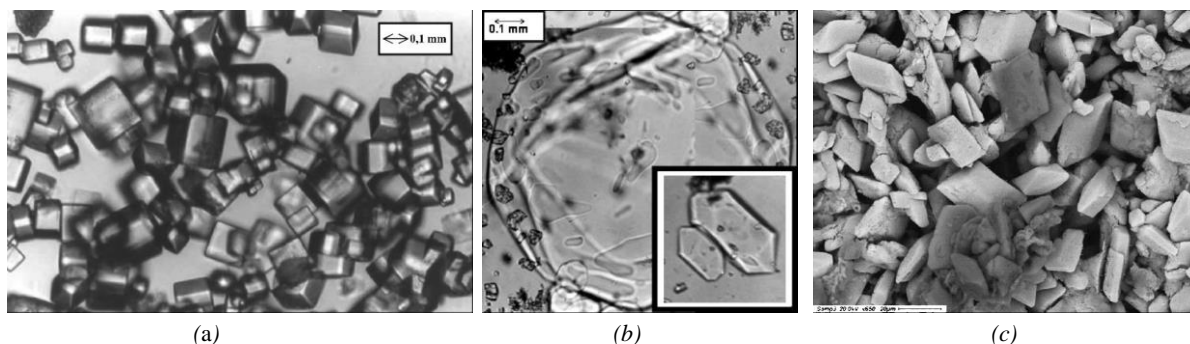


Figure 3.2: Crystal images obtained in the study by Drioli et al. [14]. (a) NaCl, (b)  $MgSO_4 \cdot 7H_2O$ , (c)  $CaCO_3$ .

The European funded project: *Membrane Based Desalination: An Integrated Approach (MEDINA)* was launched in 2006. This project focused on integrated membrane systems for improving the efficiency of desalination. Integrated systems consisting of MF, NF, RO with a membrane crystallizer coupled to NF and RO can achieve a water recovery factor as high as 92.4 %, thus approaching zero liquid discharge, total utilization of raw materials and low energy consumptions [17]. Integrated membrane systems are also very interesting from an economical point of view [18]–[20]. The exergetic efficiency is decreasing when MD or MCr are introduced, mainly due to the requirement of steam when operating the thermal processes with respect to electrical energy demand in pressure driven membrane operations [20]. Nevertheless, the water recovery factor increases significant (Table 3.1) with the introduction of MD and MCr from only 40 % in RO (flow sheet 1) to above 90 % for integrated operations (flow sheet 7). In general integrated membrane systems increase the water production cost. However, the numbers shown in Table 3.1 do not consider the economic advantage of selling the produced salts (flow sheet number 4-7). If the sale of  $CaCO_3$ ,  $MgSO_4 \cdot 7H_2O$  and NaCl is considered the water production cost can be negative (Table 3.2) [20]. These numbers indicate that the actual desalination process might no longer be targeted for water production but directed towards minerals production. In this case the desalinated fresh water can just be a by-product in mineral production. This is a very interesting case to minimize mineral depletion. Moreover, minerals can be also be produced from other industrial wastewater solutions.

Table 3.1: Economic analysis of various integrated membrane systems. [20]

Flow sheet	Configuration	Water recovery factor [%]	Water cost [\$/m <sup>3</sup> ]			
			Without energy recovery		With Pelton turbine	
			With thermal energy available:			
			No	Yes	No	Yes
1	RO	40.1	0.61		0.40	
2	NF-RO	52.0	0.47		0.40	
3	MF-NF-RO	49.2	0.46		0.39	
4	MF-NF(-MCr)-RO	71.6	0.68	0.55	0.63	0.51
5	MF-NF-RO(-MCr)	70.4	0.59	0.47	0.54	0.43
6	MF-NF(-MCr)-RO(-MD)	88.6	0.74	0.55	0.71	0.69
7	MF-NF(-MCr)-RO(-MCr)	92.8	0.73	0.54	0.51	0.51

Table 3.2: Water production cost of several integrated membrane systems when the sale of the produced salt is considered [20].

Flow sheet	Configuration	Water cost [\$/m <sup>3</sup> ]			
		Without energy recovery		With Pelton turbine	
		With thermal energy available:			
		No	Yes	No	Yes
4	MF-NF(-MCr)-RO	-0.40	-0.52	-0.44	-0.57
5	MF-NF-RO(-MCr)	0.077	-0.041	0.032	-0.086
6	MF-NF(-MCr)-RO(-MD)	-0.49	-0.68	-0.53	-0.71
7	MF-NF(-MCr)-RO(-MCr)	-0.13	-0.32	-0.16	-0.36

### 3.2 INDUSTRIAL WASTEWATER TREATMENT

Today, many industrial processes require post-treatment on their wastewaters due to more strict environmental regulations. The problem of industrial waste is the associated higher cost of post-treatment without any economic gain. Nevertheless, if waste could be turned into resources it might add several benefits to the industrial process. In this logic membrane crystallizers is very interesting since it is able to treat almost all types of feed waters, no concentration limits, it is able to produce fresh water which can be used elsewhere in the industry and it can also recover the valuable resources, which is present in the wastewaters.

Curcio et al. [21] recovered Na<sub>2</sub>SO<sub>4</sub> from simulated wastewater obtained in production of base raw materials (Ni-H) for special rechargeable batteries. The system consisted of NF and MCr in integrated membrane operations. At time of crystallization, NF and MCr system achieved an overall water recovery factor of 87 %. The produced crystals have been found to be of the anhydrous form (Thenardite) and of very high quality in terms of uniform crystal size with coefficient of variation as low as 23 % [21]. Less favorable results have been obtained in the first study by Tun et al. [22], who studied MD with Na<sub>2</sub>SO<sub>4</sub> and NaCl solutions near saturation. The authors achieved a promising flux of 20 l/m<sup>2</sup>h at feed temperatures of 60 °C and ΔT of 40 °C. However, they have also observed a drastically flux reduction due to extensive scaling on membrane surface [22]. These results indicate that sufficient care has not been taken to avoid scaling on membrane surface. In 2011, Tun and Groth [23], treated effluent from a SO<sub>2</sub> scrubber with MF-NF-MCr for water and Na<sub>2</sub>SO<sub>4</sub> production and energy recovery. In this study high purity (above 95 %) anhydrous Na<sub>2</sub>SO<sub>4</sub> crystals have been achieved. Moreover, also high quality fresh water has been produced with only 1.11 ppm of Na<sup>+</sup> and 2.82 ppm S<sup>-2</sup> in the distillate [23]. Sodium sulfate solutions can also be a by-product from SO<sub>2</sub> removal in flue gas. In the study by Li et al. [24] an integrated membrane system (RO and MCr) has been suggested for Na<sub>2</sub>SO<sub>4</sub> reclamation from these types of solutions. The membrane crystallization unit in this study has not been based on DCMD but instead on OMD using a draw solution of NaCl. The isothermal process of OMD has been carried out at 20 °C and for this reason the authors found, as different for the other studies, that sodium sulfate has been formed as Na<sub>2</sub>SO<sub>4</sub>·10H<sub>2</sub>O (Mirabilite) (Figure 3.3). Moreover, the feed solution has been contaminated by the NaCl draw solution, thus the crystals produced have also been contaminated by chloride ions [24]. As also stated by the authors the operative conditions influence the chloride contamination. To lower extent, produced Na<sub>2</sub>SO<sub>4</sub>·10H<sub>2</sub>O has also been contaminated with aluminum and magnesium ions. The contamination of Cl<sup>-</sup> might be solved by using DCMD unless Na<sub>2</sub>SO<sub>4</sub>·10H<sub>2</sub>O is the desired polymorphic form. The authors have also found preliminary results on how feed and permeate flow rates influence the incorporation of impurities into the crystal [24]. To increase the purity further optimized operative conditions might be required.

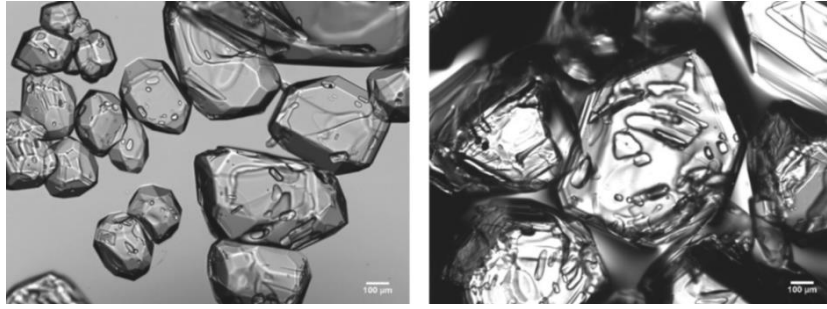


Figure 3.3:  $\text{Na}_2\text{SO}_4 \cdot 10\text{H}_2\text{O}$  crystals obtained in the study by Li et al. [24].

Recently, membrane crystallizers have also been suggested in  $\text{CO}_2$  capture [25]–[28]. Most common for  $\text{CO}_2$  capture is absorption such as amine-based. Also more environmentally friendly processes, such as reaction with alkaline solutions, and membrane technology have been investigated [25]. An example is the reaction with  $\text{NaOH}$  for production of  $\text{Na}_2\text{CO}_3$ . Luis et al. [27], have applied osmotic MCr to treat  $\text{Na}_2\text{CO}_3$  solutions using  $\text{NaCl}$  and  $\text{MgCl}_2$  solutions as draw agents. The authors have also recommended a draw solution at higher concentration than 150 mg/L based on an exergy analysis. The polymorphic structure obtained in this study is  $\text{Na}_2\text{CO}_3 \cdot 10\text{H}_2\text{O}$  [27]. Similarly in the studies by Ye et al. [25], [26], it has been found that  $\text{Na}_2\text{CO}_3 \cdot 10\text{H}_2\text{O}$  is produced by utilizing a OMD configuration with  $\text{NaCl}$  as draw solution. As a result of  $\text{NO}_x$  and  $\text{SO}_x$  in flue gasses, the influence of  $\text{NaNO}_3$  and  $\text{Na}_2\text{SO}_4$  on crystal habit has also been investigated. The authors have found that only  $\text{Na}_2\text{SO}_4$  has some impact on crystal morphology, whereas no impurities of  $\text{Na}_2\text{SO}_4$ ,  $\text{NaNO}_3$  or  $\text{NaCl}$  (from draw solution) have been observed within the crystals [25], [26]. Therefore, MCr is able to produce ultrapure  $\text{Na}_2\text{CO}_3 \cdot 10\text{H}_2\text{O}$  which can be a potential application in  $\text{CO}_2$  capture. Ye et al. [28] have also conducted similar experiments by utilizing dense membranes in FO and PRO mode. Similar results on polymorph and purity has been obtained. The authors have stated that a higher purity of sodium carbonate (>99.98%) can be obtained using this configuration with respect to their results obtained utilizing MCr [28]. Nevertheless, the results have to be seen in perspective to the results achieved in their previous study with the lowest purity given as 99.10 % [26]. Moreover, the main problem in both osmotic MCr and FO is the draw solution which should be re-concentrated for constant flux and more efficient draw solutions might be required. As previously mentioned, the loss of  $\text{Cl}^-$  from draw solution to feed might be solved by using DCMD.

Membrane based crystallization has also been suggested for the agricultural sector [29]–[31]. FO and MD have been applied for the recovery of phosphorus in the form of Struvite ( $\text{MgNH}_4\text{PO}_4 \cdot 6\text{H}_2\text{O}$ ) from anaerobically digested sludge [29]. In this study, FO is the crystallizing unit. The draw agent in this study is  $\text{MgCl}_2$  solution, which according to the authors are promoting struvite formation since the reverse salt flux increases the concentration of  $\text{Mg}^{2+}$  in the digested sludge. The MD unit served as re-concentrator of the draw solution. In case the MD process has directly been applied on the sludge severe organic fouling has been observed on the membrane surface and the trans-membrane flux decreases from 10 to 2  $\text{l/m}^2\text{h}$ . However, similar decrease has been observed during FO treatment and the authors stated that the fouling in FO is reversible and cleaning could be performed to restore some of the membrane performance. The authors have also added some magnesium to further promote the struvite crystallization. They have achieved a pure orthorhombic structure, with an average size of 40  $\mu\text{m}$  [29].



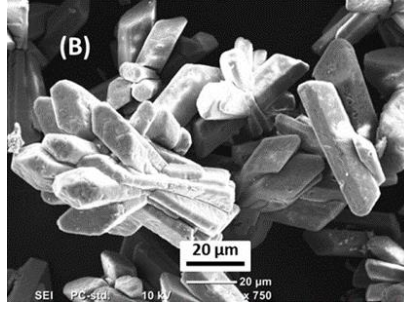


Figure 3.4: Struvite crystals obtained in the study by Xie et al. [29].

Another example of MCr in treatment of wastewater is for rare-earth wastewater and fertilizer plant wastewater, where high amount of ammonium salts are present. You et al. [30] have suggested MCr in VMD mode for recovery of ammonium salt. Two solutions of 20 %  $\text{NH}_4\text{Cl}$  and  $(\text{NH}_4)_2\text{SO}_4$  have been tested. Volatile ammonium has to be minimized by controlling pH in order to avoid it to move to permeate. In treatment of  $\text{NH}_4\text{Cl}$  solution, the authors have been able to maintain the total nitrogen low and stable in permeate whereas for  $(\text{NH}_4)_2\text{SO}_4$  it increased rapid after 400 min of operation. Total of  $125.7 \text{ kg/m}^3$  and  $58.4 \text{ kg/m}^3$  for  $\text{NH}_4\text{Cl}$  and  $(\text{NH}_4)_2\text{SO}_4$ , respectively, could be obtained for the highest saturation factor. It has been found that the crystal size decreases with increase in saturation and moreover, that  $\text{NH}_4\text{Cl}$  has dendritic structure and  $(\text{NH}_4)_2\text{SO}_4$  crystals is being lamellar (Figure 3.5) [30].

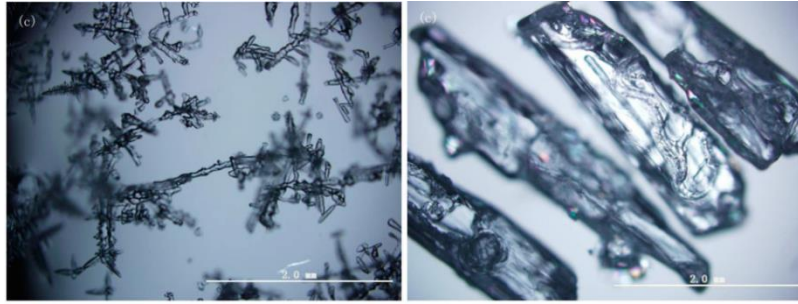


Figure 3.5: Ammonium salts obtained during MCr in VMD configuration, (a)  $\text{NH}_4\text{Cl}$  and (b)  $(\text{NH}_4)_2\text{SO}_4$  [30].

In membrane crystallization of inorganic salts, it is particular important to ensure appropriate control of scaling and other types of fouling. Especially as the concentration approaches saturation. Scaling is more prominent in pressure driven membrane operations caused by the higher convective flux, which endorse more likely saturation near membrane surface. Furthermore, in all membrane operations the membrane promotes heterogeneous secondary nucleation. Secondary nucleation occurs when the nuclei are formed on already existing surfaces of the crystallizing material. The nucleation can occur on the membrane surface due to decrease in the energetic barrier needed for stable nuclei to be formed [32]. The energetic barrier of heterogonous nucleation on a porous membrane can be estimated through Eq. 3.1 [33].

$$\frac{\Delta G_{het}^*}{\Delta G_{hom}^*} = \frac{1}{4} (2 + \cos\theta)(1 - \cos\theta)^2 \left[ 1 - \varepsilon \frac{(1 + \cos\theta)^2}{(1 - \cos\theta)^2} \right]^3 \quad (Eq. 3.1)$$

where  $\Delta G_{hom}^*$  is the homogenous nucleation,  $\theta$  is contact angle and  $\varepsilon$  is surface porosity. Both positive and negative aspects can occur due to heterogeneous nucleation, such as the positive of controlled growth on the surface for crystallization of macromolecules or the negative consequence of surface scaling. If scaling appears it can decline the process performance and also promote wetting of the membrane. Optimal operative conditions and adequate design of the system can minimize this phenomenon. Nevertheless, several studies have reported the negative aspects of scaling in membrane crystallization e.g. the ones described by Gryta [34], [35]. The author reported partial wetting of the

membrane and a rapid crystallization on the membrane surface in crystallization of NaCl after 138 h of experiment [34]. Despite the long duration of the carried out experiments, scaling might have been avoided by selecting better operative conditions [34]. The nature of the salt also influences the potential of scaling, if characterized by a positive or negative enthalpy of solution. Tun et al. [22] have investigated the deposition of salts on the membrane surface by utilizing a salt with positive temperature-solubility coefficient (NaCl) and a salt with negative temperature-solubility coefficient ( $\text{Na}_2\text{SO}_4$ ). Due to temperature polarization, the temperature near the membrane surface decreases compared to the bulk, causing a salt with negative solubility coefficient to crystallize in the bulk rather than on the membrane surface. For this reason, higher saturation degrees are achieved for  $\text{Na}_2\text{SO}_4$  compared to NaCl. The research activities carried out by Tun et al. [22] indicate that the control of temperature of the crystallizing solution is an crucial parameter for the process. However, the authors have described that after the feed attaining a critical level of concentration, the flux declined drastically and reaches zero, due to the deposits of salts on the membrane surface. Different procedures can be applied to avoid scaling on the membrane surface. The membrane modules can be placed vertical to incorporate the effect of gravity and let the crystals to flow to the feed tank instead of remaining in the module. A crystal recovery system can be used to separate the produced crystals from the mother liquid, hence lowering the risk of scaling [36], [37]. Not only long term performance, but also low salts solubility, can negatively influence the membrane performance due to scaling on the membrane surface. For example, in literature it can be found that, in the crystallization of NF/RO brine, calcium carbonates and sulfates can precipitate and cause scaling due to the extensive concentration [38]. This problem can be solved by removal of calcium with chemical treatment with  $\text{Na}_2\text{CO}_3$  [14], [36]. In fact with a crystal recovery system and removal of calcium the membrane crystallization unit is able to be in crystallization mode for more than nine hours without particular reduction in flux [36]. Moreover, fouling by organic substances can also occur on the membrane surface. Higher is organic concentration, inferior will be the membrane performance due to membrane pore blocking and decrease in heat transfer. A reduction of flux at 8 % in the beginning of RO brine treatment (30 % water recovery) and 13 % near to precipitation of NaCl for a natural seawater solution compared to a synthetic solution has been observed by Ji et al. [39]. Moreover, organics influence the produced crystals (for example, in the crystallization of NaCl in presence of humic acid, crystals exhibit small size, low growth rate and high coefficient of variation [36]).

The described examples of positive and negative aspects of membrane crystallizers show that membrane performance and crystal quality depend strongly upon the selected operative conditions. Similar trend is observed when membrane crystallizers are applied in protein crystallization. This is interesting, in particularly due to the higher value of the final product which can accelerate the commercialization of membrane crystallizers and, furthermore, the well-controllable nucleation and growth in MCr might be more competitive with respect to existing crystallizers.

### 3.3 CRYSTALLIZATION OF BIOMOLECULES

Crystallization of proteins and other macromolecules is important in chemical and pharmaceutical industry. In particular in separation and purification, in the study of the biological activity which is strongly related to the molecular structure of the biomolecule and for designing new drug molecules [40], [41]. In determination of crystal structure, by X-ray or neutron crystallography and nuclear magnetic resonance (NMR) spectroscopy, it is important to have adequate spatial arrangement [40]. In this regard membrane crystallizers are a promising technology. Some of the first proteins, which has been crystallized by means of MCr is hen egg-white lysozyme (Figure 3.6) with concentration gradient provided by NaCl and  $\text{MgCl}_2$  solutions as driving force [40]–[43]. These first studies highlight many of the advantages of MCr, such as highly defined structure, low induction times and controllable crystal

kinetics [42]. Simone et al. [44] and Zhang et al. [45] have studied the effect of precipitant agents in the crystallization of lysozyme. The former investigated interaction of cobalt and cobber ions on the crystallization process. The authors have reported that  $\text{Co}^{2+}$  coordination can lead to different morphologies, i.e. the standard shaped tetragonal form and never before observed a roof-like morphology. Using cobber as ligand, only one polymorph structure has been observed, but large crystal sizes up to 700–800  $\mu\text{m}$  have been achieved [44]. Zhang et al. [45] studied the effect of several precipitants and additives at different concentrations by evaluating trans-membrane flux, IR spectra, size distributions and induction time. The authors have found that the best crystals are obtained using NaCl and NaSCN. In case of the additives, the shorter induction times and larger crystals are obtained with glycerol, PEG4000 and PEG6000 [45].

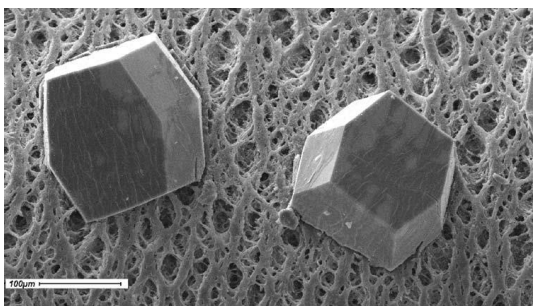


Figure 3.6: Hen egg-white lysozyme crystallization by means of MCr [42].

Another important parameter in crystallization is the polymorph structure. Even if the compound has the same chemical composition, polymorphs differ in bioavailability, solubility, dissolution rate, chemical stability, physical stability, melting point, color, filterability, density, flow behavior, and many other properties [46]. These factors are particularly important in the fabrication of drugs as different polymorphs can affect drug efficacy, bioavailability and safety [46]. Membrane crystallizers are able to tune different polymorph structures. This has been reported in several studies, which have proved that by changing operative conditions and eventually by the use of antisolvent crystallization, different polymorphic structures can be obtained as reported for  $\alpha$ - and  $\gamma$ -glycine (Figure 3.7) [11], [47], form I and II of paracetamol [48], tetragonal, orthorhombic and bipyramidal of lysozyme [49],  $\alpha$ - and  $\beta$  L-glutamic acid [50], and form A and B of L-histidine [51].

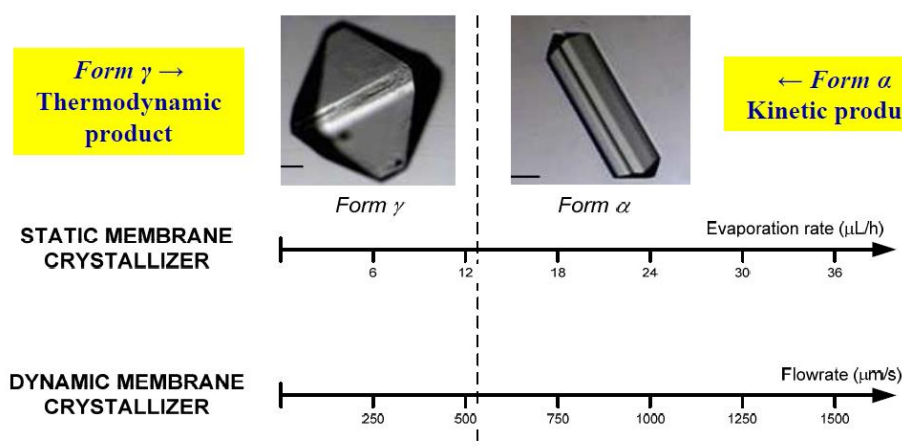


Figure 3.7: Tunable polymorph structure of Glycine by changing operative conditions in MCr [11].

Several other compounds have been found to be produced or recovered by means of membrane crystallizers. These includes fumaric acid recovered from MBr effluent used for the production of L-malic acid [52], Lyophilized bovine pancreas (BPT) and porcine pancreas (PPT) trypsin [53], [54]. Lysozyme (Figure 3.6) and trypsin (Figure 3.8) crystallization are excellent examples of the uniform crystal product and well-define morphology obtainable in MCr utilizing the surface of the membrane as heterogeneous support. The active pharmaceutical compound: 1-(5-bromo-fur-2-il)-2-bromo-2-nitroethane (G-1), has been recovered from wastewater in the configuration of osmotic membrane crystallizer [55]. L-asparagine monohydrate having up to two times more narrow size distribution compared to batch stirred crystallizers has been obtained in standalone membrane hollow fiber crystallizer [56]. Polymer-coated drug crystals have been produced by antisolvent crystallization using the drug Griseofulvin coated by a thin layer of the polymer Eudragit RL100 [57]. Recently, membranes with hydrogel layer have been fabricated for supported heterogeneous support of tailored protein crystallization [58]. The hydrogel layer allows to have controlled nano-architecture (mesh size) and different morphologies so that crystals appear at lower protein concentration and enhance diffraction features [58].

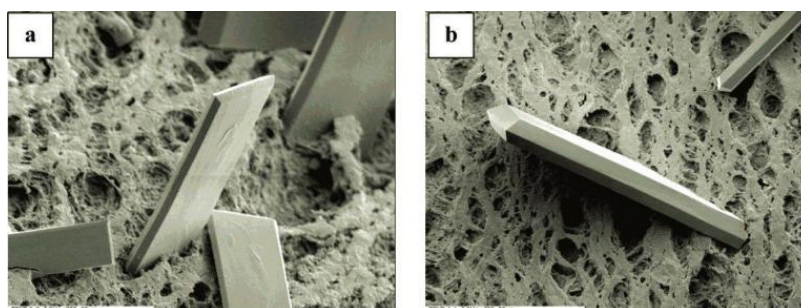


Figure 3.8: Trypsin crystallized on microporous membrane by means of MCr [53].

### 3.4 SUMMARY

Membrane crystallization is a new process, first suggested less than 30 years ago. Despite the young age membrane crystallization has continued to grow and mature and is today a very promising technology although the publication rate each year is not comparable with similar processes as membrane distillation. Furthermore, membrane crystallization is not yet fully commercialized. Nevertheless, membrane crystallization provides several advantages with respect to conventional methodologies including controlled nucleation and crystal growth, uniform crystal size distribution, tunable polymorph selection etc. The results achieved in previous studies on MCr proves that a wide range of applications are possible ranging from inorganic salts in desalination and wastewater treatment to crystallization of biomolecules. The easy scale-up and down of membrane operations, in particular, is of great importance. For instance in the crystallization of single molecules for diffraction analysis, the equipment should be small scale and still be able to control the process. The opposite applies to applications in desalination where e.g. a single plant might need to process 500,000 m<sup>3</sup>/d of brine and this is surely to increase in future. This provides another positive aspect to membrane crystallizers, i.e. for the recovery of rare and expensive minerals from brine or other wastewater sources as a contribution to the existing mining industry. However, membrane development, flux enhancement and more focus on targeted salts with respect to operative conditions is required to enable the fully success of membrane crystallization. The following chapters will seek to address positive and negative features on membrane requirements and operational conditions for several feed solutions.

## REFERENCES

- [1] R. Azoury, J. Garside, and W. G. Robertson, "Crystallization processes using reverse osmosis," *J. Cryst. Growth*, vol. 79, pp. 654–657, 1986.
- [2] Y. Wu, Y. Kong, J. Liu, J. Zhang, and J. Xu, "An experimental study on membrane distillation-crystallization for treating waste water in taurine production," *Desalination*, vol. 80, pp. 235–242, 1991.
- [3] J. T. M. Sluys, D. Verdoes, and J. H. Hanemaaijer, "Water treatment in a Membrane-Assisted Crystallizer (MAC)," *Desalination*, vol. 104, no. 1–2, pp. 135–139, Apr. 1996.
- [4] J. H. Henemaaijer and D. Verdoes, "Method for removing at least one constituent from a solution," Patent No EP 0669898 A11995.
- [5] R. Lakerveld, J. Kuhn, H. J. M. Kramer, P. J. Jansens, and J. Grievink, "Membrane assisted crystallization using reverse osmosis: Influence of solubility characteristics on experimental application and energy saving potential," *Chem. Eng. Sci.*, vol. 65, no. 9, pp. 2689–2699, May 2010.
- [6] J. Kuhn, R. Lakerveld, H. J. M. Kramer, J. Grievink, and P. J. Jansens, "Characterization and Dynamic Optimization of Membrane-Assisted Crystallization of Adipic Acid," *Ind. Eng. Chem. Res.*, vol. 48, no. 11, pp. 5360–5369, Jun. 2009.
- [7] L.-F. Liu, L.-L. Yang, K.-Y. Jin, D.-Q. Xu, and C.-J. Gao, "Recovery of l-tryptophan from crystallization wastewater by combined membrane process," *Sep. Purif. Technol.*, vol. 66, no. 3, pp. 443–449, May 2009.
- [8] B. Tang, G. Yu, J. Fang, and T. Shi, "Recovery of high-purity silver directly from dilute effluents by an emulsion liquid membrane-crystallization process," *J. Hazard. Mater.*, vol. 177, no. 1–3, pp. 377–83, May 2010.
- [9] J. Campbell, L. G. Peeva, and A. G. Livingston, "Controlling Crystallization via Organic Solvent Nano filtration : The Influence of Flux on Griseofulvin Crystallization," *Crystal growth and design* vol. 14, pp. 2192–2200, 2014.
- [10] E. Curcio, A. Criscuoli, and E. Drioli, "Membrane Crystallizers," *Ind. Eng. Chem. Res.*, vol. 40, pp. 2679–2684, 2001.
- [11] G. Di Profio, S. Tucci, E. Curcio, and E. Drioli, "Selective Glycine Polymorph Crystallization by Using Microporous Membranes," *Cryst. Growth Des.*, vol. 7, pp. 526–530, 2007.
- [12] R. H. Perry and D. Green, *Perry's chemical engineers' handbook*. McGraw Hill Book CO, 1987.
- [13] D. Weckesser and a. König, "Particle Shape and Purity in Membrane Based Crystallization," *Chem. Eng. Technol.*, vol. 31, no. 1, pp. 157–162, Jan. 2008.
- [14] E. Drioli, E. Curcio, A. Criscuoli, and G. Di Profio, "Integrated system for recovery of CaCO<sub>3</sub>, NaCl and MgSO<sub>4</sub>·7H<sub>2</sub>O from nanofiltration retentate," *J. Memb. Sci.*, vol. 239, no. 1, pp. 27–38, Aug. 2004.
- [15] a Pérez-González, a M. Urriaga, R. Ibáñez, and I. Ortiz, "State of the art and review on the treatment technologies of water reverse osmosis concentrates," *Water Res.*, vol. 46, no. 2, pp. 267–83, Feb. 2012.
- [16] E. Drioli, A. Criscuoli, and E. Curcio, "Integrated membrane operations for seawater desalination," *Desalination*, vol. 147, pp. 77–81, 2002.
- [17] E. Drioli, A. Criscuoli, and F. Macedonio, Eds., *Membrane Based Desalination: An Integrated Approach (Medina) (European Water Research)*. IWA Publishing, London, UK, 2011.
- [18] F. Macedonio, G. Di Profio, E. Curcio, and E. Drioli, "Integrated membrane systems for seawater desalination," *Desalination*, vol. 200, no. 1–3, pp. 612–614, Nov. 2006.

- [19] E. Drioli, E. Curcio, G. Di Profio, F. Macedonio, and a. Criscuoli, “Integrating Membrane Contactors Technology and Pressure-Driven Membrane Operations for Seawater Desalination,” *Chem. Eng. Res. Des.*, vol. 84, no. 3, pp. 209–220, Mar. 2006.
- [20] F. Macedonio, E. Curcio, and E. Drioli, “Integrated membrane systems for seawater desalination: energetic and exergetic analysis, economic evaluation, experimental study,” *Desalination*, vol. 203, no. May 2006, pp. 260–276, 2007.
- [21] E. Curcio, X. Ji, A. M. Quazi, S. Barghi, G. Di Profio, E. Fontananova, T. Macleod, and E. Drioli, “Hybrid nanofiltration–membrane crystallization system for the treatment of sulfate wastes,” *J. Memb. Sci.*, vol. 360, no. 1–2, pp. 493–498, Sep. 2010.
- [22] C. M. Tun, A. G. Fane, J. T. Matheickal, and R. Sheikholeslami, “Membrane distillation crystallization of concentrated salts—flux and crystal formation,” *J. Memb. Sci.*, vol. 257, no. 1–2, pp. 144–155, Jul. 2005.
- [23] C. M. Tun and A. M. Groth, “Sustainable integrated membrane contactor process for water reclamation, sodium sulfate salt and energy recovery from industrial effluent,” *Desalination*, vol. 283, pp. 187–192, Dec. 2011.
- [24] W. Li, B. Van der Bruggen, and P. Luis, “Integration of reverse osmosis and membrane crystallization for sodium sulphate recovery,” *Chem. Eng. Process. Process Intensif.*, vol. 85, pp. 57–68, Nov. 2014.
- [25] W. Ye, J. Lin, J. Shen, P. Luis, and B. Van Der Bruggen, “Membrane Crystallization of Sodium Carbonate for Carbon Dioxide Recovery: Effect of Impurities on the Crystal Morphology,” *Crystal Growth and design*, vol. 13, 2362-2372, 2013.
- [26] W. Ye, J. Lin, P. Luis, and B. Van Der Bruggen, “Carbon Dioxide Recovery by Membrane Assisted Crystallization,” *International Scholarly and Scientific Research and innovation*, vol. 7, no. 7, pp. 1507–1509, 2013.
- [27] P. Luis, D. Van Aubel, and B. Van der Bruggen, “Technical viability and exergy analysis of membrane crystallization: Closing the loop of CO<sub>2</sub> sequestration,” *Int. J. Greenh. Gas Control*, vol. 12, pp. 450–459, Jan. 2013.
- [28] W. Ye, J. Wu, F. Ye, H. Zeng, A. T. K. Tran, J. Lin, P. Luis, and B. Van der Bruggen, “Potential of Osmotic Membrane Crystallization Using Dense Membranes for Na<sub>2</sub>CO<sub>3</sub> Production in a CO<sub>2</sub> Capture Scenario,” *Cryst. Growth Des.*, vol. 15, no. 2, pp. 695–705, Feb. 2015.
- [29] M. Xie, L. D. Nghiem, W. E. Price, and M. Elimelech, “Toward Resource Recovery from Wastewater: Extraction of Phosphorus from Digested Sludge Using a Hybrid Forward Osmosis – Membrane Distillation Process,” *Environ. Sci. Technol. Lett.*, vol. 1, pp. 191–195, 2014.
- [30] W.-T. You, Z.-L. Xu, Z.-Q. Dong, and M. Zhang, “Vacuum membrane distillation–crystallization process of high ammonium salt solutions,” *Desalin. Water Treat.*, vol. 55, no. 2, pp. 368–380, Jun. 2014.
- [31] C. A. Quist-Jensen, F. Macedonio, and E. Drioli, “Membrane technology for water production in agriculture: Desalination and wastewater reuse,” *Desalination*, vol. 364, pp. 17–32, May 2015.
- [32] E. Drioli, E. Curcio, and G. di Profio, “State of the Art and Recent Progresses in Membrane Contactors,” *Chem. Eng. Res. Des.*, vol. 83, no. 3, pp. 223–233, Mar. 2005.
- [33] E. Curcio, E. Fontananova, G. Di Profio, and E. Drioli, “Influence of the Structural Properties of Poly(vinylidene fluoride) Membranes on the Heterogeneous Nucleation Rate of Protein Crystals,” *J. Phys. Chem. B*, vol. 4, no. 1, pp. 12438–12445, 2006.
- [34] M. Gryta, “CONCENTRATION OF NaCl SOLUTION BY MEMBRANE DISTILLATION INTEGRATED WITH CRYSTALLIZATION,” *Sep. Sci. Technol.*, vol. 37, pp. 3535–3558, Feb. 2002.
- [35] M. Gryta, “Direct Contact Membrane Distillation with Crystallization Applied to NaCl Solutions,” in *Chemical Paper*, 2002, vol. 56, no. May 2001, pp. 14–19.



- [36] F. Macedonio and E. Drioli, "Hydrophobic membranes for salts recovery from desalination plants," *Desalin. Water Treat.*, vol. 18, pp. 224–234, 2010.
- [37] F. Macedonio, L. Katzir, N. Geisma, S. Simone, E. Drioli, and J. Gilron, "Wind-Aided Intensified eVaporation (WAIIV) and Membrane Crystallizer (MCR) integrated brackish water desalination process: Advantages and drawbacks," *Desalination*, vol. 273, no. 1, pp. 127–135, Jun. 2011.
- [38] F. Macedonio, C. a. Quist-Jensen, O. Al-Harbi, H. Alromaih, S. a. Al-Jlil, F. Al Shabouna, and E. Drioli, "Thermodynamic modeling of brine and its use in membrane crystallizer," *Desalination*, vol. 323, pp. 83–92, Aug. 2013.
- [39] X. Ji, E. Curcio, S. Al Obaidani, G. Di Profio, E. Fontananova, and E. Drioli, "Membrane distillation-crystallization of seawater reverse osmosis brines," *Sep. Purif. Technol.*, vol. 71, no. 1, pp. 76–82, Jan. 2010.
- [40] E. Curcio, G. Di Profio, and E. Drioli, "Membrane crystallization of macromolecular solutions," *Desalination*, vol. 145, pp. 173–177, 2002.
- [41] E. Curcio, G. Di Profio, and E. Drioli, "A new membrane-based crystallization technique : tests on lysozyme," *Journal of crystal growth*, vol. 247, pp. 166–176, 2003.
- [42] G. Di Profio, E. Curcio, A. Cassetta, D. Lamba, and E. Drioli, "Membrane crystallization of lysozyme: kinetic aspects," *J. Cryst. Growth*, vol. 257, pp. 359–369, Oct. 2003.
- [43] E. Curcio, S. Simone, G. Di, E. Drioli, A. Cassetta, and D. Lamba, "Membrane crystallization of lysozyme under forced solution flow," *Journal of membrane science*, vol. 257, pp. 134–143, 2005.
- [44] S. Simone, E. Curcio, G. Di Profio, M. Ferraroni, and E. Drioli, "Polymeric hydrophobic membranes as a tool to control polymorphism and protein–ligand interactions," *J. Memb. Sci.*, vol. 283, no. 1–2, pp. 123–132, Oct. 2006.
- [45] X. Zhang, M. S. El-Bourawi, K. Wei, F. Tao, and R. Ma, "Precipitants and additives for membrane crystallization of lysozyme.," *Biotechnol. J.*, vol. 1, no. 11, pp. 1302–11, Nov. 2006.
- [46] A. Llinàs and J. M. Goodman, "Polymorph control: past, present and future.," *Drug Discov. Today*, vol. 13, no. 5–6, pp. 198–210, Mar. 2008.
- [47] G. D. I. Profio, C. Stabile, A. Caridi, E. Curcio, and E. Drioli, "Antisolvent Membrane Crystallization of Pharmaceutical Compounds," *J. Pharm. Sci.*, vol. 98, pp. 4902–4913, 2009.
- [48] G. Di Profio, S. Tucci, E. Curcio, and E. Drioli, "Controlling Polymorphism with Membrane-Based Crystallizers : Application to Form I and II of Paracetamol," *Chem. Mater.*, vol. 19, pp. 2386–2388, 2007.
- [49] X. Zhang, P. Zhang, K. Wei, Y. Wang, and R. Ma, "The study of continuous membrane crystallization on lysozyme," *Desalination*, vol. 219, no. 1–3, pp. 101–117, Jan. 2008.
- [50] G. Di Profio, E. Curcio, S. Ferraro, C. Stabile, and E. Drioli, "Effect of Supersaturation Control and Heterogeneous Nucleation on Porous Membrane Surfaces in the Crystallization of L - Glutamic Acid Polymorphs," *Cryst. Growth Des.*, vol. 9, pp. 2179–2186, 2009.
- [51] G. Di Profio, A. Caridi, R. Caliendo, A. Guagliardi, E. Curcio, and E. Drioli, "Fine Dosage of Antisolvent in the Crystallization of l -Histidine: Effect on Polymorphism," *Cryst. Growth Des.*, vol. 10, no. 1, pp. 449–455, Jan. 2010.
- [52] E. Curcio, G. Di Profio, and E. Drioli, "Recovery of fumaric acid by membrane crystallization in the production of L -malic acid," *Sep. Purif. Technol.*, vol. 33, pp. 63–73, 2003.
- [53] G. Di Profio, G. Perrone, E. Curcio, A. Cassetta, D. Lamba, and E. Drioli, "Preparation of Enzyme Crystals with Tunable Morphology in Membrane Crystallizers," *Ind. Eng. Chem. Res.* vol 44, pp. 10005–10012, 2005.
- [54] G. Di Profio, E. Curcio, and E. Drioli, "Trypsin crystallization by membrane-based techniques.," *J. Struct. Biol.*, vol. 150, no. 1, pp. 41–9, Apr. 2005.

- [55] M. Brito Martínez, N. Jullok, Z. Rodríguez Negrín, B. Van der Bruggen, and P. Luis, “Membrane crystallization for the recovery of a pharmaceutical compound from waste streams,” *Chem. Eng. Res. Des.*, vol. 92, no. 2, pp. 264–272, Feb. 2014.
- [56] D. M. Zarkadas and K. K. Sirkar, “Antisolvent crystallization in porous hollow fiber devices,” *Chem. Eng. Sci.*, vol. 61, no. 15, pp. 5030–5048, Aug. 2006.
- [57] D. Chen, D. Singh, K. K. Sirkar, and R. Pfeffer, “Continuous synthesis of polymer-coated drug particles by porous hollow fiber membrane-based antisolvent crystallization.,” *Langmuir*, vol. 31, no. 1, pp. 432–41, Jan. 2015.
- [58] G. Di Profio, M. Polino, F. P. Nicoletta, B. D. Belviso, R. Caliandro, E. Fontananova, G. De Filpo, E. Curcio, and E. Drioli, “Tailored Hydrogel Membranes for Efficient Protein Crystallization,” *Adv. Funct. Mater.*, vol. 24, no. 11, pp. 1582–1590, Mar. 2014.





---

# CHAPTER 4:

## MEMBRANE FEATURES FOR TREATMENT OF CONCENTRATED SOLUTIONS

---

### 4.1 INTRODUCTION

Membrane properties, such as hydrophobicity, porosity and pore size are of great importance in the performance of membrane distillation. For commercialization of membrane distillation and crystallization, appropriate membranes specifically developed for these applications are of great importance. The commercial membranes typically used in membrane distillation and membrane crystallization are normally fabricated for pressure-driven filtration processes (in particular for microfiltration) rather than for concentration/temperature-driven processes [1]. However, mass and heat transfer in MD and MCr are different from transport mechanism found in pressure driven membrane operations. Therefore, membranes have to be developed taking into consideration the specific mechanism of MD/MCr. In current chapter, a detail description of mass and heat transfers in MD and MCr are described. The trans-membrane flux ( $J$ ) in MD can be expressed by a simple empirical correlation:

$$J = B \cdot \Delta P \quad (\text{Eq. 4.1})$$

The membrane-based parameter,  $B$ , is a function of membrane properties (pore size, thickness, porosity and tortuosity), operative temperatures and the properties of the vapor transported across the membrane (molecular weight and diffusivity). The vapor pressure difference between feed and permeate side ( $\Delta P$ ) can be described through the Antoine equation for the DCMD configuration.

$$P_{H_2O} = \left[ A - \frac{B}{C + T} \right] \quad (\text{Eq. 4.2})$$

$$P_{feed} = \alpha_{H_2O} \cdot P_{H_2O}(T) \quad (\text{Eq. 4.3})$$

$$P_{permeate} = P_{H_2O}(T) \quad (\text{Eq. 4.4})$$

$P_{H_2O}$  is the vapor pressure of pure water in [Pa] and  $A$ ,  $B$  and  $C$  are constants, which depends on the component. For water the constants are  $A = 23.1965$ ,  $B = 3816.44$ ,  $C = -46.13$ . [22].  $T$  is the temperature in Kelvin [K].

Water activity coefficients ( $\alpha_{H_2O}$ ) can be estimated through different equations and different software are also available for water activity estimation including MINEQL, MINTEQ and PHREEQC. MINEQL uses the Debye-Hückel law (Eq. 4.5), nevertheless this model can only be used for diluted solutions and therefore not applicable for modeling of highly concentrated brines, such as SWRO brine.

$$\log(\gamma) = -|Z_M Z_X| A I^{1/2} \quad (\text{Eq. 4.5})$$

$\gamma$  is the activity coefficient,  $z$  is the charge number for ion  $M$  and  $X$ ,  $A$  is a constant depending on the solution and  $I$  is the ionic strength of the solution [27]. MINTEQ is also not appropriate for high concentrated solutions. In PHREEQC multiple databases can be selected, especially a database in which the Pitzer approach can be used to estimate the activity coefficient [28]. The Pitzer approach, in contrast to Debye-Hückel, can be used for highly concentrated solutions, due to a long range term between the

ions and a short range term between solute species [29]. The activity coefficient for the Pitzer approach is estimated by Eq. 4.6 - Eq. 4.9 for a 1:1 electrolyte [30].

$$\ln(\gamma) = |Z_M Z_X| f^\gamma + m \left( \frac{2v_M v_X}{v} \right) B_{MX}^\gamma + m^2 \left( \frac{2(v_M v_X)}{v} \right) C_{MX}^\gamma \quad (\text{Eq. 4.6})$$

$$f^\gamma = -A \left[ \frac{I^{1/2}}{1 + bI^{1/2}} + \frac{2}{b} \ln(1 + bI^{1/2}) \right] \quad (\text{Eq. 4.7})$$

$$B_{MX}^\gamma = 2\beta_{MX}^{(0)} + \frac{2\beta_{MX}^{(1)}}{\alpha^2 I} \left[ 1 - e^{-\alpha I^{1/2}} - (1/2)\alpha^2 I \right] \quad (\text{Eq. 4.8})$$

$$C_{MX}^\gamma = (3/2)C_{MX}^\phi \quad (\text{Eq. 4.9})$$

$m$  is the molality,  $v_M$  and  $v_X$  are the moles of ion  $M$  and  $X$ , respectively and  $v_M + v_X = v$ . As seen in Eq. 4.6, the term  $|Z_M Z_X| f^\gamma$  is similar to the Debye-Hückel term in Eq. 4.5.  $B_{MX}^\gamma$  and  $C_{MX}^\gamma$  are second and third virial coefficients accounting for the deviation from the Debye-Hückel equation as an interaction between pairs and triplets of ions, respectively [30]. The third virial coefficient is often assumed to be independent of ionic strength and can be overlooked if the three ions in the triplet have the same charge [31].  $\beta^{(0)}$ ,  $\beta^{(1)}$  and  $C^{(\phi)}$  is interaction constants between  $M$  and  $X$  ions available for large variety of salts e.g. in publications by Pitzer and Hajbi et al. and others [29]–[32].  $b$  and  $\alpha$  are constants depending on the solutes. For a 2:2 electrolyte solution an additional term ( $\beta_{MX}^{(2)}$ ) is added in the second virial coefficient [32]. However, for the approach of estimation of activity coefficients for seawater and brine a model for pure electrolytes is not applicable, therefore two additional parameters have been added to the Pitzer model to account for mixing of electrolytes. The parameters are accounting for interactions between cation-cation (between two different cations) and cation-cation-anion, (between two different cations and an anion) [31]. The Pitzer equations have been validated for osmotic and activity coefficients up to ionic strengths equal to 6 M [31]. Harvie and Weare [33] have tested the Pitzer model for a multicomponent seawater system, consisting of  $\text{Na}^+$ ,  $\text{K}^+$ ,  $\text{Mg}^{2+}$ ,  $\text{Ca}^{2+}$ ,  $\text{Cl}^-$ ,  $\text{SO}_4^{2-}$  and found that the Pitzer approach shows good agreement for this particular system. Hajbi et al. [29] investigated evaporation of reverse osmosis brine, including an implementation of the Pitzer approach to experimental data. The authors presented good agreements between the theoretical and experimental studies and found that halite, glauberite, anhydrite, gypsum, epsomite and hexahydrate are the salts that precipitated with discontinuous evaporation from the composition considered. The Pitzer approach, through the PHREEQC software, has been used in current work to model the vapor pressure of various feed solution, which as mentioned previously, is the driving force in membrane distillation. In membrane distillation the hydrophobic microporous membrane entails only transport of volatile components through the membrane and thereby acts solely as a contactor between two interfaces and not as a separation unit as in pressure driven membrane operations. Wetting of the membrane pores is avoided by maintaining the pressure below the liquid entry pressure ( $LEP$ ) (Eq. 4.10).

$$LEP = -\frac{2\Theta\gamma\cos\theta}{r} \quad (\text{Eq. 4.10})$$

where  $\Theta$  is a geometric factor, determined by pore structure and is equal to 1 for cylindrical pores.  $\gamma$  is the surface tension,  $\theta$  is the liquid-solid contact angle and  $r$  is the largest pore radius [22], [34]. The liquid entry pressure is reduced if surfactants or detergents are present due to reduction of surface tension [22], [34]. When the membrane is wetted, it is not possible to restore the un-wetted conditions by decreasing the pressure below the liquid entry pressure [35]. Contact angle ( $\theta$ ) can be estimated through

the Young's equation (Eq. 4.11) based on a smooth and homogenous surface. However, to predict contact angle on porous membranes ( $\theta^*$ ), Eq. 4.12 should be taken into account [36].

$$\gamma_L \cos \theta = \gamma_S - \gamma_{SL} \quad (\text{Eq. 4.11})$$

$$\cos \theta^* = f_1 \cos \theta - f_2 \quad (\text{Eq. 4.12})$$

where  $\gamma_L$ ,  $\gamma_S$  and  $\gamma_{SL}$  are the surface tension for liquid, the surface energy of the polymer, and the solid-liquid surface tension, respectively.  $f_1$  and  $f_2$  are the fractions of liquid-solid and liquid-air surfaces, respectively.

Heat transfer in membrane distillation occurs by heat transported through the boundary layer in the feed solution and through the membrane by two mechanisms: heat conduction through the membrane material and latent heat of vaporization associated with vapors (Figure 4.1). Heat on the permeate side is transferred from the membrane surface to the bulk through the boundary layer. The boundary layer heat transfer resistance is a crucial step in membrane distillation, termed temperature polarization. A temperature polarization coefficient (TPC) is defined as Eq. 4.13 and is in generally used to quantify the boundary layer resistances. TPC is often used as a measure of heat transfer efficiency of the MD process, and if it is approaching 1, the design of the MD process is improving [37].

$$TPC = \frac{T_f^m - T_p^m}{T_f - T_p} \quad (\text{Eq. 4.13})$$

Correspondingly to the heat transfer, the mass transfer through the boundary layer on both sides involves concentration polarization. However, concentration polarization contributes less to overall resistance to mass transfer than thermal polarization due to relative low flux and thermal nature of the process [23]. Similar to the heat transfer, the mass transfer resistance is dependent upon the boundary layers resistances and the resistance offered by the membrane. When pure water is used as the condensing fluid, the resistances to mass transfer on permeate side can be omitted. Knudsen diffusion (collision of molecule with the membrane wall), molecular diffusion (collision between molecules) or viscous flow are the resistance influencing mass transfer through the membrane in DCMD [37]–[39] (Figure 4.1).

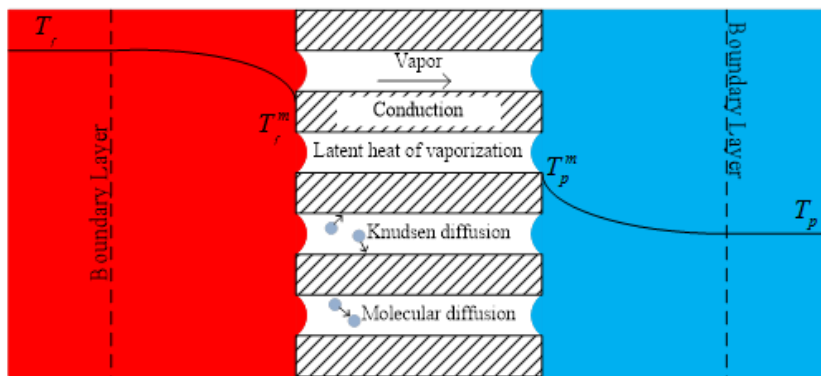


Figure 4.1: Membrane distillation concept with heat and mass transfer resistance.

To meet the requirements of membranes and by taking into account the transport mechanisms in MD and MCr, researchers have been trying to modify or design new membranes, in recent years, specifically for MD applications. Khayet [2] presents 10 requirements which have to be fulfilled in order to prepare the best suitable membrane for MD applications [2]: 1) The membrane must be hydrophobic and porous; 2) Appropriate pore size and pore size distribution are required. Large pore size prompts a high mass

transfer, however with a higher probability for wetting due to decrease in the liquid entry pressure; 3) The tortuosity factor should be small; 4) High overall porosity; 5) Low thickness of the hydrophobic layer is desirable in order to decrease mass transfer resistance. However, in this case high heat losses takes places, therefore multi-layer membrane might be preferable in order to obtain overall large thickness and small membrane resistance; 6) Low thermal conductivity of the membrane material is necessary to prevent heat losses (according to Al-Obaidani increase in thermal conductivity from 0.05 to 0.5 W/mK reduces the flux 26 % [27]); 7) High fouling resistance, 8) High thermal stability; 9) High chemical resistance and 10) Long-term stability in terms of steady performance is essential [2].

To meet membrane requirements, the objective of this study is to evaluate the performance of membrane distillation and membrane crystallization using various types of membrane characteristics to discover the most appropriate membrane structures. Each membrane type is characterized in terms of flux, permeate quality, stability towards wetting and crystal quality, including middle diameter, deviation from the mean crystal size and crystal growth rate, which will be linked to the specifically membrane features, such as pore size and porosity. Membrane material and specific features are important for the performance both in MD and MCr. Membrane hydrophobicity is vital for the MD and MCr process and in particular materials such as poly(vinylidene fluoride) (PVDF), polypropylene (PP) and polytetrafluoroethylene (PTFE) are used in MD. In general fluoropolymers have low surface tension, high thermal stability and improved chemical resistance making them sufficient for membrane operations [3]. The hydrophobicity of PVDF is not as high as PP or PTFE, but PVDF has the advantage that it can be easily dissolved in common solvents offering easy processing [4]. Moreover, other studies focus on preparing PVDF membranes utilizing green solvents, which are an advantages for the overall sustainability of the MD and MCr process [5].

## 4.2 MATERIALS AND METHODS

### 4.2.1 MEMBRANE CHARACTERISTICS

Various lab-made PVDF membranes have been tested in membrane distillation and membrane crystallization. The membrane preparation procedure can be found elsewhere [6]. Table 4.1 reports the physical parameters for different kind of membranes used.

*Table 4.1: Characteristics of the prepared membranes.*

Fiber type	O.D. [mm]	I.D. [mm]	Thickness [mm]	Pore size [ $\mu\text{m}$ ]	Porosity
M1	1.75	0.94	0.40	0.43	80.77
M3	1.60	1.15	0.23	0.52	83.39
M4	1.78	1.40	0.19	0.29	65.44

Membrane type M1 is a symmetric sponge-like membrane. However, M1 contains some macrovoids in the outer layer of structure (Figure 4.2). M3 is an asymmetric membrane with a sponge type arrangement in the outer structure, with thickness of 0.055 mm, and inside a finger-like layer (Figure 4.3). M4 have a symmetric sponge structure and is the membrane with the smallest thickness used in the conducted experiments (Figure 4.4). Three membrane fibers have been assembled in small glass modules with length of 17 cm.

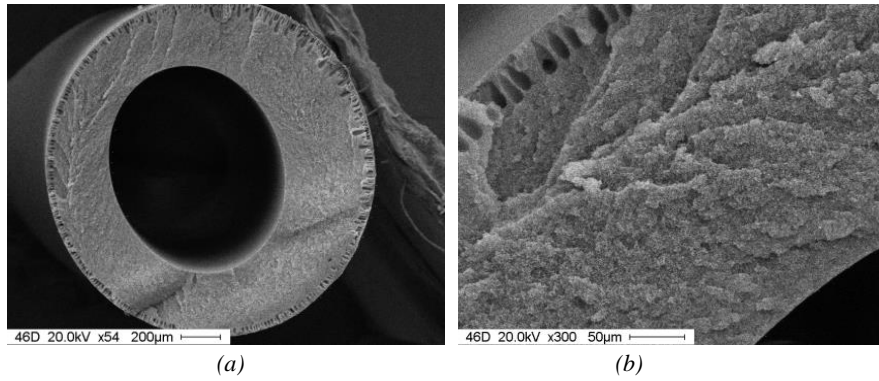


Figure 4.2: SEM images of membrane M1. (a) Cross section (54x). (b) Enlarged cross section (300x).

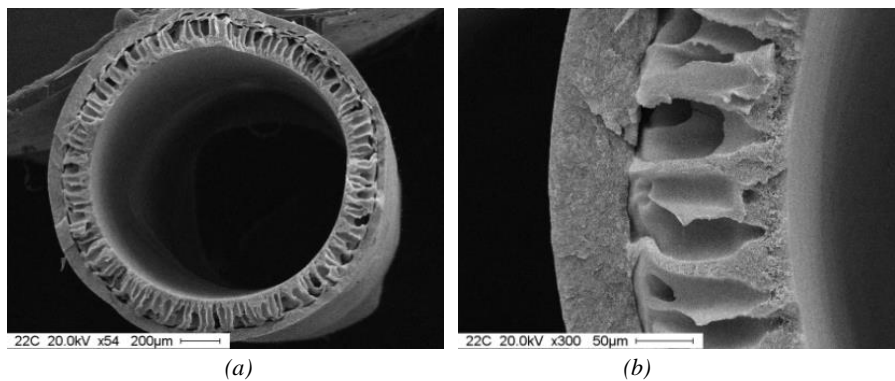


Figure 4.3: SEM images of M3. (a) Cross section (54x). (b) Enlarged cross section (300x).

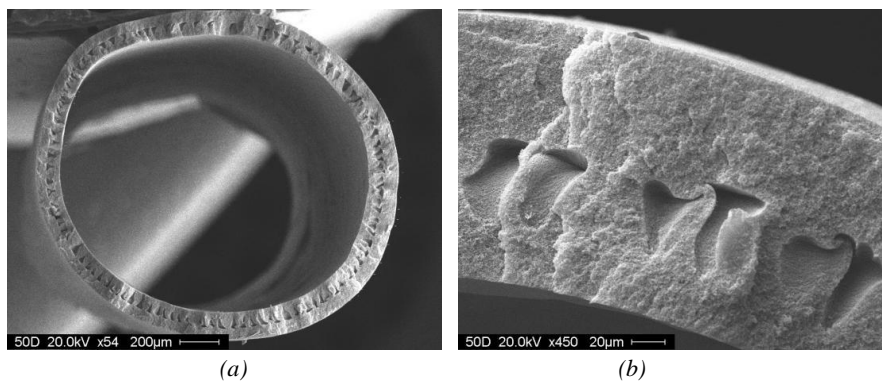


Figure 4.4: SEM images of M4. (a) Cross section (54x). (b) Enlarged cross section (450x).

#### 4.2.2 EXPERIMENTAL SETUP

Direct-contact membrane distillation (DCMD) and membrane crystallization (MCR) have been carried out on a small lab-scale plant, built to fit the membrane modules. The plant is shown in Figure 4.5 and consists of a 500 ml feed tank immersed in a heating bath to maintain the required temperature. The flux is calculated by measuring the increment in volume by using a 250 ml graduated cylinder immersed in a cooling bath. The flow rate is obtained by two peristaltic pumps and inlet temperatures are measured with thermocouples on retentate and permeate sides. DCMD has been performed with feed solution in lumen side of the module and with distillate in shell side. Feed and permeate are introduced in counter-flow into the membrane module at feed flow rates of 40 ml/min and 20 ml/min, respectively. In MCR,

the membranes have been tested with feed solution in shell side, due to complications with pore blocking when membrane crystallization has been performed with feed in lumen side. In this case feed flow rates have been set for 100 and 140 ml/min and permeate flow rate at 20 ml/min. The flows have been introduced in counter-flow mode.

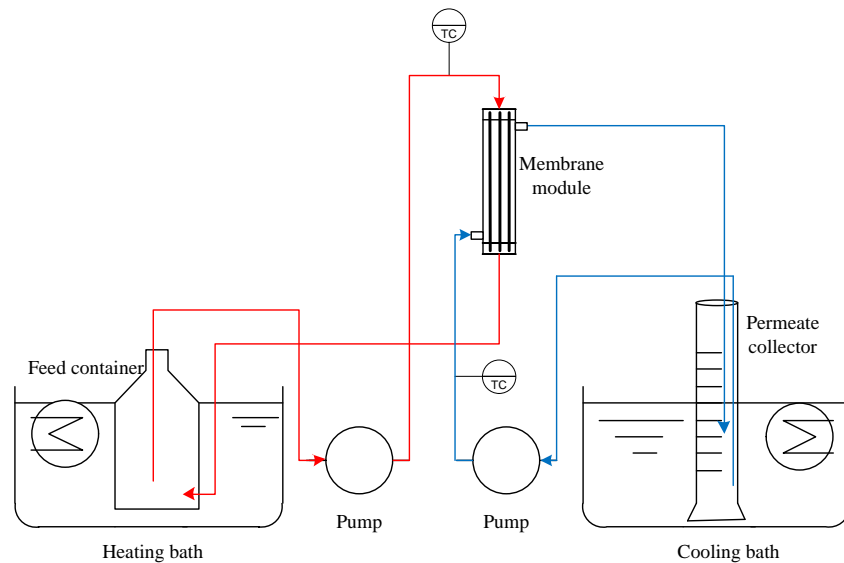


Figure 4.5: Schematic representation of the lab-scale membrane distillation plant used for evaluating the membrane performance.

#### 4.2.3 UTILIZED FEED SOLUTIONS

The membranes have first been tested by using distilled water as feed in DCMD configurations. Afterwards the membrane performance has been evaluated using single salt solutions (NaCl, 28.02 g/l and 57.18 g/l) and synthetic seawater and brine (Table 4.2). The permeate side consist of distillate water. For the evaluation of permeate quality, conductivity is measured at start and after completion of the experiment.

Table 4.2: Composition of synthetic seawater and brine <sup>a</sup>.

Composition	Synthetic seawater [ppm]	Synthetic brine [ppm]
Na <sup>+</sup>	12500	26478
Mg <sup>2+</sup>	1520	3101
Ca <sup>2+</sup>	490	20
Cl <sup>-</sup>	22300	45500
SO <sup>4-</sup>	3189	6507
HCO <sub>3</sub> <sup>-</sup>	150	107

<sup>a</sup> The composition of RO brine has been estimated on the following assumptions: (1) Seawater intake has a salinity at 4.0 %; (2) the recovery factor of RO is 51 %; (3) salt rejection is 99.7 %; (3) The brine is assumed to be pre-treated with addition of Na<sub>2</sub>CO<sub>3</sub> for removal of 98% of calcium to prevent gypsum scaling on membrane surface.

In MCr experiments single salt NaCl solutions with concentration 353.7 g/L and single salt MgSO<sub>4</sub>·7H<sub>2</sub>O with concentration 652.6 g/L have been tested. MCr experiments have also been carried out using synthetic brine as feed solution. The initial concentration of these experiments is four times the concentration with respect to Table 4.2.

#### 4.2.4 CHARACTERIZATION OF ACHIEVED CRYSTALS

The solution has been treated to super-saturation level and the time when crystals have been detected in the feed tank, suspension samples have been withdrawn from the tank. The mother liquid containing the crystals is spread on a glass slide and analyzed visually by using transmitted optical microscope (ZEISS model Axiovert 25). The images have been recorded by applying a video camera model VISIOSCOPE Modular System equipped with optical head (10/100 x). The recorded images have been analyzed by using Image J software version 1.48V from Wayne Rasband, National Institute of Health, USA. Nucleation and crystal growth have been analyzed by taking a sample after every 30 minutes. The obtained images are applied to calculate population density, growth rate, average crystal size, crystal size distribution and coefficient of variation (CV) at different time intervals after onset of crystallization for all the conditions analyzed.

### 4.3 RESULTS AND DISCUSSION

#### 4.3.1 DIRECT CONTACT MEMBRANE DISTILLATION

The first evaluation of membrane performance in terms of trans-membrane flux is carried out by having distillate water as feed solution. Testing with distilled water allows checking the membrane performance without solution effects (possible scaling, vapor pressure depreciation etc.). In Figure 4.6, the average flux for the three membranes (M1, M3 and M4) has been illustrated. Referring to the membrane characteristics (Table 4.1), thickness is one of the parameters deciding the membrane performance. Low membrane thickness implies reduced mass transfer resistance caused by the membrane. Knudsen diffusion (collision of molecule with the membrane wall), molecular diffusion (collision between molecules) or viscous flow are the resistance influencing mass transfer through the membrane in DCMD [2]. However, a conflict exists between the requirements of high mass transfer associated with thinner membranes and low conductive heat losses obtainable by using thicker membranes. In fact, thermal efficiency in DCMD increases gradually with increase in membrane thickness and an optimum thickness has to be found. Therefore, the highest average flux is observed for membrane M4 due to the smallest thickness and similar the lowest flux is observed for the membrane with the highest thickness (M1). As described previously in this chapter, pore size and porosity are also parameters deciding the overall flux. Membrane M1 has a lower pore size and porosity with respect to M3, which can explain the lower flux. However, M4 has the lowest pore size of  $0.29 \mu\text{m}$  and porosity of only 65 %, but are still the membrane achieving the higher flux. As a consequence of these results it appears that thickness is the overall determining parameter for the observed performance.

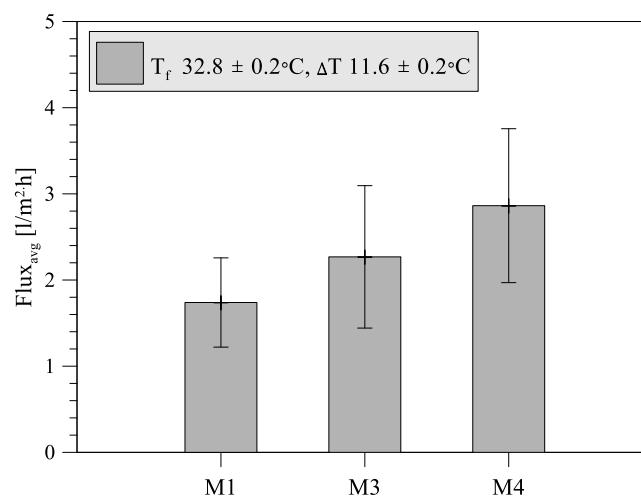


Figure 4.6: Average flux of DCMD tests using distillate water as feed solution.



In the same logic as the previous described experiments, synthetic seawater and brine have been tested as feed solution. The average flux is shown in Figure 4.7. In the low feed temperature range, no great difference between the three membranes has been observed, although M3 appears to achieve the lowest flux. However, for the higher temperature difference (i.e., driving force), the tendency is more clear, where M3 shows the lowest flux compared to M1 and M4 working at the same driving forces. This trend is unexpected taking into account the results obtained previously using distillate water. The decrease in flux for M3 can be explained by wettability and stability towards hydrophobicity quantified in terms of conductivity of permeate after finalizing the experiments. Membranes M1 and M4 show lower permeate conductivity for each experiment with respect to M3 (Figure 4.8). The microporous structure of M3 (Figure 4.3) having finger/like layer near the lumen side of the membrane makes it easier for solution to penetrate this morphology causing wetting. Likewise, the higher porosity and pore size can have positive impact on flux, but are also decreasing the liquid entry pressure. Due to the presence of macrovoids, it shows good performance using distillate water as feed solution, but in the treatment of concentrated solution the performance decreases because of higher wetting potential.

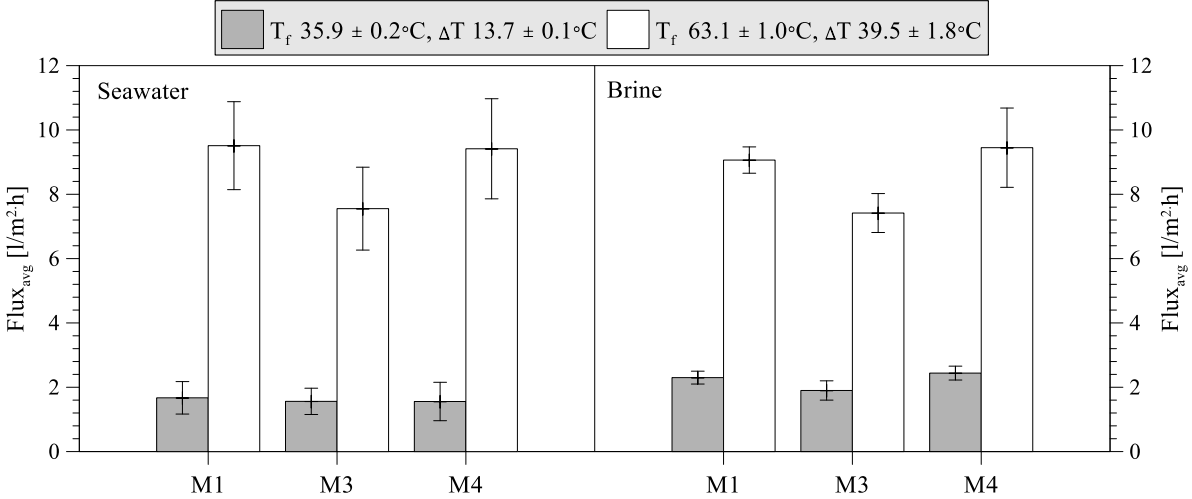


Figure 4.7: Average flux of DCMD tests utilizing synthetic seawater and brine as feed solution.

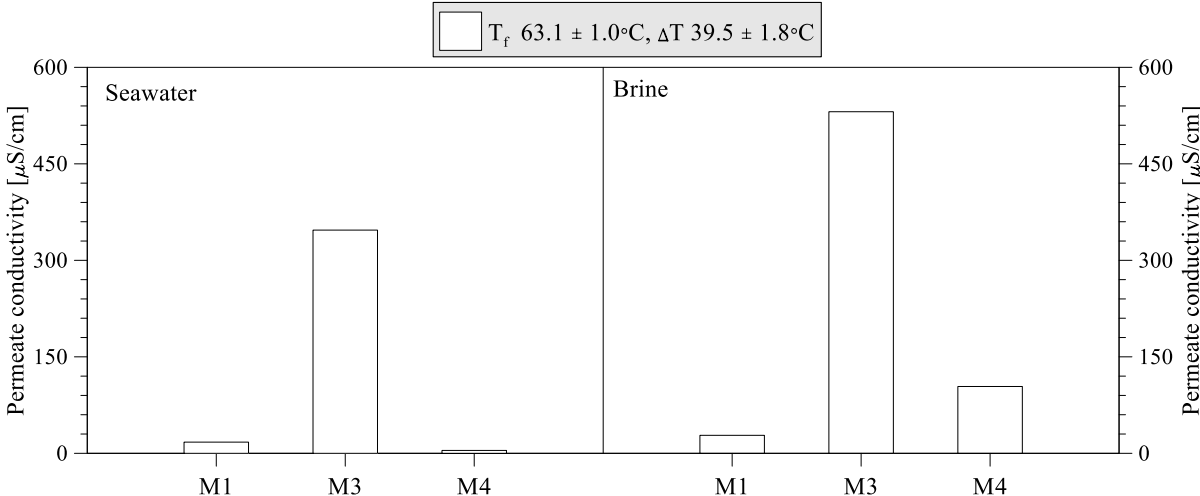


Figure 4.8: Permeate quality of DCMD tests utilizing synthetic seawater and brine as feed solution.

### 4.3.2 MEMBRANE CRYSTALLIZATION OF NaCl

Trans-membrane flux in membrane crystallization experiments of single salt NaCl solution shows the same tendency as in DCMD of concentrated solutions. The flux for membrane M3 is the lowest with respect to the other two membranes (Figure 4.9). Moreover, the flux for M3 decreases rapidly i.e. the final flux is less than half of initial stage. The lower flux is again explained by wetting of the membrane pores. Conductivity of permeate is much higher as compared to the membrane M1 and M4 (Figure 4.10). Membrane M3 is not found suitable for DCMD and MCr in the treatment of concentrated solutions, and has therefore, not been considered further in the subsequent evaluations of the most appropriate membranes for MD and MCr.

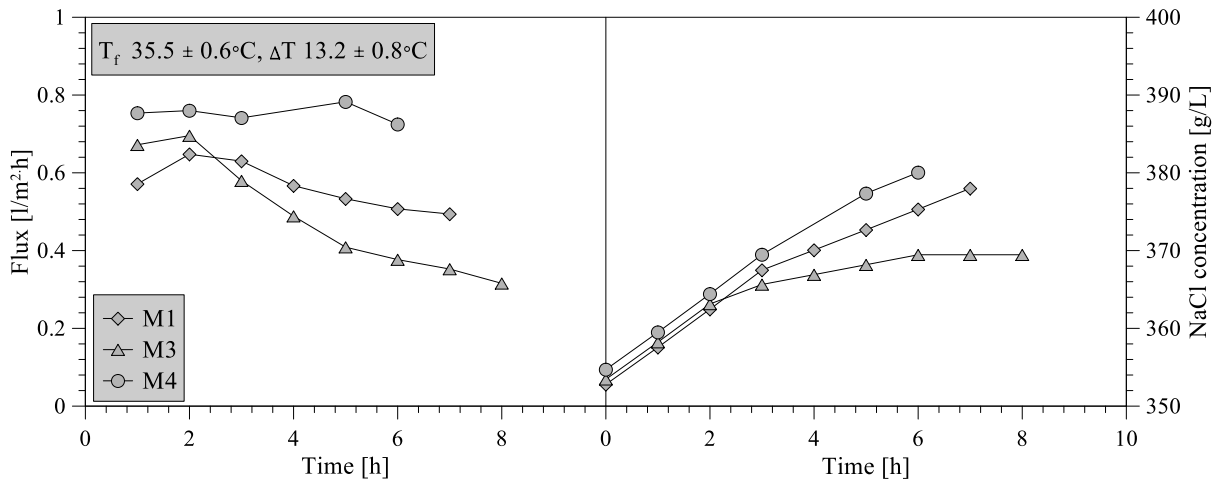


Figure 4.9: Trans-membrane flux of MCr tests in the crystallization of NaCl.

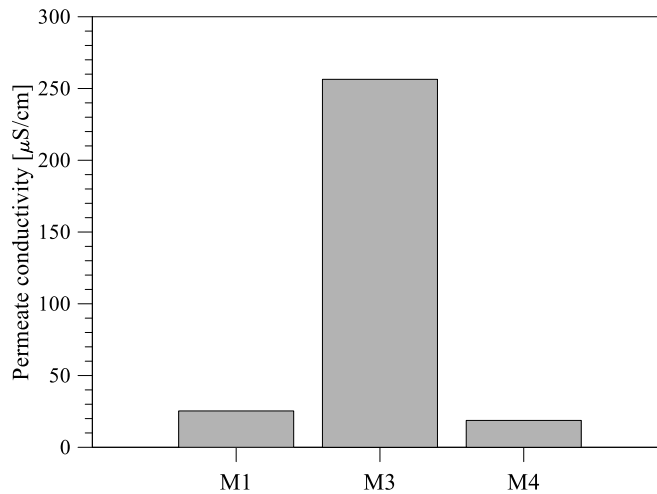


Figure 4.10: Permeate quality of MCr tests in the crystallization of NaCl.

### 4.3.3 MEMBRANE CRYSTALLIZATION OF EPSOMITE

Membrane M1 and M4 have been tested in membrane crystallization of  $MgSO_4 \cdot 7H_2O$  (Epsomite). M1 have also been tested with different flow rates (100 ml/min and 140 ml/min). Trans-membrane flux and temperature difference are shown in Figure 4.11. M4 provides better performance with respect to M1. Higher feed flow rates provide a higher flux which is expected due to decrease in boundary layer resistance and thereby temperature polarization [21].

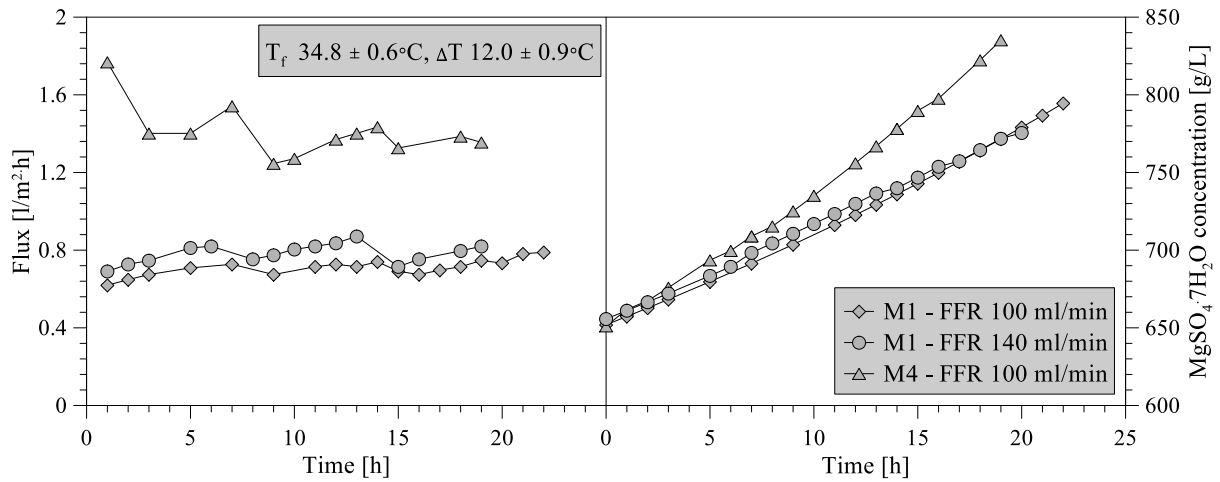


Figure 4.11: Trans-membrane flux and  $MgSO_4$  concentration for MCr treatment of  $MgSO_4$  solution (Initial concentration = 651 g/L)

An example of the produced crystals has been shown in Figure 4.12. Quality of the obtained Epsomite crystals has only been characterized by utilizing membrane M1 at different feed flow rates. The crystals have been characterized in terms of mean diameter ( $d_m$ ), coefficient of variation ( $CV$ ), and growth rate ( $G$ ). Coefficient of variation is estimated by Eq. 4.14, whereas growth rates and nucleation rates are estimated on the basis of the Randolph-Larson model shown in Eq. 4.15 and Eq. 4.16.



Figure 4.12: Epsomite crystals produced by means of MCr.

$$CV = \frac{F_{80\%} - F_{20\%}}{2F_{50\%}} \quad (\text{Eq. 4.14})$$

$$\ln(n) = -\frac{L}{Gt} + \ln(n^0) \quad (\text{Eq. 4.15})$$

$$B^0 = n^0 G \quad (\text{Eq. 4.16})$$

where  $F$  is the cumulative percent function given by the crystal length at the indicated percentage.  $n$  is the population density,  $L$  is crystal size,  $G$  is growth rate,  $t$  is retention time and  $n^0$  is population density at  $L$  equal to zero.

The time of crystals recovery is reported in Table 4.3. In each test two crystals samples have been extracted from the feed tank and analyzed. It has been observed that, as expected, nucleation occurs earlier at the highest flow rate. This suggested that effectively, trans-membrane flux has been higher in the test carried out utilizing the highest feed flow rate thus allowing achieving faster supersaturation. For the highest flow rate, the mean diameter and crystal growth rate are larger compared to a flow rate of 100 ml/min. Coefficient of variations for all the samples are lower with respect to what has normally been reported for conventional crystallizer (~50%), validating the superior crystal product obtainable from an MCr unit.

*Table 4.3: Crystal characteristics obtained with membrane M1 at different flow rates.*

Membrane type	Time of recovery		Mean diameter		Coefficient of Variation		Growth rate	
	[h]		[ $\mu\text{m}$ ]		[%]		[ $\mu\text{m}/\text{min}$ ]	
	Sample		Sample		Sample		Sample	
	1	2	1	2	1	2	1	2
M1 100 ml/min	21	22	367.2	361.5	33.58	41.44	0.1111	0.09752
M1 140 ml/min	19	20	589.2	598.4	40.95	30.52	0.3576	0.4478

#### 4.3.4 MEMBRANE CRYSTALLIZATION OF NaCl FROM RO BRINE

From the previous data it is noticed that membrane M4 is superior for treating saline solutions, due to improved trans-membrane flux and low wetting probability compared to the other prepared membranes. Therefore, the following section includes only experiments regarding membrane M4. Synthetic RO brine has been utilized in DCMD and MCr test. The membrane has been tested at the exact concentration as shown in Table 4.2. However, the tests have been extended further in order to test the membrane M4 at higher feed concentration and for the crystallization of NaCl from RO brine.

The performance of the membrane crystallization tests, at concentration factor = 4.0, in terms of trans-membrane flux is initially not differing much with flow rate (Figure 4.13). In both the experiments, crystallization occurs after 1.5 hours, thus nucleation and growth on membrane surface can be responsible for the decrease in flux promoted by the higher flow rate or the longer experimentation time. Scaling on membrane surface can easily be avoided by introducing temperature control in the feed tank, thus having slightly different temperature in the module and in the feed tank. The effect of presence of the produced crystals in the system can also easily be solved by applying a continuous removal of crystals as performed in the study by Macedonio et al. 2010 [7]. Wetting of the membrane has previously been described as a parameter decreasing the flux. Despite the permeate conductivity is slightly higher for the higher flow rate (Figure 4.14), it is unlikely that this small difference, which is nothing like the conductivity measured by utilizing membrane M3, can be responsible for the lower flux. The membrane M4 has previously proved the less wetting probability compared to other lab-made membranes illustrated by the relative low permeate conductivity (Figure 4.14) even at high concentration of a mixture of ions.

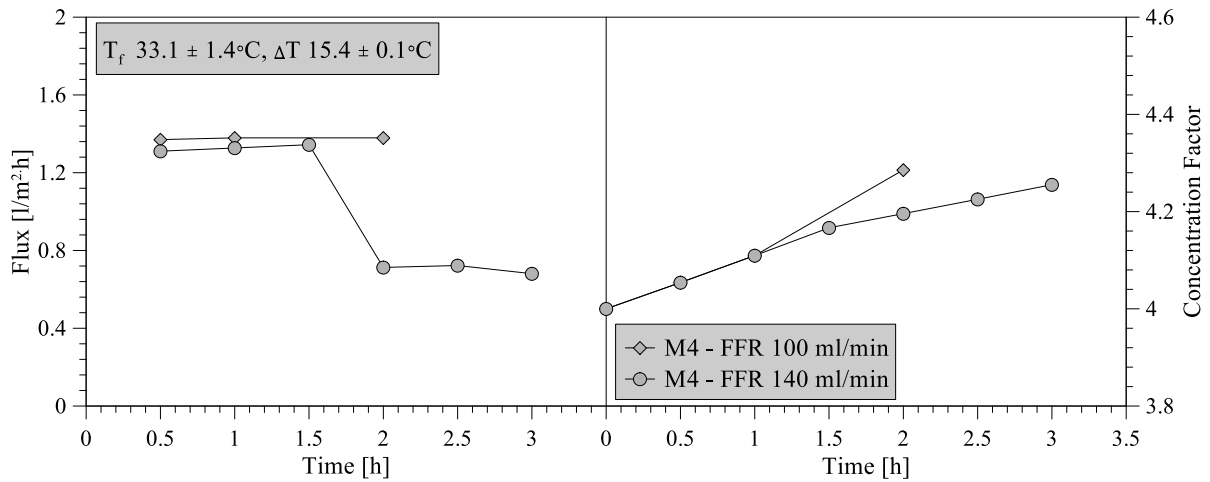


Figure 4.13: Trans-membrane flux and concentration factor for MCr tests at an initial brine concentration factor = 4.0.

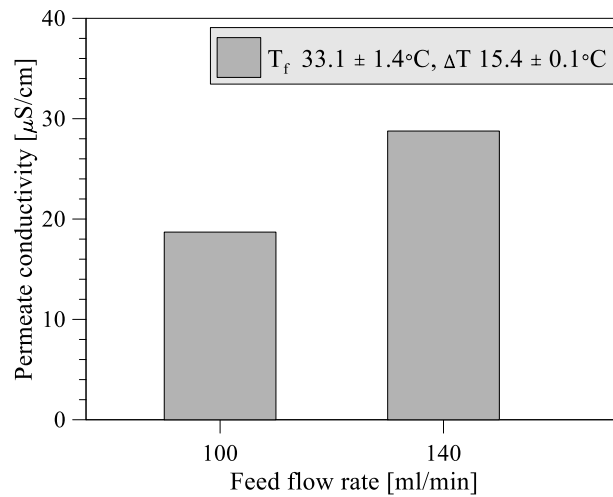


Figure 4.14: Permeate conductivity for MCr treatment of saline solutions. For MCr tests at an initial brine concentration factor = 4.0.

Crystal characteristics have been estimated according to previous described procedure. The estimated parameters for flow rates at 100 ml/min and 140 ml/min are reported in Table 4.4 and Table 4.5, respectively. Crystals have been withdrawn from the mother solution when the first crystals have been observed and hereafter with 30 min intervals.

Table 4.4: Crystal characteristics for membrane crystallization of RO brine at feed flow rate = 100 ml/min.

Sample	1	2
Sample taking [min]	90	120
Mean diameter ( $d_m$ ) [ $\mu\text{m}$ ]	33.22	22.04
Coefficient of Variation (CV) [%]	34.18	57.06
Growth rate (G) [ $\mu\text{m}/\text{min}$ ]	0.2889	0.1013
Nucleation rate ( $B^0$ ) [no./L·min]	442,178	596,367

Table 4.5: Crystal characteristics for membrane crystallization of RO brine at feed flow rate = 140 ml/min.

Sample	1	2	3
Sample taking [min]	90	120	150
Mean diameter ( $d_m$ ) [ $\mu\text{m}$ ]	16.16	29.11	27.46
Coefficient of Variation (CV) [%]	36.96	49.62	51.12
Growth rate (G) [ $\mu\text{m}/\text{min}$ ]	0.08726	0.1231	0.09767
Nucleation rate ( $B^0$ ) [no./( $L \cdot \text{min}$ )]	1,192,222	629,542	461,430

Mean diameter and growth rate for crystallization at flow rate = 100 ml/min (Table 4.4) are decreasing from sample 1 to 2 caused by the increased nucleation rate. The higher nucleation rate can also justify the high CV for sample 2, which creates more variation in crystal size due to both nucleation and growth of existing crystals. The opposite tendency is observed for the higher flow rate (Table 4.5), where mean diameter and growth rate increases from sample 1 to 2 whereas it slightly decreases again in sample 3. In Table 4.5, the nucleation rate is very high in the first sample inclining that mainly nucleation has occurred which explains the low mean diameter and the low CV due to less growth of crystals and hereby less variation in crystal size. Increased growth rate and less nucleation in sample 2 and 3 enlarge the variation in size, thus giving higher CV values.

The influence of nucleation and growth is also illustrated in terms of CSD (Figure 4.15), which describes the numbers of crystals according to a specific length range of the crystals. Therefore CSD can provide information about the uniformity of the produced crystals. The first samples for both flow rates are more uniform compared to the later withdrawn samples. In sample 2 and 3 the main part of the analyzed crystals are within the small crystal size, though with some small peaks at higher range caused by the effect of both nucleation and growth. Crystal breakage could possibly have occurred from sample 1 to 2 at low flow rate due to the movement of the CDS curve towards the left side (Figure 4.15 a) also exemplified by the decrease in mean diameter (Table 4.4) emphasizing better crystallization process control and eventually crystal recovery.

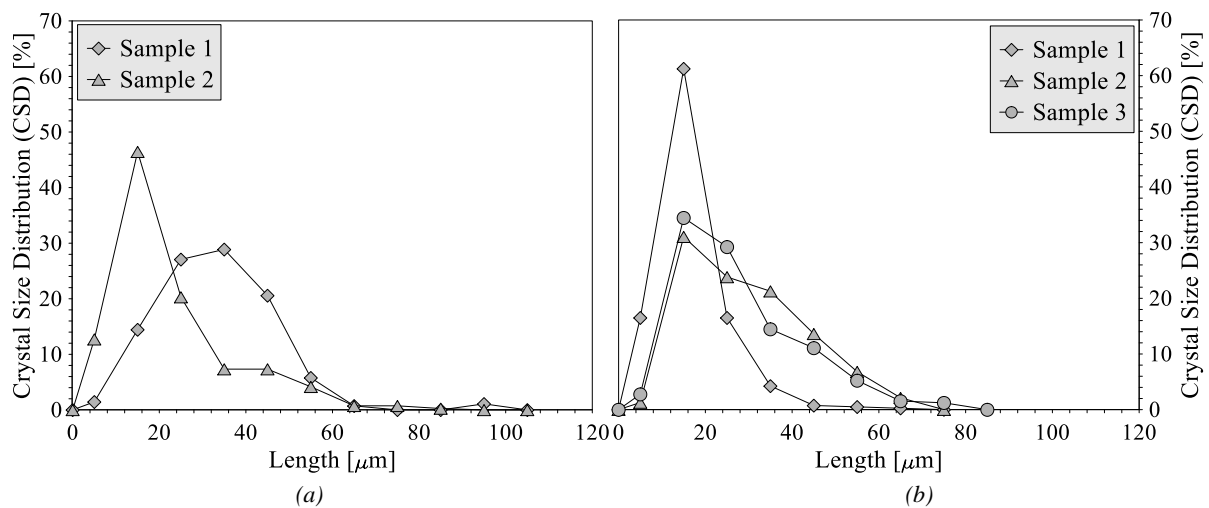


Figure 4.15: Crystal size distribution for membrane crystallization at different feed flow rates. (a) Flow rate = 100 ml/min. (b) Flow rate = 140 ml/min.

Sodium chloride exhibit a cubic structure in nature which can be affected by impurities, thus the length to width ratio is estimated for the analyzed crystals (Figure 4.16). In all the samples, more than 60 % crystals have a length to width ratio less than 1.3, which validates the cubic structure of NaCl. The eventually impurities affecting the crystal structure have been evaluated by scanning electron microscopy (SEM) and energy dispersive X-ray (EDX).

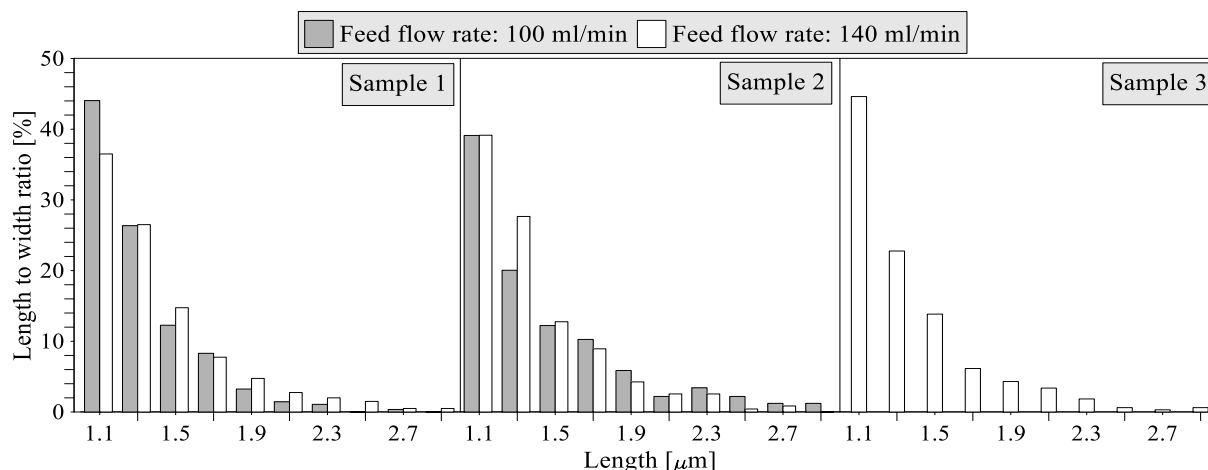


Figure 4.16: Length to width ratio for membrane crystallization at different flow rates.

A sample of the crystals obtained in the membrane crystallization tests have been analyzed with SEM and EDX in order to confirm the nature of the crystallized product and to identify any impurities incorporated into the crystal lattice. In Figure 4.17 the characteristic cubic sodium chloride crystals are observed through SEM at different magnifications. The crystallization of NaCl from RO brine is also confirmed by EDX (Table 4.6 and Figure 4.18). However, EDX analysis shows a small amount of magnesium present in NaCl crystals (Table 4.6 and Figure 4.18).

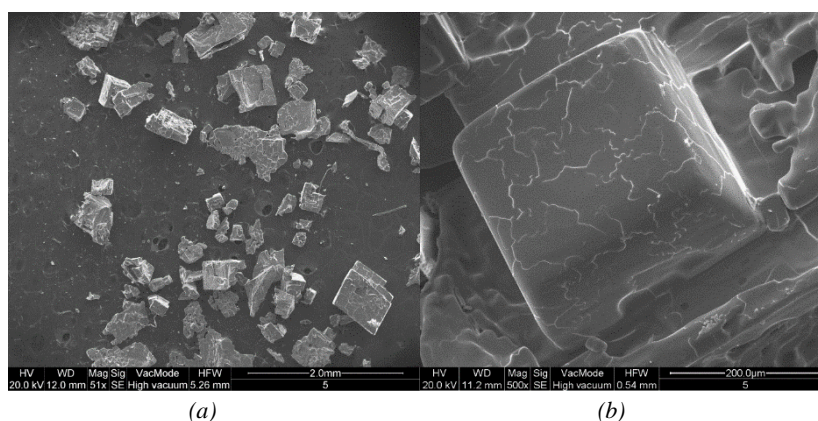


Figure 4.17: Scanning electron microscopy images of NaCl crystallized from RO brine (a) Magnification 51x (b) Magnification 500x.

Table 4.6: Energy-dispersive X-ray (EDX) analysis of NaCl crystallized from RO brine.

	Na	Cl	Mg
Weight %	33.36	66.43	0.21

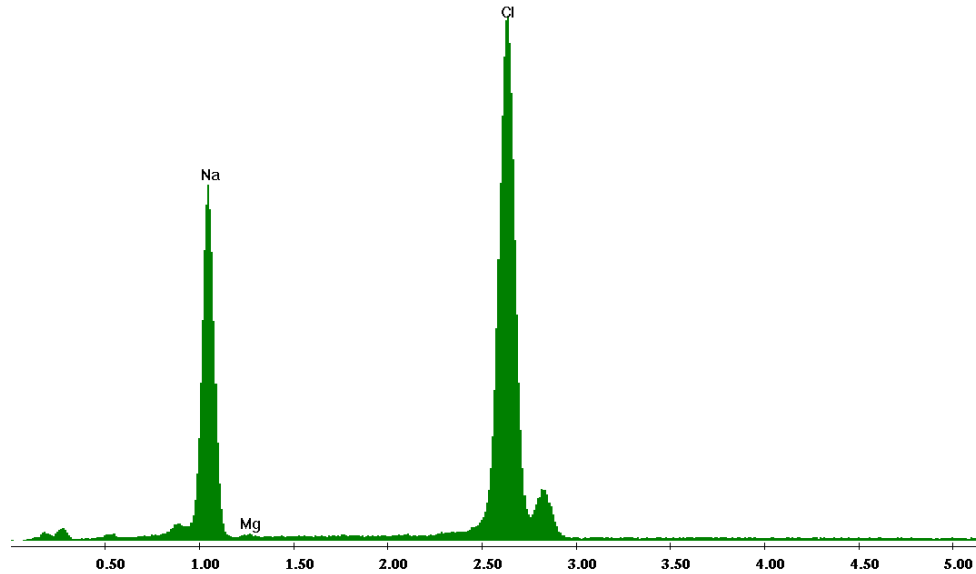


Figure 4.18: Energy-dispersive X-ray (EDX) spectra of NaCl crystallized from RO brine.

#### 4.4 SUMMARY

Testing of lab-made membranes for treatment of highly concentrated solutions have been discussed in this study. Membrane M3 achieved promising results in DCMD using distillate water as feed. However, moving towards treatment of highly concentrated solutions, the membrane has not been able to maintain the good results due to higher wetting properties caused by finger-like structure. The best membranes found in this study are M1 and M4, which are symmetric membranes, unlike the asymmetric structure of M3. In this particular case of lab-made PVDF membranes, the thickness appears to be the determining parameter for high flux achievement, thus M4 membrane obtain the highest flux in all the carried out experiments. However, thin membranes can cause more heat losses in practical applications. M1 and M4 are also stable during crystallization and both membranes are able to achieve a crystal product of high quality. The longest experimental duration has been used in the crystallization of Epsomite (more than 20 hours) and stable membrane performance is easily maintained for M1 and M4 by slightly cleaning with distillate water after end experimentation and eventually drying. Therefore, the membrane stability for M1 and M4 appears to be sufficient for membrane crystallization.

#### REFERENCES

- [1] S. Al-Obaidani, E. Curcio, F. Macedonio, G. Di Profio, H. A-Hinai, and E. Drioli, "Potential of membrane distillation in seawater desalination: Thermal efficiency, sensitivity study and cost estimation," *J. Memb. Sci.*, vol. 323, pp. 85–98, 2008.
- [2] M. Khayet, "Membranes and theoretical modeling of membrane distillation: a review.," *Adv. Colloid Interface Sci.*, vol. 164, no. 1–2, pp. 56–88, May 2011.
- [3] Z. Cui, E. Drioli, and Y. M. Lee, "Recent progress in fluoropolymers for membranes," *Prog. Polym. Sci.*, Jul. 2013.
- [4] F. Liu, N. A. Hashim, Y. Liu, M. R. M. Abed, and K. Li, "Progress in the production and modification of PVDF membranes," *J. Memb. Sci.*, vol. 375, pp. 1–27, Jun. 2011.
- [5] Z. Cui, N. T. Hassankiadeh, S. Y. Lee, J. M. Lee, K. T. Woo, A. Sanguineti, V. Arcella, Y. M. Lee, and E. Drioli, "Poly(vinylidene fluoride) membrane preparation with an environmental diluent via thermally induced phase separation," *J. Memb. Sci.*, vol. 444, pp. 223–236, Oct. 2013.



- [6] E. Drioli, A. Ali, S. Simone, F. Macedonio, S. A. AL-Jlil, F. S. Al Shabonah, H. S. Al-Romaih, O. Al-Harbi, A. Figoli, and A. Criscuoli, “Novel PVDF hollow fiber membranes for vacuum and direct contact membrane distillation applications,” *Sep. Purif. Technol.*, vol. 115, pp. 27–38, Aug. 2013.
- [7] F. Macedonio and E. Drioli, “Hydrophobic membranes for salts recovery from desalination plants,” *Desalin. Water Treat.*, vol. 18, pp. 224–234, 2010.

---

## CHAPTER 5:

# RECOVERY OF SODIUM SULFATE FROM WASTEWATER

---

### 5.1 INTRODUCTION

Untreated wastewater streams have negative impact on environment and economy. Treatment of these streams cannot only reduce/eliminate the associated hazards but does also provide the opportunity to recover valuable components encountering zero liquid discharge. This study evaluates the potential of using MD and MCr for treatment of wastewater containing high amounts of sodium sulfate. Sodium sulfate is a valuable material used in various industries for cleaning detergents, glass, pulp and paper [1]. Traditionally,  $\text{Na}_2\text{SO}_4$  is extracted from salt lake brines and through mining processes. China is the largest producer with more than 70 % of world production [1]. Sodium sulfate can also be recovered as by-product from i.e. battery reclamation, cellulose and silica pigments etc. [1]. Certain wastewater streams also contain significant quantities of  $\text{Na}_2\text{SO}_4$ . The treatment of these streams can reduce their negative impact on environment and, simultaneously contribute in achieving the objective of sustainable consumption of sodium sulfate and water.

Different polymorphs of sodium sulfate exist, where the anhydrous (thenardite) and decahydrate (mirabilite) forms are the most common. Sodium sulfate solubility changes greatly with temperature and the polymorph formed is also dependent on relative humidity (RH) (Figure 5.1 and Figure 5.2).

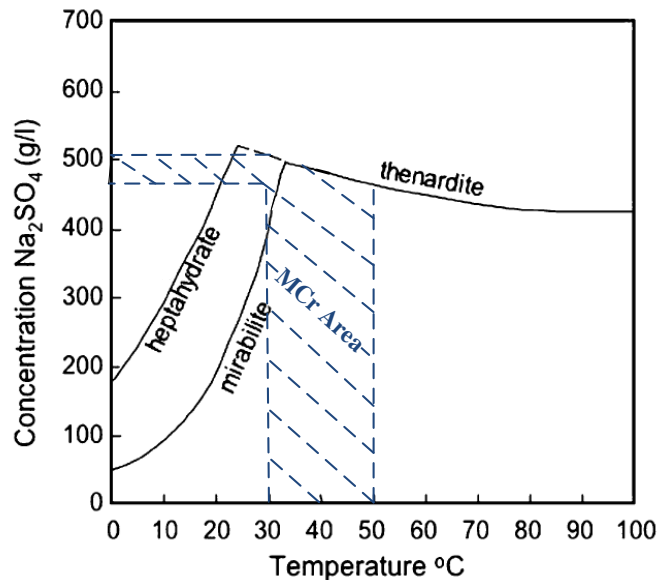


Figure 5.1: Solubility of sodium sulfate with temperature. Modified from [2]

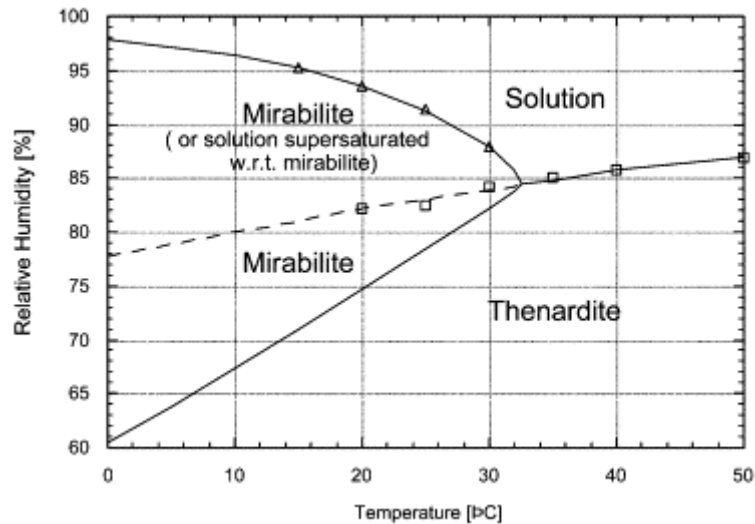


Figure 5.2: Phase diagram of sodium sulfate: dependence on relative humidity and temperature [3]

Sodium sulfate solubility increases with temperature in the range 0-30°C whereupon it decreases. In the range 30-50°C (i.e., the temperature utilized in the carried out MD/MCr tests), if the solution is supersaturated, it is precipitated as the anhydrous (Thenardite) form. This corresponds with the results obtained by Curcio et al. [4] (Described in chapter 3), who found that  $\text{Na}_2\text{SO}_4$  precipitate as Thenardite when using DCMD configuration in proper operative conditions. In contrast, Li et al. [5] found that  $\text{Na}_2\text{SO}_4$  crystallizes as Mirabilite when an isothermal osmotic MD configurations is being utilized (T: 20°C, Flow rate:5-100 ml/min), also corresponding to the phase diagram.

In this study MD and MCr have been utilized to concentrate and precipitate  $\text{Na}_2\text{SO}_4$  from wastewater solutions and also from wastewater, which has been treated with NF prior to MD/MCr.

## 5.2 MATERIALS AND METHODS

### 5.2.1 MD SETUP AND MEMBRANE USED

A semi pilot-scale MD and MCr plant has been utilized in the treatment of wastewater and recovery of  $\text{Na}_2\text{SO}_4$ . A generalized scheme has been provided in Figure 5.3. It consists of membrane modules (E) placed vertical and a feed tank (F) with external cooling control (A). The increment of mass in the permeate tank (L) is measured with a balance (I). Moreover the plant is equipped with centrifugal pumps (B), flow meters (C), heater (D) and cooler (A) for the feed and permeate side, respectively. The plant is equipped with two commercial polypropylene membranes from Microdyn-Nadir (Table 5.1).

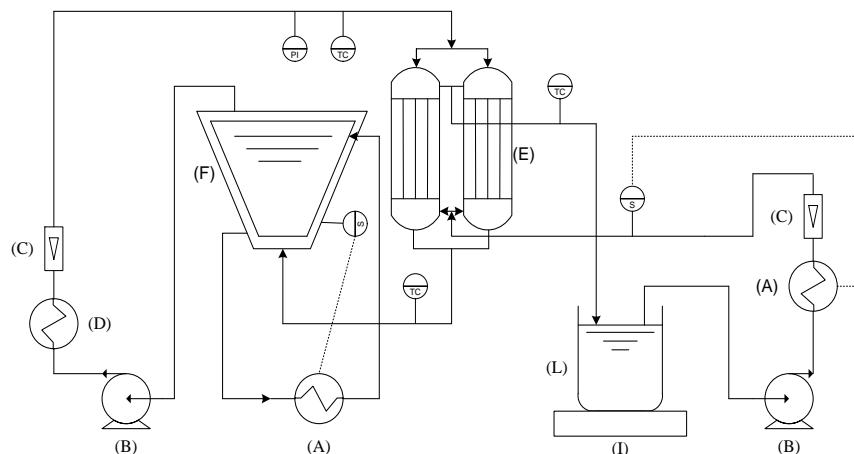


Figure 5.3: Schematic diagram of the set-up used for MCr

Table 5.1: Detailed description of membrane modules from Microdyn-Nadir (MD020CP2N)

Material	Polypropylene (PP)
Type	Hollow fiber
No. of fibers	40
Internal diameter of the fibers	1.8 mm
Membrane thickness	450 $\mu\text{m}$
Length of the fibers	45 cm
Surface area	0.1 $\text{m}^2$
Nominal pore size	0.2 $\mu\text{m}$
Shell diameter	2.1 cm

## 5.2.2 WASTEWATER CHARACTERISTICS

Besides sodium sulfate, the composition of the wastewater solution (Table 5.2) also contains magnesium and calcium. Calcium precipitation during membrane treatment is a challenging problem in many membrane operations. In this study the feed solutions are concentrated until precipitation of  $\text{Na}_2\text{SO}_4$ . Therefore calcium scaling has to be considered in both MD and MCr processes.

Table 5.2: Characteristics of the utilized wastewater.

pH	4-5
$\text{Na}_2\text{SO}_4$	4.5-5.5 w%
Ca	approx. 60 mg/L
Mg	approx. 3-5 mg/L

## 5.2.3 MD AND MCr EXPERIMENTS

The raw wastewater has been treated twice (referred to as solution # 1 and solution # 2) with MD and MCr following the structure in Table 5.3. Different flow rates (100 and 200 l/h) and feed temperature conditions (ranging from 31 to 51  $^{\circ}\text{C}$ ) have been utilized. The permeate flow rate has been kept on 100 l/h throughout the experiments. The wastewater has also been treated with nanofiltration prior to MD and MCr. Experiments on nanofiltered wastewater have been conducted at two different initial concentrations, i.e. 93.46 g/l  $\text{Na}_2\text{SO}_4$  (solution # 3) and 132.0 g/l  $\text{Na}_2\text{SO}_4$  (solution # 4). Pretreatment with nanofiltration decreases the time needed to reach sodium sulfate crystallization, thus only two different experimental conditions have been conducted for the NF pretreated wastewater (Table 5.3). The final crystallization processes have been carried out by using the conditions: feed flow rate 200 l/h and feed temperature around 37  $^{\circ}\text{C}$ . The quality of permeate has been scrutinized in terms of conductivity.

Table 5.3: DCMD and MCr experiments for the treatment of wastewater.

Experimental condition	Feed flow rate [L/h]	Feed temperature (inlet) [ $^{\circ}\text{C}$ ]	Distillate temperature (inlet) [ $^{\circ}\text{C}$ ]	Tested on solution No.:
MD 1	100	37.8 +/- 0.9	22.6 +/- 3.0	1 - 2
MD 2	200	31.4 +/- 0.6	19.4 +/- 2.9	1 - 2
MD 3	200	49.4 +/- 2.0	38.3 +/- 6.6	1 - 2 - 3 - 4
MD and MCr	200	37.4 +/- 2.3	24.1 +/- 7.7	1 - 2 - 3 - 4

## 5.2.4 CRYSTAL CHARACTERISTICS

The produced crystals have been characterized by optical microscope, energy dispersive x-ray (EDX) and scanning electron microscopy (SEM) analysis. The characterization follows the procedure found in Chapter 4. SEM and EDX are utilized for polymorph and purity estimations.

### 5.3 RESULTS AND DISCUSSION

The treatment of wastewater (without NF pretreatment) has been repeated twice, referred to as solution #1 and solution #2. The treatment of solution # 1 and 2 has been conducted under the same operative conditions (Table 5.3). The small deviations achieved in trans-membrane flux (Figure 5.4) indicate good reproducibility of the treatment by means of MD and MCr.

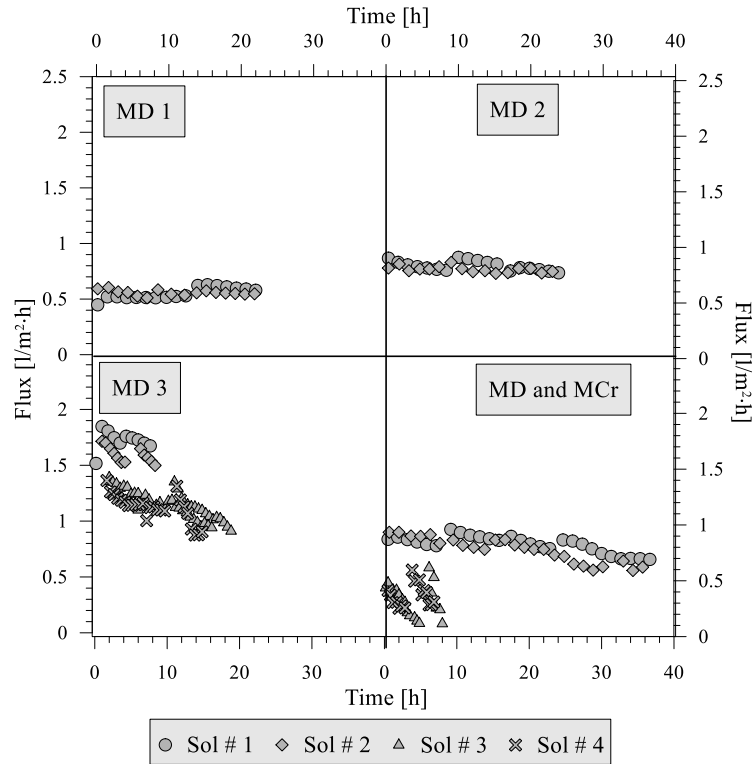


Figure 5.4: Trans-membrane flux vs. time for different experimental conditions.

The flux achieved utilizing the highest driving force (MD 3) is slightly higher for solution # 1 as compared to solution # 2. Nevertheless, the same trend is observed for the vapor pressure gradient (Figure 5.5). Driving forces in DCMD and MCr are mainly implied by temperature. However, high solution concentrations can also influence the driving force. Therefore, driving forces have been estimated on the basis of log mean pressure gradient (Eq. 5.1).

$$\Delta P_{\ln} = \frac{(P_{r,in} - P_{p,out}) - (P_{r,out} - P_{p,in})}{\ln\left(\frac{P_{r,in} - P_{p,out}}{P_{r,out} - P_{p,in}}\right)} \quad (Eq. 5.1)$$

Where  $\Delta P_{\ln}$  is the log mean vapor pressure difference and  $P_r$  and  $P_p$  is the actual vapor pressure in [Pa] of the retentate and permeate, respectively.

The vapor pressure is estimated on the basis of Eq. 4.2 – Eq. 4.4 in Chapter 4. Evolution of activity coefficients during the experiments (by use of PHREEQC) has been estimated based on the actual bulk temperatures for feed and permeate and also by taking into account the feed concentrations at the given time. Initial feed concentrations for solution # 1 and 2 are based on Table 5.2. Here the calcium and magnesium concentrations have also been considered. Increase in concentration during the experiment is based on trans-membrane flux. Calcium and magnesium content of solution # 3 and 4 is higher with respect to solution # 1 and 2 due to the nanofiltration pretreatment. However, the exact composition has

not been identified and calcium and magnesium content have, therefore, not been included solution # 3 and 4. As expected the highest flux (Figure 5.4) is obtained using the highest driving force (vapor pressure difference) according to the relationship discussed in Chapter 4. The flux decreases slightly in some tests, due to similar decrease in driving force (Figure 5.5). Therefore, the flux decline is not likely a result of scaling. Furthermore, to ensure stable performance, the wastewater solutions have been removed from the lab-scale plant every 10 hours and the plant has been cleaned slightly with distilled water. For the reason of the slight cleaning and also difficulties in obtaining steady state, some interrupted lines of both trans-membrane flux and driving force can be observed.

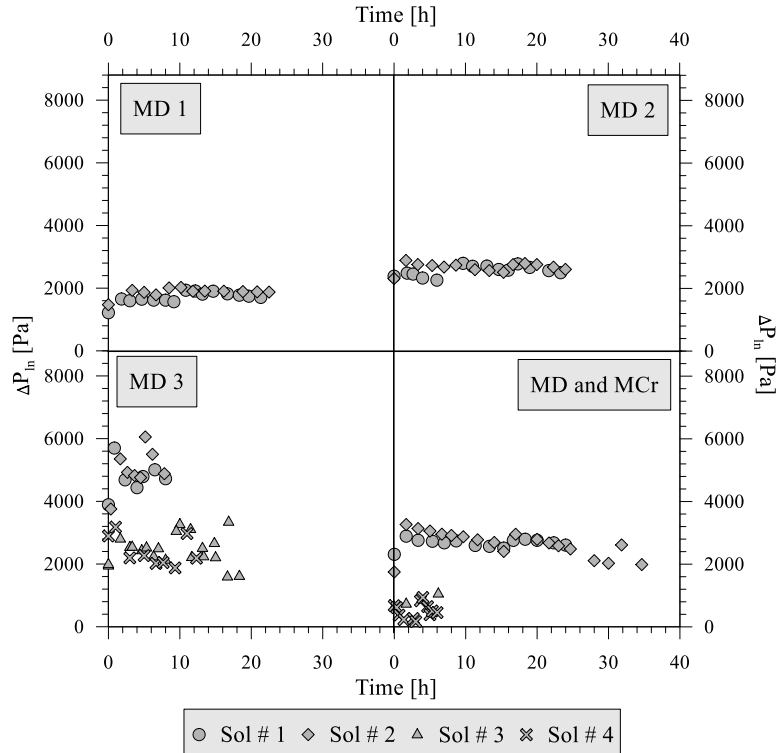


Figure 5.5: Driving force vs. time for different experimental conditions.

Trans-membrane flux for solution # 3 and solution # 4 (the nanofiltered solutions) is lower as compared to solution # 1 and 2 (Figure 5.4). Nevertheless, the same behavior is observed for vapor pressure (Figure 5.5). To eliminate the impact of the difference in driving forces between the experiments, trans-membrane flux has been normalized according to Eq. 5.2.

$$Normalized\ Flux = \frac{J}{\Delta P_{in}} \quad (Eq. 5.2)$$

Where  $J$  is the trans-membrane flux in  $[l/m^2h]$  and  $\Delta P_{in}$ , is the log mean vapor pressure difference. Normalized flux (Figure 5.6) for solution # 1 and 2 shows a very similar and steady trend, whereas for solution # 3 and 4, the normalized flux is not steady. In particular during crystallization a drastic reduction in flux is observed, which is accounted for the faster increase of concentration of ions and to a higher initial concentration of calcium and magnesium ions.

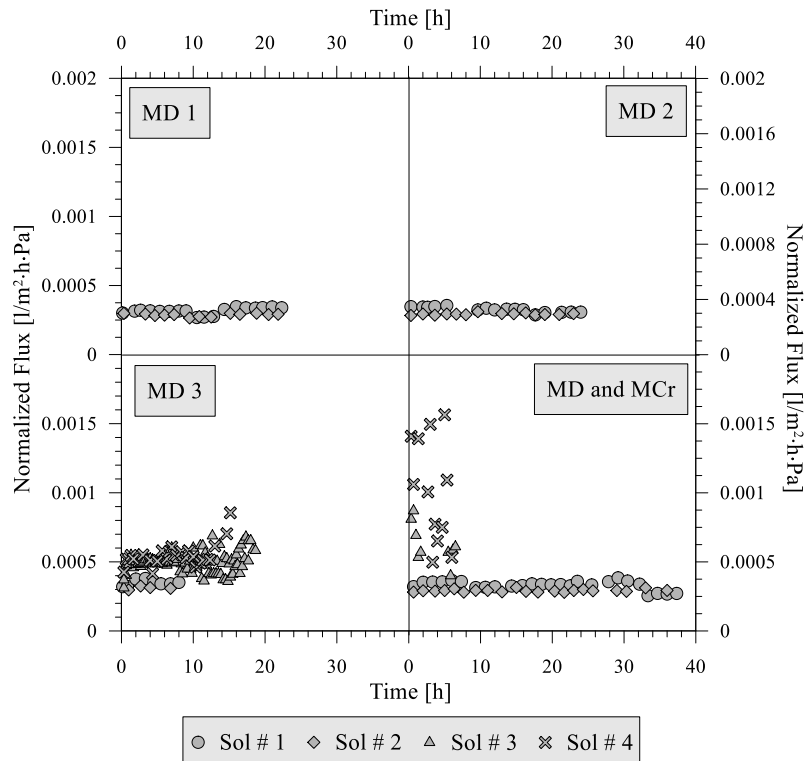


Figure 5.6: Normalized flux vs. time for different experimental conditions.

### 5.3.1 POTENTIAL SCALING STUDIES

Calcium compounds, in particular calcium sulfates and calcium carbonates are high risk scaling components. In reverse osmosis, scaling is normally avoided by adding proper antiscalants before the membrane operation. However, chemical treatment is not aligned with the process intensification strategy and sustainable development. In literature [6], it has been proved that calcium can be removed from feed solution through chemical treatment with  $\text{Na}_2\text{CO}_3$ . Nevertheless, in this study, the wastewater has not been treated chemically prior or during MD/MCr.

The conductivity of permeate has been measured frequently during the tests in order to detect eventual wetting of the membrane. In all the carried out tests, permeate conductivity at the end of each test has been lower with respect to its value at the start of the experiment. This demonstrated that the intrusion of feed solution through the membrane pores is negligible. Therefore, the utilized polypropylene membranes preserved the crucial requisite of hydrophobicity during the operative time of these experiments. The MD/MCr treatment has been carried out for 92, 90, 28 and 22 hours for solution # 1, 2, 3 and 4, respectively, thus the membranes have proven their long term stability. Moreover, not any particular cleaning has been carried out to minimize scaling. The only cleaning, beside distillate water, has been cleaning with citric acid for one hour followed by rinsing with distillate water. This has only been performed after precipitation of  $\text{Na}_2\text{SO}_4$ , means only before beginning of experimentation with a new solution.

### 5.3.2 CRYSTALLIZATION OF SODIUM SULFATE

In terms of concentrations, precipitation of  $\text{Na}_2\text{SO}_4$  has been observed at concentrations around 370.3 g/L for solution # 1 and 2 (Figure 5.7). For the nanofiltered solutions crystallization has been observed at 318.4 and 319.4 g/L. The lower observed saturation might have been reduced, due to the higher concentration of bivalent ions in the nanofiltered wastewater.

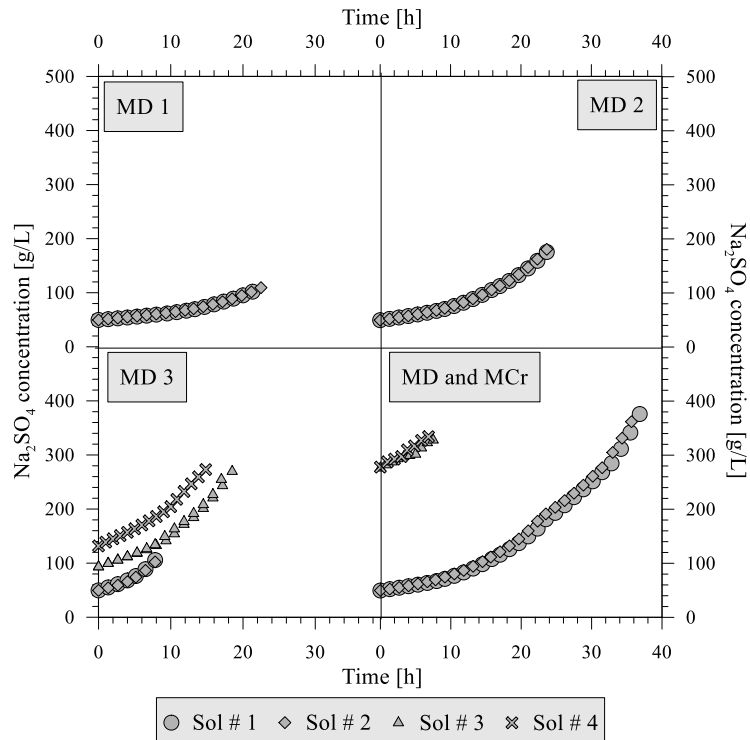


Figure 5.7:  $\text{Na}_2\text{SO}_4$  concentration for different test conditions.

Sodium sulfate crystals produced from solution # 2 have been characterized according to different parameters. Samples of the mother liquid containing crystals have been withdrawn from the retentate tank every 30 minutes, and examined visually (via an optic microscope) in order to determine crystals shape, dimension and crystal size distribution. Moreover, a sample of mother liquid and crystals, at this stage, has also been filtered to recover crystals for SEM and EDX analysis. Knowledge of the evolution of particle size distribution as function of time allows evaluating quality, mean diameter ( $d_m$ ), coefficient of variation (CV) and growth rate of the produced crystals. From microscopic pictures, the  $\text{Na}_2\text{SO}_4$  crystals exhibited mainly the conventional elongated habit with orthorhombic symmetry found for anhydrous  $\text{Na}_2\text{SO}_4$  (Figure 5.8) [7].



Figure 5.8. Sodium sulfate produced from "wastewater solution # 2".



Coefficient of variation (CV) has been estimated through Eq. 4.14, whereas growth and nucleation rate have been estimated on the basis of the Randolph-Larson model (Eq. 4.15 and Eq. 4.16, respectively). Illustration of CSD and data of crystal characterization are reported in Figure 5.9 and Table 5.4, respectively. CSD of the samples are in general narrow also confirmed by CV below 50% for all the samples. CV is an industrially relevant parameter since it measures the scatterings of crystal size around its mean. The CV of ideal mixed-suspension crystallizer, widely employed in the industrial crystallization, is 50% for size-independent growth, but becomes significantly higher for size-dependent growth [8]. Low CV is characteristic of a narrow crystal size distribution and, therefore, of a better product [9]. Crystal samples collected at time of 750 min. showed the lowest CV (34.9%). These values are comparable with CV observed in other studies (initial CV: 23% and around 40% at residence time of 90 min.) [4]. Mean diameter and growth rate decrease during time possibly due to slight reduction in super-saturation level. The mean diameter obtained in this study appears to be much higher with respect to mean diameter found in other studies (around 100  $\mu\text{m}$ ) [4], [12]. Furthermore, Curcio et al. [4], have reported a linear growth rate of  $1.56 \cdot 10^{-8}$  m/s ( $=0.936$   $\mu\text{m}/\text{min}$ ), which is slightly higher than the value observed in this study. The reason in the differences might be attributed to that crystals, in this study, have been withdrawn later with respect to other studies. Overall the results indicate the potential of keeping the crystallization process of sodium sulfate steady and of good quality by utilizing MCr.

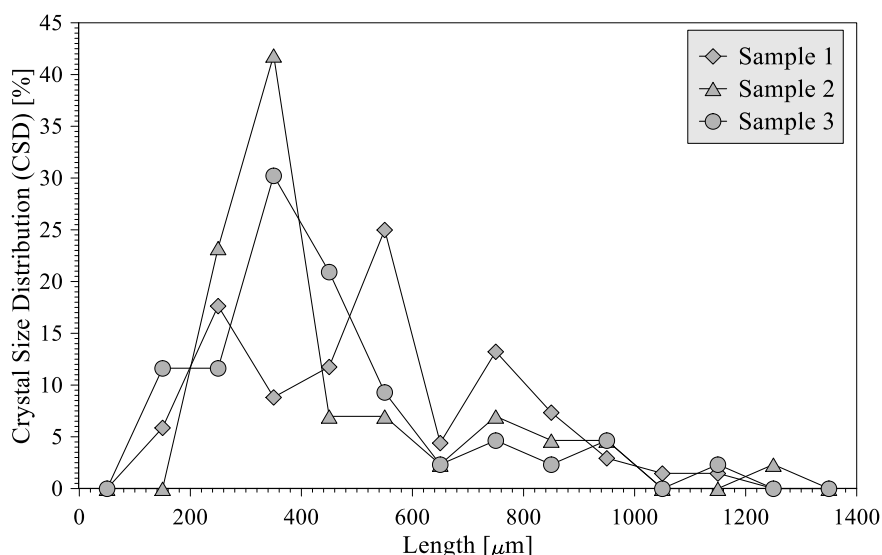


Figure 5.9. Crystal size distribution (CSD) achieved during crystallization of "wastewater solution # 2".

Table 5.4: Crystal characteristics achieved in the crystallization of "wastewater solution # 2".

Sample	1	2	3
Sample taking [min]	690	720	750
Number of crystal analyzed	68	43	43
Mean diameter ( $d_m$ ) [ $\mu\text{m}$ ]	521.03	448.26	435.93
CV [%]	42.7	46.8	34.9
Growth rate (G) [ $\mu\text{m}/\text{min}$ ]	0.6014	0.6009	0.5310
Nucleation rate ( $B^0$ ) [no./( $\text{L} \cdot \text{min}$ )]	9189	13862	11758

### 5.3.3 SEM AND EDX ANALYSIS

The recovered  $\text{Na}_2\text{SO}_4$  crystals from all the wastewater solutions have been analyzed by SEM and EDX to estimate structure and impurities. Sodium sulfate exists in different hydrate forms including the anhydrous form (Thenardite), heptahydrate and decahydrate (Mirabilite). However, the stable forms are considered as Thenardite and Mirabilite with transition around 33 wt.%  $\text{Na}_2\text{SO}_4$  and a temperature of 32 °C [10]. However, addition of NaCl up to 15 wt.% decreases the transition temperature to 25 °C as a consequence of decreased  $\text{Na}_2\text{SO}_4$ –water interactions [11]. The polymorph recovered by membrane crystallization, in DCMD configuration, is normally the form of Thenardite [4], [12], [13]. The easy control of MCr has previously shown the great potential of targeting the desired polymorphs by changing operational conditions [14] as also described in Chapter 3. The obtained SEM images of crystals recovered from different solutions can be seen in Figure 5.10 at different magnifications. EDX analyses have been performed to analyze the composition of the crystals and to estimate if any impurities are present. The EDX analysis (Figure 5.12) clearly shows that mainly sodium sulfate has been precipitated, though a very small amount of impurities of calcium and magnesium have been incorporated in solution # 3 and 4, accounted by the higher concentration of these ions in the wastewater at crystallization time due to the nanofiltration pretreatment. The weight percent of Thenardite and Mirabilite have been estimated by analyzing the molar mass of each component with respect to the total mass of Thenardite and Mirabilite, respectively. Since EDX does not measure hydrogen, it has not been considered in the total molar mass of Mirabilite. The weight percent estimations indicate that Thenardite has been precipitated since the weight percent of oxygen in case of Mirabilite should be much higher (~74%).

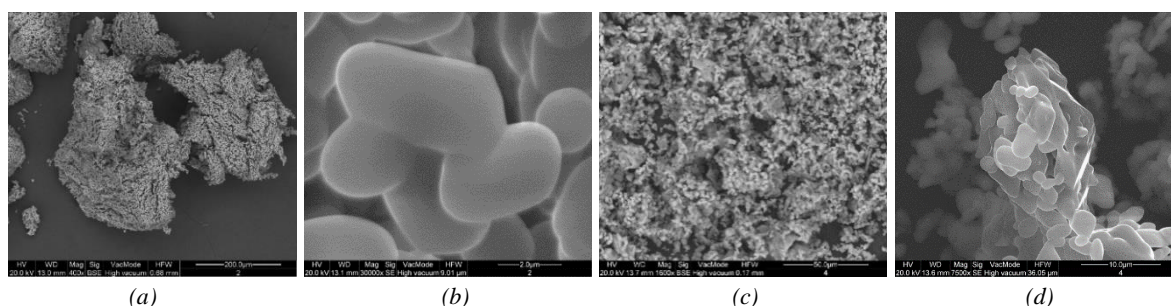


Figure 5.10. SEM images of (a)  $\text{Na}_2\text{SO}_4$  from solution # 1 – magnification 400x, (b)  $\text{Na}_2\text{SO}_4$  from solution # 1 – magnification 30000x, (c)  $\text{Na}_2\text{SO}_4$  from solution # 2 – magnification 1600x and (d)  $\text{Na}_2\text{SO}_4$  from solution # 2 – magnification 75000x.

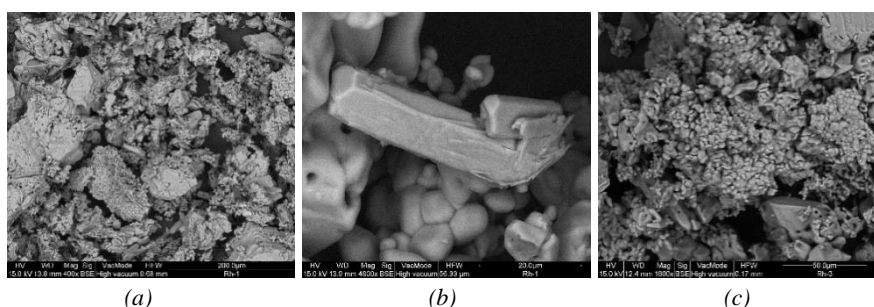


Figure 5.11. SEM images of (a)  $\text{Na}_2\text{SO}_4$  from solution # 3 – magnification 400x, (b)  $\text{Na}_2\text{SO}_4$  from solution # 1 – magnification 4800x, (c)  $\text{Na}_2\text{SO}_4$  from solution # 4 – magnification 1600x and (d)  $\text{Na}_2\text{SO}_4$  from solution # 4 – magnification.

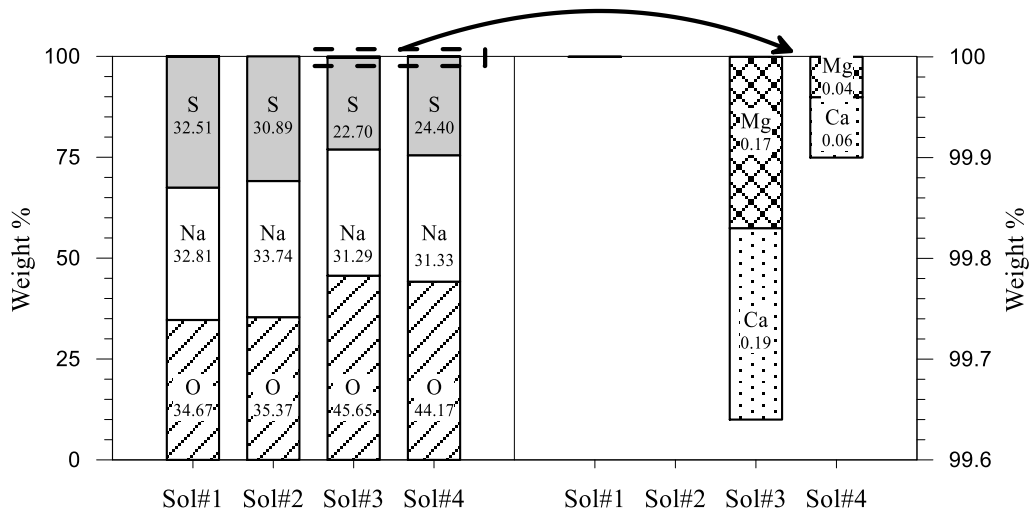


Figure 5.12. EDX analysis of  $\text{Na}_2\text{SO}_4$  recovered through MCr.

### 5.3.4 UNTREATED WASTEWATER VS. PRETREATED WASTEWATER

In this study a higher normalized flux is achieved for the nanofiltration solutions, indisputably in a more scattered and uncontrollable version. Despite the additional efforts required to achieve stable performance of MD/MCr in terms of steady trans-membrane flux, the nanofiltered solutions has a positive effect on experimental duration for achieving super-saturation of  $\text{Na}_2\text{SO}_4$  and can also reduce the membrane area required for MD/MCr. Moreover, pretreatment enhances the prospects of avoiding scaling. However, if MD is applied from the untreated wastewater, a stream of high quality fresh water is obtained. Nanofiltration permeate still contains ions, mainly monovalent, thus additional treatment for meeting stringent discharge requirements are necessary. The recovery factor (Eq. 5.3) of the ultrapure permeate is illustrated in Figure 5.13, where the recovery factor is above 60 % for all the treated wastewater solutions. Taking into account the stable performance in terms of trans-membrane flux for solution # 1 and 2 (also during  $\text{Na}_2\text{SO}_4$  precipitation), the experimentation could have been extended, thus further approaching the objective of zero liquid discharge. Therefore, the stable performance of the unfiltered wastewater is weighted higher than the NF treated wastewater.

$$\text{Recovery Factor} = \frac{\text{Total volume}_{\text{permeate}}}{\text{Total volume}_{\text{feed, initial}}} \quad (\text{Eq. 5.3})$$

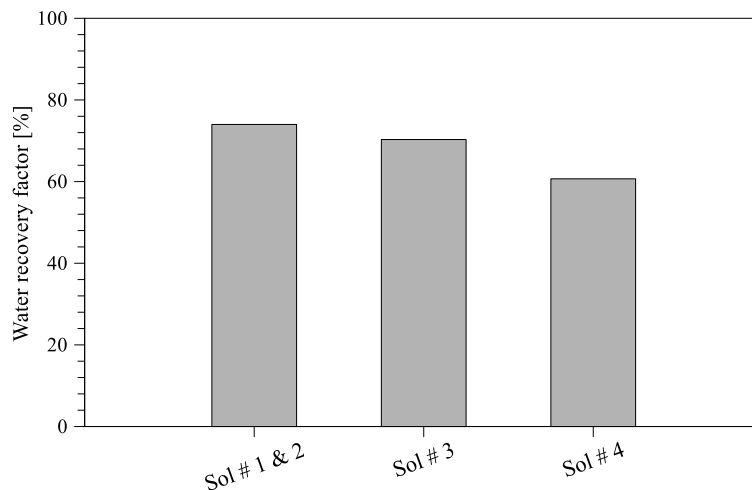


Figure 5.13: Recovery factor of the four wastewater solutions

## 5.4 SUMMARY

Membrane distillation and membrane crystallization have been utilized for treatment of wastewater containing high amounts of sodium sulfate. Two tests on raw wastewater (solution # 1 and 2) and two tests on wastewater which have been treated by nanofiltration prior to the MD/MCr process (solution # 3 and 4) have been carried out. The untreated wastewater showed the most stable performance for more than 90 h with no decline in trans-membrane flux despite the very high scaling potential of components such as calcium and magnesium. Sodium sulfate has been recovered as a high quality product in terms of narrow size distribution, low coefficient of variation, constant growth rate and low incorporation of impurities. Crystallization from the nanofiltered wastewater indicated a higher incorporation of impurities into the crystal lattice caused by the higher amounts of bivalent ions with respect to the unfiltered wastewater. Therefore, due the stable performance and reduced incorporation of impurities, the unfiltered wastewater might be more suitable for directly treatment by means of MD and MCr.

## REFERENCES

- [1] U.S. Geological Survey, “Mineral Commodity Summaries - Sodium sulfate,” 2013.
- [2] S. Genkinger and A. Putnis, “Crystallisation of sodium sulfate: supersaturation and metastable phases,” *Environ. Geol.*, vol. 52, no. 2, pp. 329–337, Nov. 2007.
- [3] R. J. Flatt, “Salt damage in porous materials: how high supersaturations are generated,” *J. Cryst. Growth*, vol. 242, no. 3–4, pp. 435–454, Jul. 2002.
- [4] E. Curcio, X. Ji, A. M. Quazi, S. Barghi, G. Di Profio, E. Fontananova, T. Macleod, and E. Drioli, “Hybrid nanofiltration–membrane crystallization system for the treatment of sulfate wastes,” *J. Memb. Sci.*, vol. 360, no. 1–2, pp. 493–498, Sep. 2010.
- [5] W. Li, B. Van der Bruggen, and P. Luis, “Integration of reverse osmosis and membrane crystallization for sodium sulphate recovery,” *Chem. Eng. Process. Process Intensif.*, vol. 85, pp. 57–68, Nov. 2014.
- [6] F. Macedonio and E. Drioli, “Hydrophobic membranes for salts recovery from desalination plants,” *Desalin. Water Treat.*, vol. 18, pp. 224–234, 2010.
- [7] H. G. Wiedemann and W. Smykatz-Kloss, “Thermal studies on Thenardite,” *Thermochim. Acta*, vol. 50, pp. 17–29, 1981.
- [8] S.J. Jancic and P. A. M. Grootcholten, *Industrial crystallization*. Delft, Holland: Delft University Press, 1984.
- [9] E. Curcio and E. Drioli, “Membrane Distillation and Related Operations — A Review,” *Separation and Purification Reviews*, vol. 34, pp. 35–86, 2005.
- [10] K. Thomsen, “Aqueous Salt Solutions.” . <http://www.phasediagram.dk>
- [11] P. Bharmoria, P. S. Gehlot, H. Gupta, and A. Kumar, “Temperature-Dependent Solubility Transition of Na<sub>2</sub>SO<sub>4</sub> in Water and the Effect of NaCl Therein : Solution Structures and Salt Water Dynamics,” *J. Phys. Chem. B*, vol. 118, pp. 12734-12742, 2014.
- [12] C. M. Tun, A. G. Fane, J. T. Matheickal, and R. Sheikholeslami, “Membrane distillation crystallization of concentrated salts—flux and crystal formation,” *J. Memb. Sci.*, vol. 257, no. 1–2, pp. 144–155, Jul. 2005.
- [13] C. M. Tun and A. M. Groth, “Sustainable integrated membrane contactor process for water reclamation, sodium sulfate salt and energy recovery from industrial effluent,” *Desalination*, vol. 283, pp. 187–192, Dec. 2011.
- [14] G. Di Profio, S. Tucci, E. Curcio, and E. Drioli, “Controlling Polymorphism with Membrane-Based Crystallizers : Application to Form I and II of Paracetamol,” *Chem. Mater.*, vol. 19, pp. 2386–2388, 2007.



---

## CHAPTER 6:

# RECOVERY OF NaCl FROM PRODUCED WATER

---

### 6.1 INTRODUCTION

Produced water is by-product coming from oil and gas industry. It represents the largest wastewater stream from oil and gas industry. Around 250 million barrels of produced water is produced each day [1]. It includes water from reservoirs and water used for injection water to force the oil to be pumped to the surface. The produced water is characterized by having high salinity and dispersion of oil and greases. Heavy metals, radionuclides, production chemicals, dissolved gases, scale products, waxes and microorganism can also be found in the produced water [1]. According to Arthur, Langhus, and Patel [2] some of the possible strategies to manage produced water are: 1) Controlling production of water by using polymer gel that blocks the water or water separators, although it is not always possible; 2) Injection back to the formations; 3) Discharge of the produced water after treatment for meeting specific standards; 4) Reuse after treatment for drilling etc.; 5) Reuse after extensive treatment for irrigation, animal watering or potable use. From an environmental point of view and for meeting regulations for discharge or reuse, treatment is of great importance. Since fresh water resources are being depleted, extensive treatment of produced water might also be a useful water source for protection of the depleting water resources.

Numerous of treatment options have been applied on produced water such as physical, chemical, biological and membrane treatment. Physical treatment includes adsorption of dissolved organics, metal removal by sand filtration, cyclones for separation of water-oil-gas phases, evaporation etc. [3]. Chemical treatment involves precipitation, oxidation, Fenton processes, ozone treatment etc. [3]. Biological treatment is mainly the activated sludge process [3]. However, these type of processes are contradicting with the process intensification strategy and green and sustainable development. The reason is the non-environmental friendly process for the use of hazardous chemicals, high costs, high energy consumptions, secondary pollution and large footprints [3].

Several studies have highlighted the positive aspects of membrane based treatment [1], [3], [4]. In the past, pressure driven membrane operations have been mostly investigated for produced water treatment. However, the conventional pressure driven membrane operations have severe problems at high salinity levels. Membrane distillation has recently gained increased attention for the treatment of oil and gas produced water [5]–[7]. This study intends to evaluate the feasibility of MCr for not only treating the produced water but also for recovering minerals from the stream. Generally very high salinity level of this stream restricts the treatment options. MCr has the capability to concentrate the solution to their saturation level, thus providing the possibility to extract fresh water and to recover valuable components from various streams. The objective of the current study is to investigate the MCr process applied for recovery of minerals and fresh water production from microfiltered oilfield produced water.

## 6.2 MATERIALS AND METHODS

### 6.2.1 FEED COMPOSITION

Produced water samples have been initially pretreated by microfiltration and activated carbon filtration for oil separation, removal of suspended solids and removal of H<sub>2</sub>S. The water contains 248 g/L of TDS and traces of volatile compounds. Ionic analysis of the water carried out by ionic chromatograph (Metrohm 861 Advanced Compact IC) has been provided in Table 6.1. Total organic carbon (TOC) analysis has been performed according to the detailed procedure described elsewhere [8]. In membrane crystallization, calcium is often removed by chemical treatment to avoid the undesired scaling phenomena [9], [10]. Nevertheless, in this study the produced water has not been treated chemically prior to MD and MCr in order to evaluate the feasibility of direct treatment.

Table 6.1: Main properties of produced water used

Property	Value
TDS	248,000
Conductivity (mS/cm)	228.2
pH	6.15
TOC	18.10
TC	40.72
Sodium Na [ppm]	76,646
Calcium Ca [ppm]	6,065
Magnesium Mg [ppm]	8,361
Potassium K [ppm]	1,396
Chloride Cl [ppm]	144,057
Phosphate [ppm]	1055
Sulfate SO <sub>4</sub> [ppm]	1213
Nitrate NO <sub>3</sub> [ppm]	613
Fluoride F [ppm]	472

### 6.2.2 MEMBRANE CRYSTALLIZATION TESTS

To test the initial technical feasibility of MCr for simultaneous recovery of water and salt crystals from produced water, experimentation has been carried out by using small scale membrane modules. PP and PVDF membranes have been utilized (Table 6.2). MCr tests have been performed at feed temperatures of 35°C, 45°C and 55°C for each membrane while the permeate temperature has been kept constant at 10°C. For these temperatures, feed and permeate flow rates have been adjusted at 150 and 70 ml/min, respectively. In order to avoid blockage of fibers due to possible scaling, shell to lumen side configuration has been applied. The lab-scale plant has been described in details in Chapter 4. After confirming the technical feasibility of the process at small scale, the experimentation has been extended at semi-pilot scale by using commercial PP modules from Microdyn Nadir (Table 6.2) at feed and permeate inlet temperatures of 40°C and 15°C, respectively. Description of the semi-pilot scale can be found in Chapter 5. The quality of distillate has been analyzed after regular interval by monitoring its conductivity. The produced crystals have been characterized with the procedure described in Chapter 4.

Table 6.2: Membrane characteristics used in MCr treatment of produced water

Fiber type	Thickness [mm]	Pore size [μm]	Porosity [%]	Membrane area [m <sup>2</sup> ]
PP lab-made module	0.45	0.2	73	0.0056
PP commercial modules	0.45	0.2	73	0.2
PVDF	0.40	0.23	80.77	0.0021

### 6.3 RESULTS AND DISCUSSION

Trans-membrane flux for small scale modules have been illustrated in Figure 6.1. It can be noticed that, as expected, the flux is increasing by increase in feed temperature and driving force for both the utilized membranes. PVDF membrane exhibits higher flux, due to higher pore size and porosity together with a lower thickness with respect to PP membrane. Similar value of flux at low temperatures for PP membrane has been found in the larger scale system (Figure 6.2). Recovery factors, illustrated in Figure 6.1 and Figure 6.2, for most of the tests have been obtained around or above 35 %. The reason for the slightly decline in flux is the increase in concentration which suppress the vapor pressure; hence the driving force.

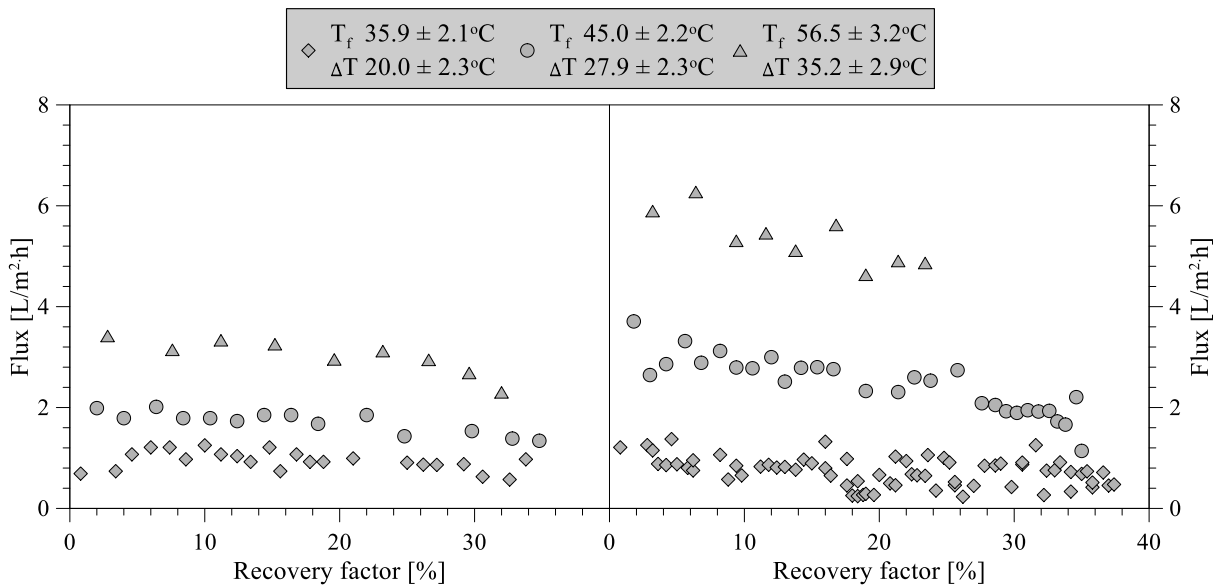


Figure 6.1: Trans-membrane flux of PP and PVDF membranes in MCr tests of produced water.

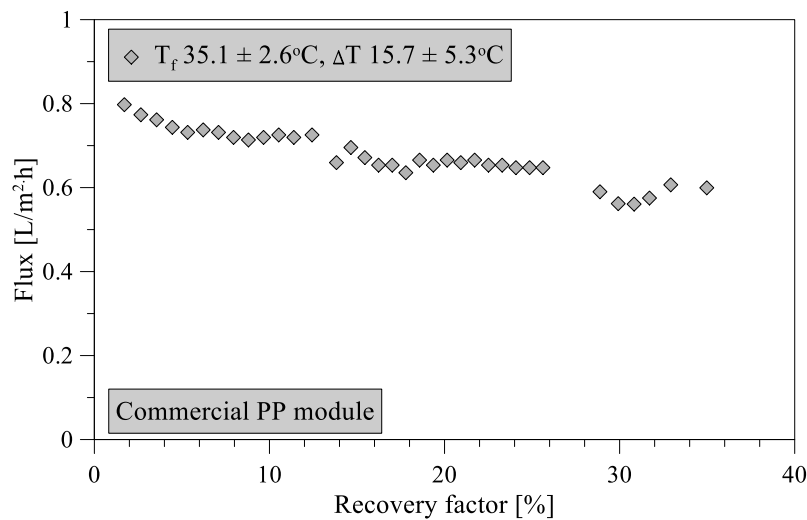


Figure 6.2: Trans-membrane flux of commercial PP module in MCr tests of produced water.



### 6.3.1 CHARACTERIZATION OF RECOVERED CRYSTALS

The recovered crystals have been analyzed with SEM, EDX and x-ray diffractometer (XRD). SEM images shown in Figure 6.3 at different magnifications illustrate a cubic structure. To analyze the composition and purity of the crystals, EDX and XRD analysis have been performed. The spectrum of one EDX analysis, given in Figure 6.4, clearly shows that only sodium chloride without any impurities detected, is crystallized from the produced water. This analysis has been confirmed by XRD (Figure 6.5) where the sample of crystals recovered from produced water shows the same peaks as for XRD spectra of NaCl from literature. The recovered crystals have been separated from the solution and have been dried to estimate experimentally the quantitative potential of crystal recovery per unit volume of feed. The weight of crystals separated from small and semi-pilot plant showed that 16.4 kg of the high quality crystals can be recovered per cubic meter of produced water at water recovery factors of 35%.

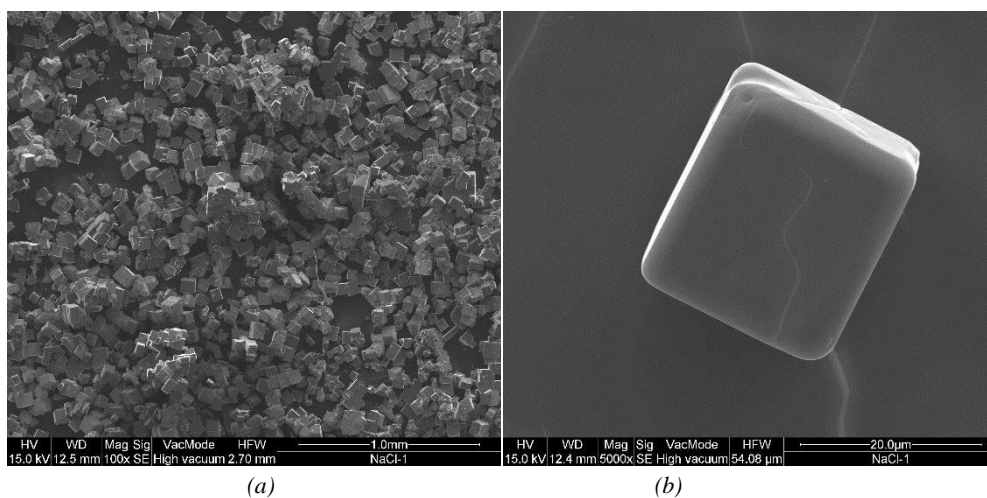


Figure 6.3: SEM images of the crystals precipitated from produced water (a) Area of crystal sample – magnification: 100x, (b) Single crystal – magnification: 5000x

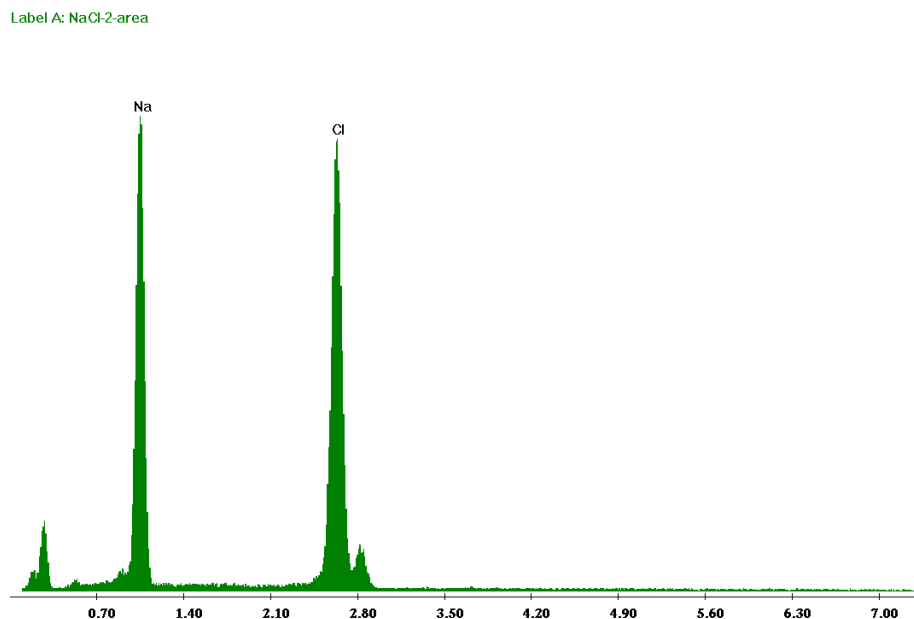


Figure 6.4: Example of EDX spectra obtained for the crystals precipitated from produced water.

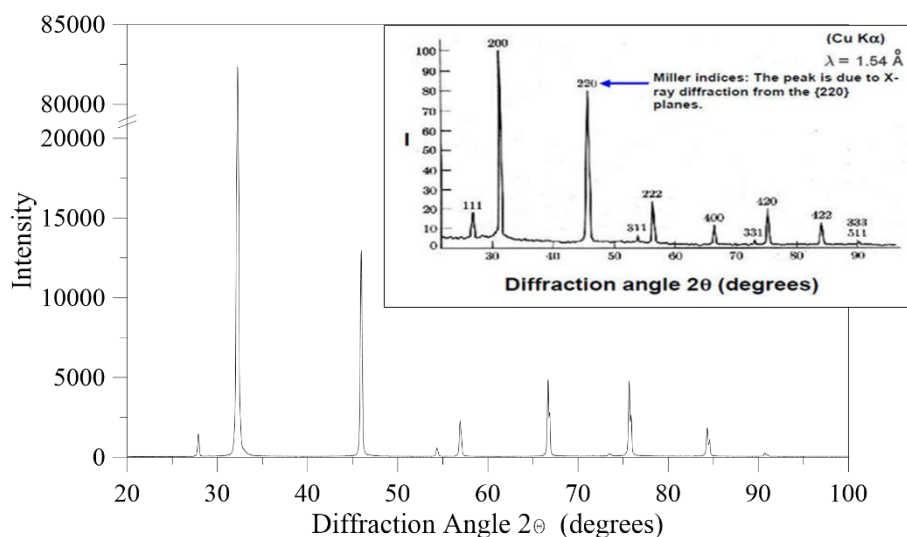


Figure 6.5: XRD spectra obtained from the recovered crystals from produced water.

Once the first crystals have been observed, a sample of mother liquid containing crystals have been analyzed by optical microscope. Mean diameters of recovered crystals at different temperatures by using two membranes, are shown in Figure 6.6. The figure indicates that mean diameter using PVDF membrane shows the trend of an increase in diameter with increasing temperature. The increasing feed temperature improves the trans-membrane flux and hereby the supersaturation gradient, which is the driving force for crystal growth. However, mean diameters of the produced crystals by using PP membrane at different feed temperatures are not showing any clear trend. Growth rate has the same trend as mean diameter, where the recovery at constant feed flow rate is higher for the highest temperature (Figure 6.7b), which is explained by the higher supersaturation ratio caused by the higher flux at 55 °C.

In comparison of PVDF and PP membrane, the growth rate by using PVDF membrane is much lower as compared to PP (Figure 6.7a). The reason is the difference in membrane surface area between the two modules, i.e. 0.0021 m<sup>2</sup> for PVDF and 0.0056 m<sup>2</sup> for PP, thus the same concentration factor can be reach sooner using PP membrane and therefore the growth rate increases.

Besides supersaturation gradients, mean diameter and crystal growth is also influenced by feed flow rates, due to a control in the transfer of material from solution to crystal interface (diffusion) and by organization of material from the interface into the crystal lattice (integration) [44], [45]. Either the diffusion or integration is the rate limiting step. If mean diameter and crystal growth increase with increasing feed flow rate, the diffusion step is rate limiting. Likewise if mean diameter and crystal growth is suppressed at higher feed flow rates, it is the integration of material into crystal lattice which is the rate determining step. In crystallization from produced water, the average mean diameter and growth rate decreases with increase in feed flow rate (Figure 6.6b and Figure 6.7b). Therefore, the limiting step of crystal growth is the integration step under the given operative conditions.

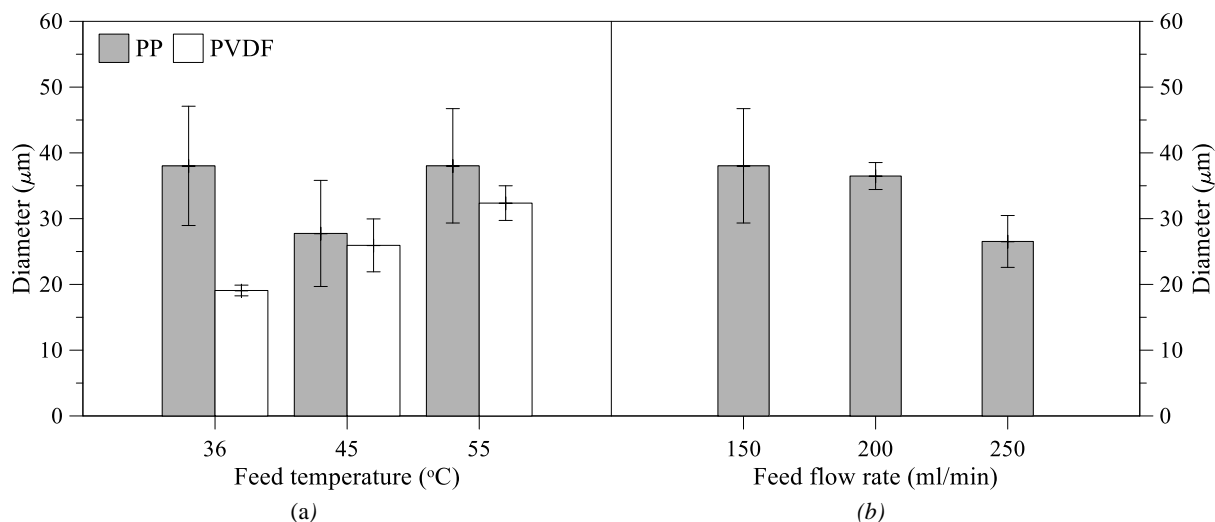


Figure 6.6: Mean diameter of the produced crystals at different feed temperatures and feed flow rates (a and b respectively).

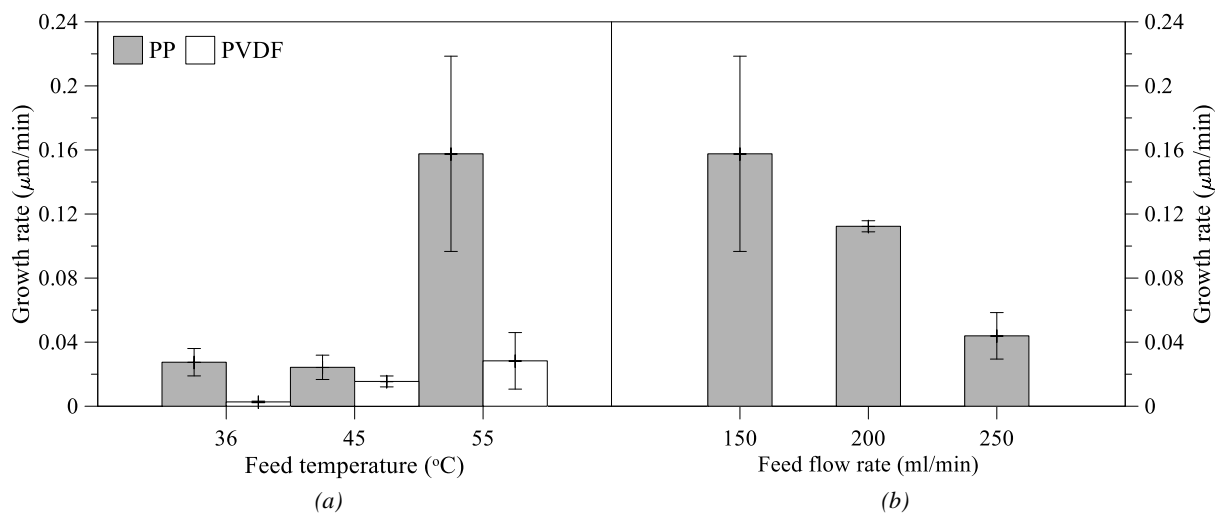


Figure 6.7: Growth rate of the produced crystals at different feed temperatures and feed flow rates (a and b respectively).

In general membrane crystallizers produce crystals of high quality in terms of uniform size distribution. In this study CV tend to have lower value with increasing temperature (Figure 6.8). This can be attributed to the easier dissolution of small particles at higher temperatures, thus making the crystal product more uniform with respect to size distribution. No clear tendency is observed for the different feed flowrates, although the majority of the obtained values show a uniform production by having CV values below 50%, which is normally obtainable for industrial crystallizers [46] and in the ranges of what have been achieved by membrane crystallization in other studies [47].

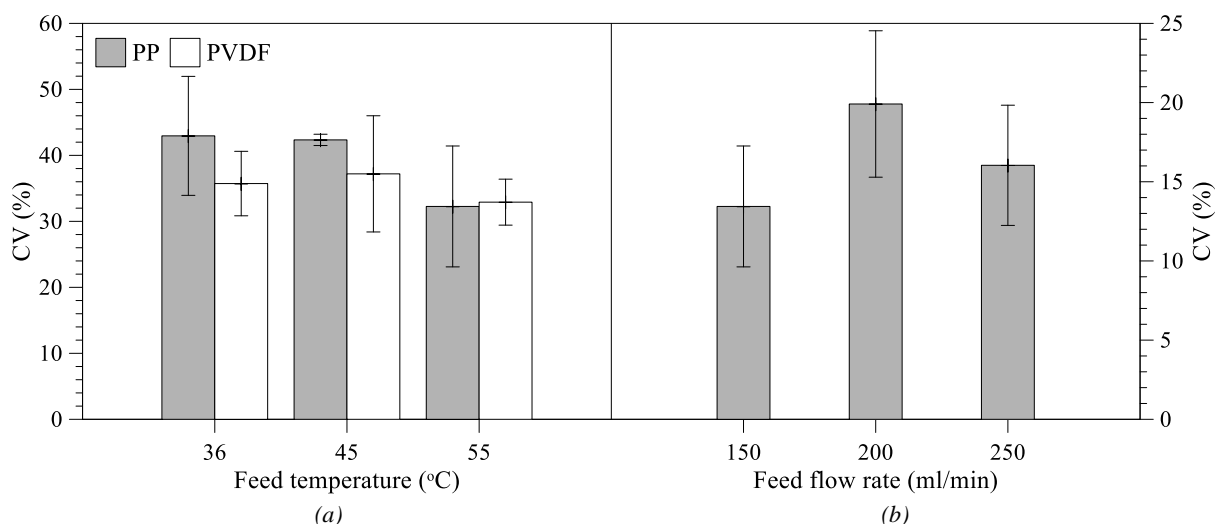


Figure 6.8: Coefficient of variation (CV) of the produced crystals at different feed temperatures and feed flow rates (a and b respectively).

Similar to lab scale units, the crystals from semi-pilot scale plant have also been recovered and characterized. Once the first crystals have been observed, a sample of mother liquid containing crystals has been analyzed by optical microscope. Sample 2 and 3 have been characterized after 20 min and 40 min from crystallization onset, respectively. From the crystal images, mean diameter, CV and growth rate have been estimated and are shown in Figure 6.9. Diameter of the crystals is increasing with passage of time due to the nature of crystal growth and the continued incorporation of materials into the crystal lattice. The relative constant increase in diameter and growth rate indicates that the crystallization process is well-controlled and no crystals are growing uncontrollable nor breaking.

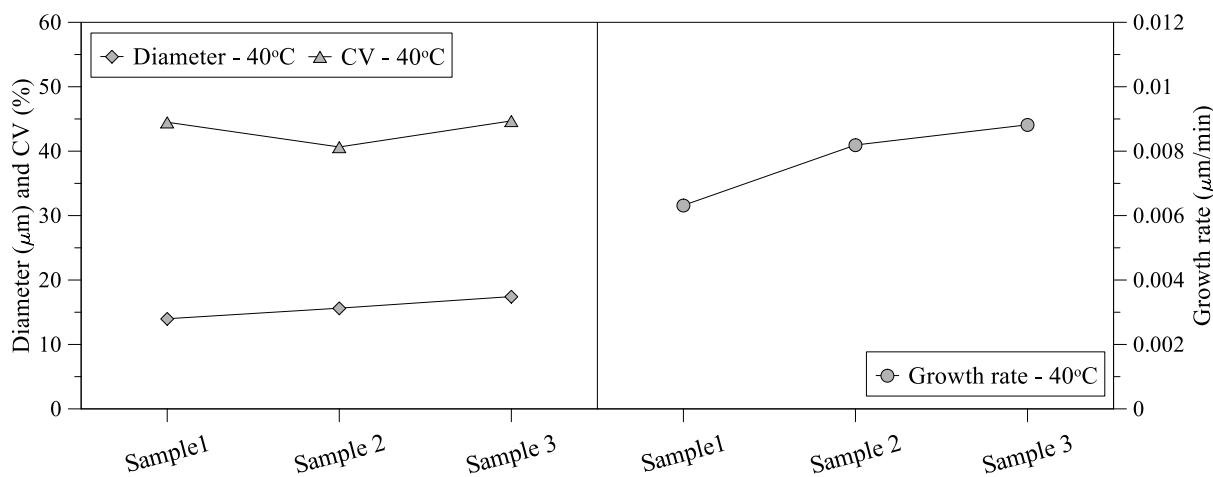


Figure 6.9: Diameter, coefficient of variation and growth rate for crystals recovered from semi-pilot plant at different time intervals

Sodium chloride which is normally characterized by having a cubic shape, shows the same tendency in this work. Deviation from cubic structure can be influenced by impurities in the solution [47]. The main part of the produced crystals shows a length to width ratio below 1.4 (Figure 6.10), illustrating the good cubic structure. No particular trend between PP and PVDF membrane and the different temperatures and flow rate is observed, thus no disturbance of the cubic crystal growth or incorporation of impurities which can impact the crystal habit has been affected by the various operative conditions.

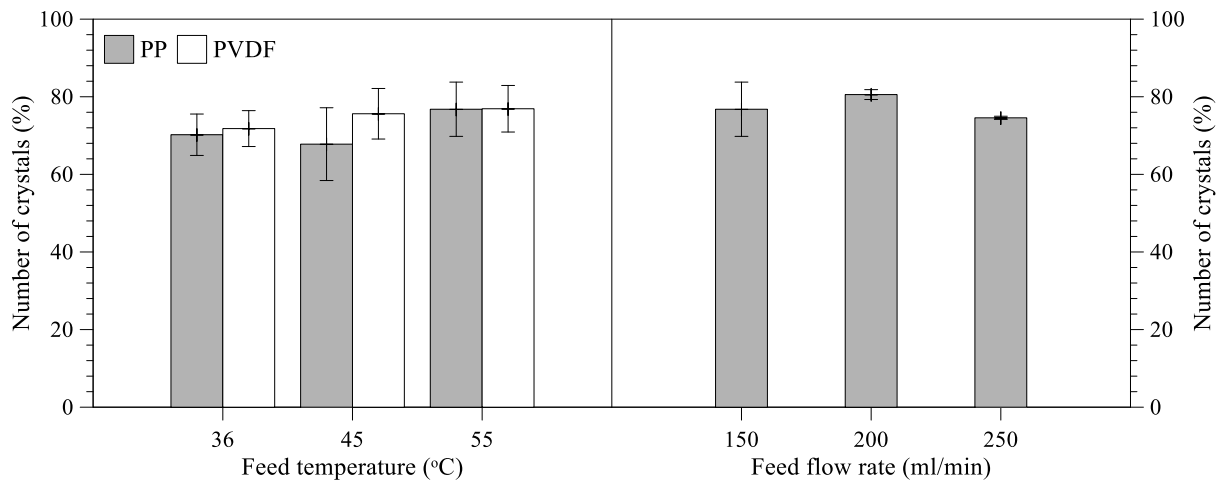


Figure 6.10: Percentages of analyzed crystals with length to width ratio below 1.4.

### 6.3.2 EVALUATION OF NEW METRICS

The impact of treatment by means of membrane crystallization has been evaluated through new metrics as described in Chapter 1. In particular, mass intensity (MI), waste intensity (WI), productivity/size ratio (PS) and productivity/weight ratio (PW) have been calculated for the utilized MD/MCr plant utilizing polypropylene membranes. Changes of mass and waste intensities and productivity with respect to size of membrane ( $0.2 \text{ m}^2$  – active surface area) and weight ( $0.467 \text{ kg}$  - module) have been identified. In the beginning of the experiment, water has only been considered the product and in the end of the experiment both water and salt have been considered. From the time of saturation, NaCl is being produced at rate of  $0.063 \pm 0.012 \text{ kg/h}$ . MI and WI decrease significantly with increase in water recovery factor (Figure 6.11) from above 35 to below 3 and 2 for MI and WI, respectively.

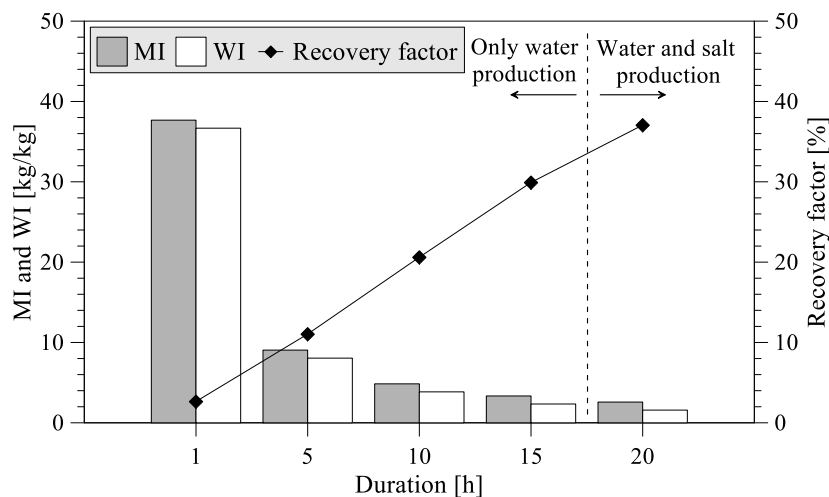


Figure 6.11: Mass and waste intensities and overall water recovery factor with duration of treatment.

PS and PW have been estimated based on membrane area and weight of module and only based on membrane system (Figure 6.12). Prior to NaCl saturation, PS is equal and PW is proportional to trans-membrane flux, respectively. The slight decrease in PS and PW is due to concentration increase, which decrease the driving force. The feed temperature utilized in this experiment has been relatively low (around  $35 \text{ }^\circ\text{C}$ ), thus the productivity can be easily increased. These numbers also indicates the flexibility of a MD/MCr plant. Moreover, PS and PW are increasing when salt is precipitating. In fact, NaCl is being recovered in similar range as water with PS of  $0.32 \text{ kg}/(\text{m}^2\text{h})$  and  $0.56 \text{ kg}/(\text{m}^2\text{h})$  for salt and water,

respectively. Furthermore, the evaluation of the new metrics has to be seen with respect to water recovery factor. In the carried out experiments a recovery factor of only 37% have been obtained and continued treatment will have improved impact on MI and WI. Taking into account the relative stable flux and no wetting of the membrane indicate that the experiment could have been continued. Nevertheless, in order to increase water and salt recovery, it is necessary to introduce a continuous crystal recovery system to avoid crystal accumulation in the MCr plant and on membrane surface.

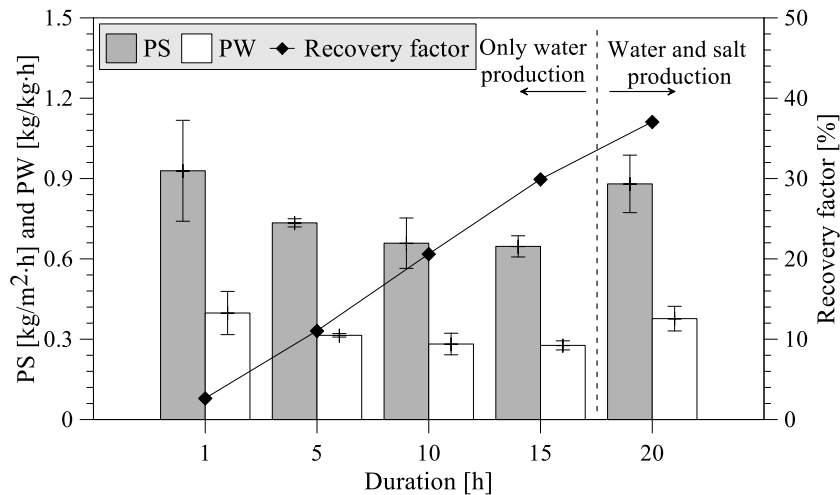


Figure 6.12: Productivity/Size, Productivity/Weight ratio and overall water recovery factor with duration of treatment

## 6.4 SUMMARY

MCr is technically feasible technique to simultaneously recover fresh water and minerals from produced water, providing the opportunity to implement the concept of process intensification strategy in produced water management. The process shows stable performance when the formed crystals are simultaneously recovered from the solution. Major decrease in flux arises from increase in solution concentration that suppresses the vapor pressure of the solution. Flux decay is higher when process is carried out at high feed temperature. High quality crystals are produced starting from water recovery factor of 33%. The crystals are characterized by having no incorporation of impurities, very uniform size distribution illustrated by low coefficient of variations and a good cubic structure. Crystal growth increases by increasing feed temperature, due to the higher super-saturation ratio achieved due to higher flux. Opposite is the trend of crystal growth with respect to feed flow rates, where the growth decreases with increase of flow rates. Therefore, the limiting step of crystal growth is the integration of material from the interface into the crystal lattice under operative conditions applied in current study.

## REFERENCES

- [1] E. T. Igunnu and G. Z. Chen, "Produced water treatment technologies," *Int. J. Low-Carbon Technol.*, pp. 1–21, Jul. 2012.
- [2] J. D. Arthur, B. G. Langhus, and C. Patel, "Technical summary of oil and gas produced water treatment technologies," *All Consulting, LLC, USA*, 2005.
- [3] A. Fakhru'l-Razi, A. Pendashteh, L. C. Abdullah, D. R. A. Biak, S. S. Madaeni, and Z. Z. Abidin, "Review of technologies for oil and gas produced water treatment.," *J. Hazard. Mater.*, vol. 170, no. 2–3, pp. 530–51, Oct. 2009.
- [4] E. Drioli, A. Ali, Y. M. Lee, S. F. Al-Sharif, M. Al-Beirutty, and F. Macedonio, "Membrane operations for produced water treatment," *Desalin. Water Treat.*, 2015.
- [5] F. Macedonio, A. Ali, T. Poerio, E. El-Sayed, E. Drioli, and M. Abdel-Jawad, "Direct contact membrane distillation for treatment of oilfield produced water," *Sep. Purif. Technol.*, vol. 126, pp. 69–81, 2014.
- [6] A. Alkhudhiri, N. Darwish, and N. Hilal, "Produced water treatment: Application of Air Gap Membrane Distillation," *Desalination*, vol. 309, pp. 46–51, Jan. 2013.
- [7] S. Zhang, P. Wang, X. Fu, and T.-S. Chung, "Sustainable water recovery from oily wastewater via forward osmosis-membrane distillation (FO-MD).," *Water Res.*, vol. 52, pp. 112–21, Apr. 2014.
- [8] F. Macedonio, A. Ali, T. Poerio, E. El-sayed, E. Drioli, and M. Abdel-jawad, "Direct contact membrane distillation for treatment of oilfield produced water," *Sep. Purif. Technol.*, vol. 126, pp. 69–81, 2014.
- [9] F. Macedonio, C. a. Quist-Jensen, O. Al-Harbi, H. Alromaih, S. a. Al-Jlil, F. Al Shabouna, and E. Drioli, "Thermodynamic modeling of brine and its use in membrane crystallizer," *Desalination*, vol. 323, pp. 83–92, Aug. 2013.
- [10] F. Macedonio and E. Drioli, "Hydrophobic membranes for salts recovery from desalination plants," *Desalin. Water Treat.*, vol. 18, pp. 224–234, 2010.
- [11] W. R. Wilcox, "Crystallization flow," *J. Cryst. Growth*, vol. 12, no. 2, pp. 93–96, Feb. 1972.
- [12] A. Mersmann, A. Eble, and C. Heyer, "Crystal growth," in *Crystallization Technology Handbook*, CRC Press, 2001.
- [13] Allan Myerson, *Handbook of Industrial Crystallization*. Elsevier Inc., 2002.

---

# CHAPTER 7: TREATMENT OF HIGH CONCENTRATED LiCl SOLUTIONS

---

## 7.1 INTRODUCTION

Conventional resources of raw materials are depleting rapidly due to increasing population and improved living standards [1], thus the development of future society is strongly related with continuous and adequate supply of raw materials. The speed of mineral extraction is higher than ever for their rapidly growing demand. However, the resources of raw materials are finite and require sustainability in terms of production, manufacturing, use and recovery. As mineral and metals depletion are becoming a reality, the primary production is getting more difficult, expensive [2] and requires more energy [3]. The problem of water availability in mining and energy production creates a new and recent realized problem to mineral extraction. Stressed nexus of raw material resources, fresh water and energy raise the question on how long time mineral production can be carried out at the speed of the required quantities/qualities at reasonable costs [3].

An example of a future possible scarce element is lithium, which is interesting, in particular, for its increasing use in lithium-ion batteries for replacing the fuel dependent transportation system with electrical or hybrid electrical vehicles. Different studies discuss the availability of lithium sources in relation to whether the available lithium in future is able to meet the demand [4]–[7]. Lithium compounds are mainly being produced from brines and hard-rock mining [8]. Several drawbacks are attributed to the state-of-the-art lithium recovery such as low lithium grades, low recovery factors, complications in making new production sites or enlarging existing areas for salt lake brines [6]. Furthermore the mining industry is harsh for the environment and associated with high level of pollution [6]. Some drawbacks are also associated with the recovery of lithium from salt-lake brine such as contaminants and separation from compounds such as magnesium [9].

Recovery of components of interest from waste streams and exploitation of nontraditional sustainable resources are the fundamental keys to realize the objective of sustainable development. As previous discussed, seawater contains all the elements present in periodic table, providing the opportunity to recover rare or expensive elements. Extraction of lithium from seawater could be an interesting pathway to bridge the gap between demand and supply of this material in perspective. Research on recovery of lithium from seawater has mainly been focused towards manganese oxide based adsorbents [10]–[13]. Publication from Umeno et al. [2002] and Chung et al. [2008] are membrane based adsorption which is centered on  $\text{Li}^+/\text{H}^+$  exchange [10], [11]. Supported liquid membranes might also be a potential lithium extractor from seawater [14]. However, the main issue for these technologies is the extraction at the low concentration contained in seawater at efficient rate and reasonable economic expenses. Another limitation of lithium recovery from seawater but also from brine is the magnesium to lithium ratio, i.e. 7000:1 in seawater. The magnesium content reduces the evaporation rate and the similar chemistries makes the recovery more difficult [15]. From economical point of view, the lithium production cost is as high as 80\$/kg, which is not compatible with recovery from spodumene (6-8\$/kg) or from salt lake brines (2-3\$/kg) [6]. Application of innovative processes (standalone or integrated with conventional processes) and more rational use of conventional separation and purification processes may be necessary to recover valuable components from non-conventional sources.

In order to cope the new challenges of better process control, low energy consumption, small footprint and excellent control on selection of polymorph [16], MCr has been proposed [17]–[19]. The largest seawater RO desalination plant of today; the Sorek plant in Israel has a capacity of 540,000 m<sup>3</sup>/d.



Extensive concentration to reach lithium saturation is required considering this type of plant. In Figure 7.1 the recovery factor of each step of the analysed process is reported together with the lithium concentration in seawater, RO brine, MD brine and MCr brine, respectively. It can be seen that when MCr is utilized for the concentration of the RO and MD brines, the concentration required to produce LiCl is around 14 mol/L. These high numbers of recovery factors might seem unrealistic, nevertheless as described in Chapter 1, many major research projects are aiming at this particular perspective. Not only aiming at the objective of utilizing the brine in a smarter way but also in fact, the global MVP project has specific targeted the recovery of lithium and strontium from the MD concentrated brine. Their recovery process is not yet membrane based, although it still gives perspective of the potential of lithium recovery using integrated membrane systems. Therefore, a preliminary investigation of lithium recovery by means of MCr has been carried out.

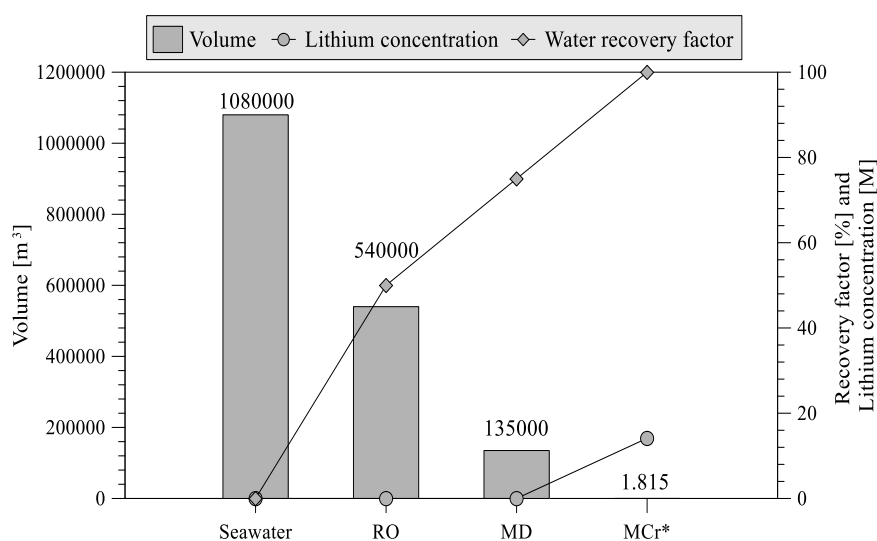


Figure 7.1: Illustration of the decrease in brine volume and increase in recovery factor for obtaining lithium recovery. (\* the bar illustrating the volume of 1.815m<sup>3</sup> cannot be seen due to the low value)

Principally, MCr can be operated in all modes of MD including direct contact, vacuum, sweep gas, air gap and osmotic shown in Figure 7.2. Beside osmotic membrane distillation (OMD), all the configurations have been described in Chapter 1. In OMD, a draw solution is used to concentrate the feed solution. All these configurations have their own merits and demerits [20]. Technical feasibility of MCr process for recovery of salts from seawater brine is well acknowledged in the literature [21]–[24] and also discussed in previous chapters. Due to its established capability to concentrate the solutions to their saturation level, MCr can be an interesting candidate for lithium recovery. MCr also possesses the potential to realize the objective of zero liquid discharge in industry. However, recovery of highly soluble components such as lithium and reaching the objective of zero liquid discharge requires the treatment of extraordinary concentrated solutions. Solubility of LiCl in aqueous solution is 15.6 mol/kg H<sub>2</sub>O (~14 M) at 20 °C [25]. At such high concentrations, the osmotic pressure of the solution can limit the migration of solvent from solution to the permeate side making the application of some MD configurations less interesting for further recovery. In current study, an experimental and theoretical comparative analysis of DCMD-MCr, OMD-MCr and VMD-MCr for treatment of highly concentrated solutions has been performed to recover crystals from single LiCl salt solutions.

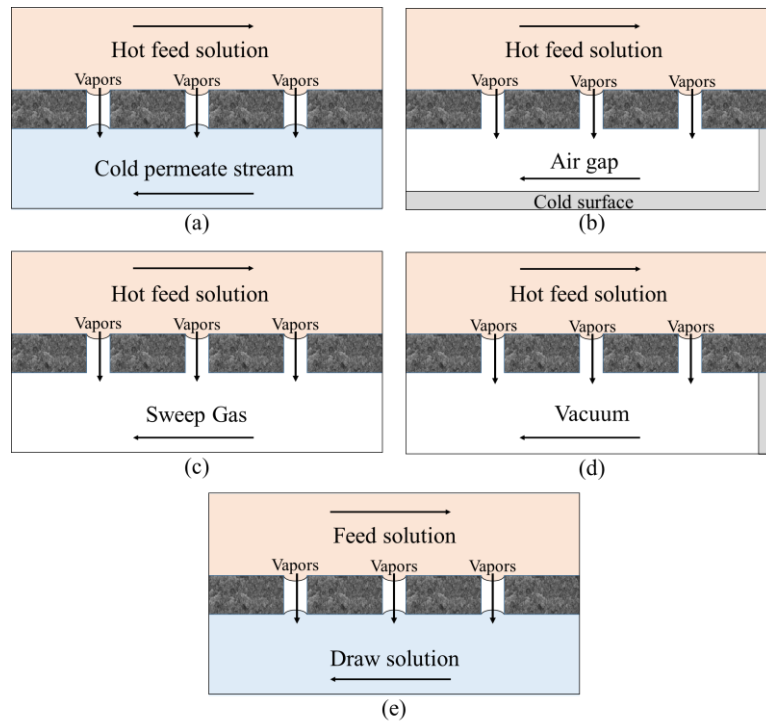


Figure 7.2: Basic configurations of membrane distillation, (a) Direct contact membrane distillation (b) Air gap membrane distillation (c) Sweep gas membrane distillation (d) Vacuum membrane distillation (e) Osmotic membrane distillation.

## 7.2 MATERIALS AND METHODS

### 7.2.1 APPLIED MEMBRANES

Two commercial polypropylene (PP) membrane modules from Microdyn-Nadir (MD020CP2N) have been used in DCMD and OMD configurations. Each module contains 40 fibers at 45 cm length with surface area of 0.1 m<sup>2</sup>. For VMD, commercial PP based hollow fibers from Membrana (Accurel® S6/2) assembled into small modules each having surface area of 0.0036 m<sup>2</sup> has been applied. The properties of applied membranes, as reported by the suppliers, can be found in Table 7.1.

Table 7.1: Properties of PP membrane applied in DCMD, OMD and VMD.

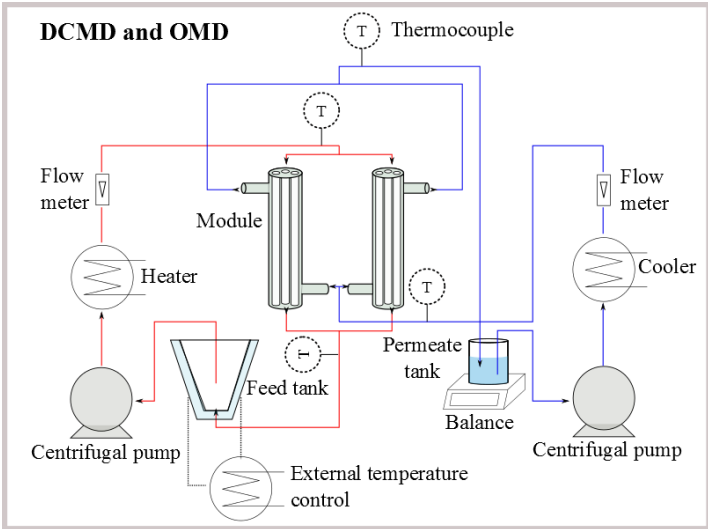
Characteristics	
Outer diameter (mm)	2.70
Inner diameter (mm)	1.80
Thickness (mm)	0.45
Average pore size (µm)	0.2
Porosity (%)	70.00
Bubble point (bar)	> 0.95

### 7.2.2 MEMBRANE DISTILLATION TESTS

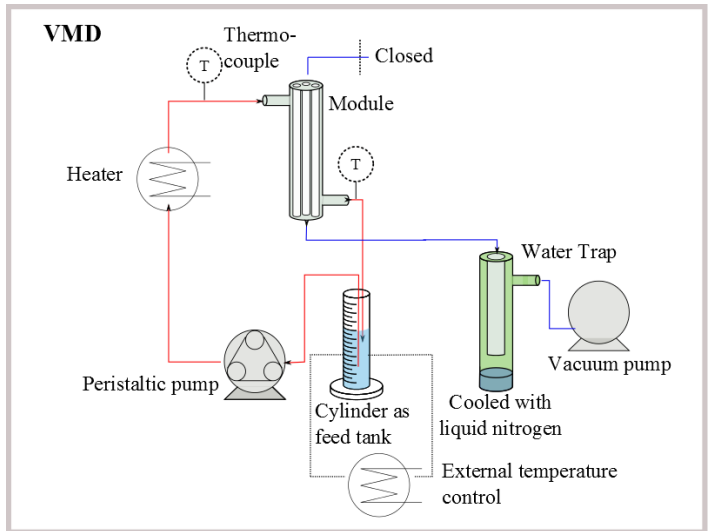
DCMD, OMD and VMD have been carried out for testing the limitations of each configuration with respect to high concentration solutions. DCMD and OMD have been carried out with feed solution in lumen side of the module and permeate in shell side. Flow rates of 100 L/h and 50 L/h have been utilized for feed and permeate side, respectively and corresponding feed and permeate temperatures have been set at 52 and 20°C at the modules inlets. OMD has been carried out in the same operative conditions but with a 4.5 M CaCl<sub>2</sub> solution as osmotic draw agent. Flow sheet of the utilized DCMD and OMD plant is illustrated in Figure 7.3a. To ensure a high driving force along the module, countercurrent flow

configurations have been applied in both cases. Detailed description of the DCMD and OMD plant can be found in Chapter 5.

In VMD, experiments have been performed at feed inlet temperatures of around 40, 50 and 60 °C and flow rates of 0.0013, 0.0025 and 0.0042 L/h corresponding to similar Reynolds numbers as used in DCMD and OMD. The flux has been determined by monitoring the decrease in feed volume using a graduated cylinder as feed tank (Figure 7.3b). The feed is transported to the shell side of the membrane module by a peristaltic pump (Masterflex – Cole Parmer Instrument Company). Feed flow rates have been adjusted directly from the peristaltic pump. Before entering into the module, feed has been heated and the temperatures have been measured at feed inlet and outlet by thermocouples. On permeate side, vacuum has been created by an oil vacuum pump (EDWARDS RV5). Permeate has been collected in a trap immersed in a dewar flask containing liquid nitrogen as the condensing liquid. The trap has been placed in between the module and vacuum pump.



(a)



(b)

Figure 7.3: Schematic representation of set-up applied for (a) DCMD and OMD, (b) VMD.

Solutions have been prepared by dissolving LiCl (VWR Chemicals, AnalaR NORMAPUR) in distillate water. Solutions of different concentrations have been prepared for use in DCMD, OMD and VMD as described in Table 7.2.

Table 7.2: Concentration of LiCl solutions used in the different configurations.

Configuration	LiCl feed concentration starting from	Permeate solution
DCMD	6 M	Distillate water
OMD	7 M	4.5 M CaCl <sub>2</sub>
VMD	8 M	(Vacuum)

For an initial characterization, produced crystals have been observed through optical microscope following the procedure described in Chapter 4.

## 7.3 RESULTS AND DISCUSSION

### 7.3.1 DIRECT CONTACT MEMBRANE DISTILLATION

DCMD flux as function of solution concentration has been shown in Figure 7.4. The figure shows that flux decreases with increase in solution concentration. The difference in vapor pressure between feed side and permeate side is the driving force for membrane distillation. The increase in concentration reduces the vapor pressure of feed solution, thus the flux approaches to zero at very high concentration. As clear from the figure, the applied membranes and operating conditions do not allow to concentrate the solution beyond 7M. The solubility of LiCl is 15.6 mol/kg H<sub>2</sub>O (~14 M) at 20 °C [25] and increases further with temperature, which is far from the possible concentration achieved in this study.

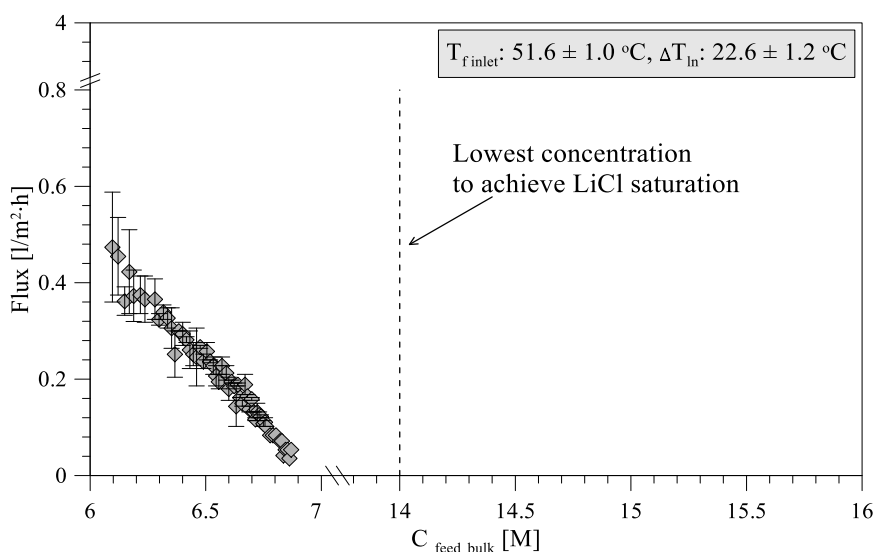


Figure 7.4: Flux for DCMD with single solute lithium chloride solution starting from 6M.

As generally acknowledged, feed concentrations play a very small role in process performance of membrane distillation [26], as also described in Chapter 1. Nevertheless, this study shows that at very high concentrations the water activity of the solution is an important parameter which decreases the vapor pressures significantly. To clarify the effect of increased concentration, a simple estimation of the flux at different feed temperatures has been carried out. Theoretical flux in MD can be described by using the following fundamental relationship

$$J = B \cdot (P_{FEED} - P_{PERMEATE}) \quad (Eq. 7.1)$$

The flux is based on the difference in vapor pressures between feed ( $P_{feed}$ ) and permeate side ( $P_{permeate}$ ). Membrane characteristic parameter  $B$  has been calculated by using Knudsen-molecular diffusion model due to close proximity of membrane pore size with mean free path of water vapors molecules (~0.11 micron) at thermal conditions considered in current study.

$$B = \left[ \frac{3\tau\delta_m}{3\epsilon r} \left( \frac{\pi RT}{8M} \right)^{1/2} + \frac{\tau\delta_m}{\epsilon} \frac{Pa}{PD} \frac{RT}{M} \right]^{-1} \quad (Eq. 7.2)$$

Where  $\tau$ ,  $\delta_m$ ,  $\epsilon$ ,  $r$ ,  $R$  and  $M$  are tortuosity factor, membrane thickness, porosity, average pore size of membrane, universal gas constant and molecular weight of water, respectively. For thermal and hydrodynamic conditions applied in current study, initial effect of temperature polarization has been incorporated by introducing a temperature polarization coefficient of 0.4 [27]. However, with increase in concentration, the temperature polarization coefficient will decrease significant making the flux lower than observed in Figure 7.5. The vapor pressure of the feed side can be estimated as a function of water activity coefficient predicted by PHREEQC [28] and vapor pressure of pure water ( $P_{water}$ ) given by the Antoine equation (Described in Chapter 4). Although, the Pitzer equations have only been validated for osmotic and activity coefficients up to ionic strengths equal to 6 M [29] and therefore might deviate at higher concentrations, this model can still indicate the problems of the decreasing vapor pressures faced in DCMD. Flux at different temperatures estimated through above scheme has been illustrated in Figure 7.5 and Figure 7.6. Feed temperature for membrane crystallization is normally between 30 and 50 °C. It can be noted from the figures that for feed inlet temperature of 30°C, the flux approaches to zero at a solution concentration of ~4M. Beyond this concentration, the osmotic effects overcome the thermal effect and a negative flux is observed. The solubility of LiCl at 30°C is above 14 M indicating that DCMD is not capable to achieve supersaturation and hence crystallization under these conditions. To maintain the positive flux by overcoming the osmotic pressure at high solution concentration, the feed temperature must be increased. The increase in feed temperature however increases further the solubility of LiCl and achievement of supersaturation still remains unachievable task. Thus, the recovery of lithium by means of DCMD configuration is impractical by using the PP membrane considered in this study.

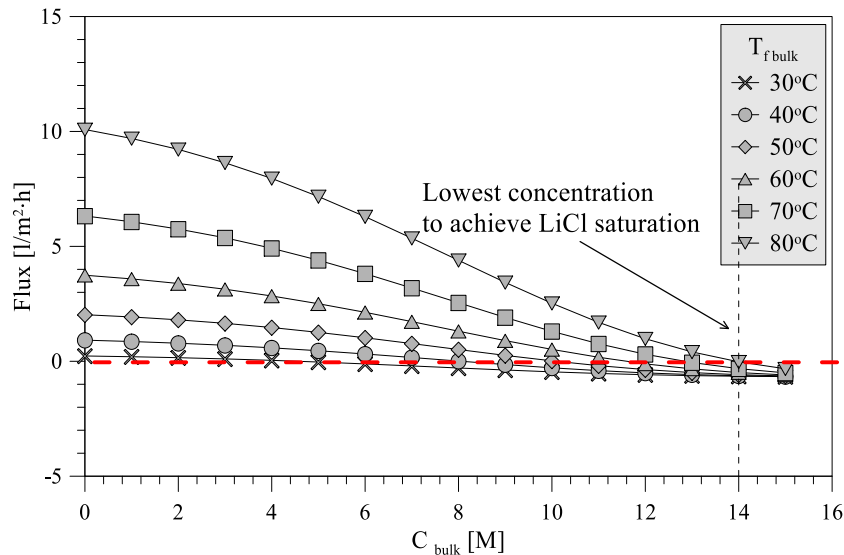


Figure 7.5 : Theoretical evaluation of trans-membrane flux at increasing LiCl concentration for several feed temperatures in the DCMD configuration. Permeate bulk temperature: 25°C.

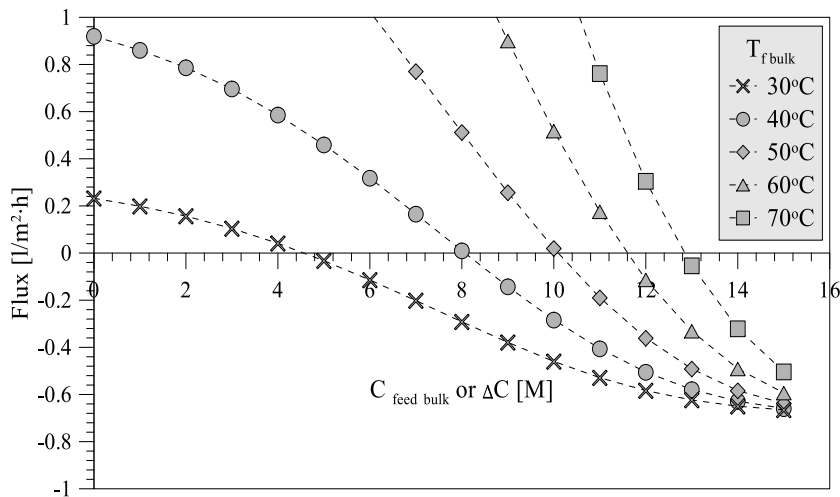


Figure 7.6: Close-up of Figure 7.5 for evaluation of negative flux.

### 7.3.2 OSMOTIC MEMBRANE DISTILLATION

Suppression of vapor pressure on permeate side can be another possible strategy to achieve higher solution concentrations in MD. This objective has been achieved by using osmotic membrane distillation (OMD). In general, OMD approach is used as isothermal membrane distillation, where the driving force is a concentration gradient. The isothermal approach allows preserving compounds which do not persist with a temperature increase. However, a combination of DCMD and OMD is more effective to increase the overall driving force and can be advantageous in recovering heat insensitive compounds such as LiCl. Thus in current study the driving force is further increased by simultaneously applying concentration difference and temperature gradient. The experimental performance of the OMD configuration is shown in Figure 7.7. OMD decreases the osmotic effect on feed side and is, therefore, able to improve the concentration factor. However, the flux declines more rapid compared to DCMD due to concentration increase on feed side and a dilution of the  $\text{CaCl}_2 \cdot 2\text{H}_2\text{O}$  solution on permeate side which further decrease the driving force. OMD in the utilized experimental conditions cannot concentrate LiCl above  $\sim 10$  M. Therefore, either more effective draw solutions with concentration restoring systems are required or another configuration has to be introduced.

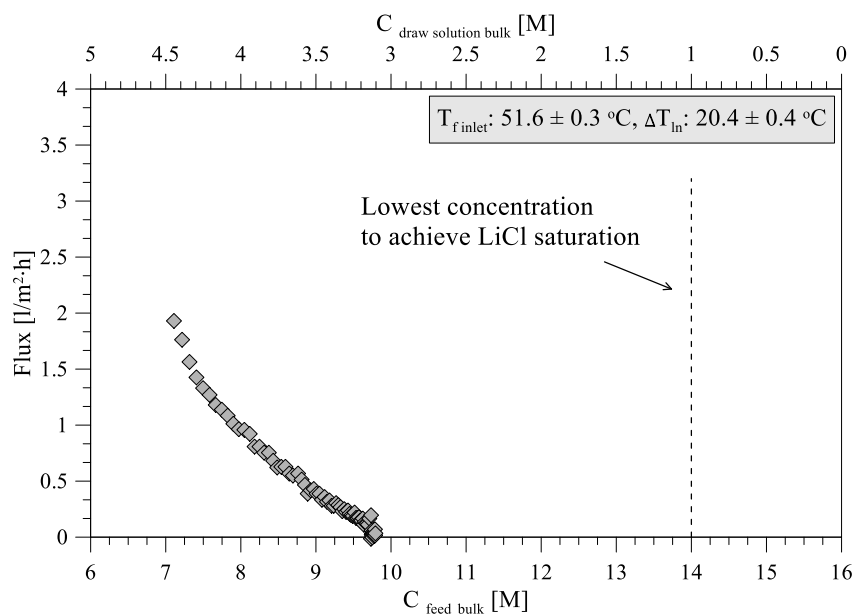


Figure 7.7: Flux for OMD with single solute lithium chloride solution starting from 7M. Draw solution: 4.5 M  $\text{CaCl}_2 \cdot 2\text{H}_2\text{O}$ .

Theoretical trans-membrane flux for OMD by using a 4.5 M  $\text{CaCl}_2 \cdot 2\text{H}_2\text{O}$  solution as draw agent has been illustrated in Figure 7.8. At feed inlet temperature of 30°C, OMD is capable to reach a solution concentration of ~9.5 M which is more than what can be achieved by using DCMD at this temperature but is still lower than the solubility limit of LiCl. Increase in feed inlet temperature to 50, 60 and 70°C allows to concentrate the solution to maximum concentrations of ~12.5, 13.5 and 14,5 M, respectively which are still lower than corresponding supersaturation concentrations at the respective temperatures. The reason for the slightly higher obtainable concentration in the theoretical estimation is due to the draw solution is considered continues re-concentrated, which is different from the experimental data. These observations indicate that combined OMD and DCMD is capable to slightly push the upper limit of maximum achievable concentration but is still not sufficient to exceed the solubility of LiCl.

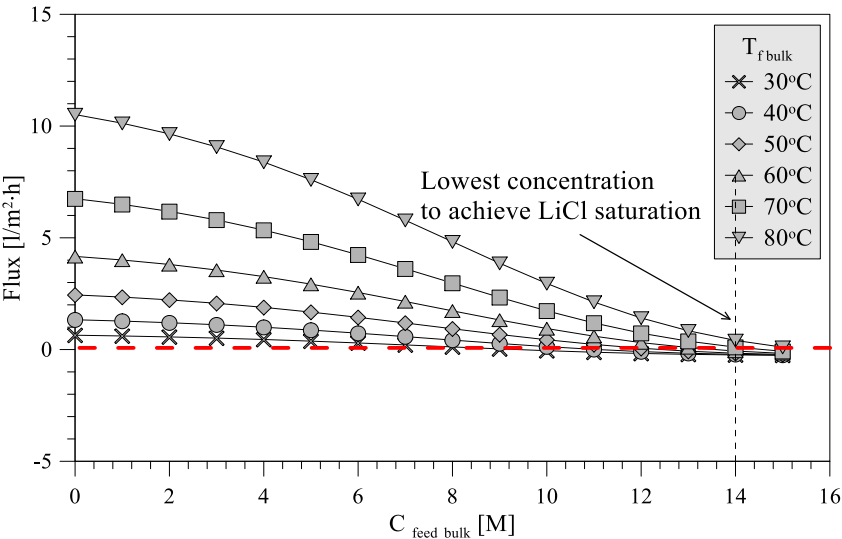


Figure 7.8: Theoretical evaluation of trans-membrane flux at increasing LiCl concentration for several feed temperatures in combined OMD and DCMD configuration. Draw solution: 4.5 M  $\text{CaCl}_2 \cdot 2\text{H}_2\text{O}$  (Continuously kept at 4.5 M), Permeate bulk temperature: 25°C.

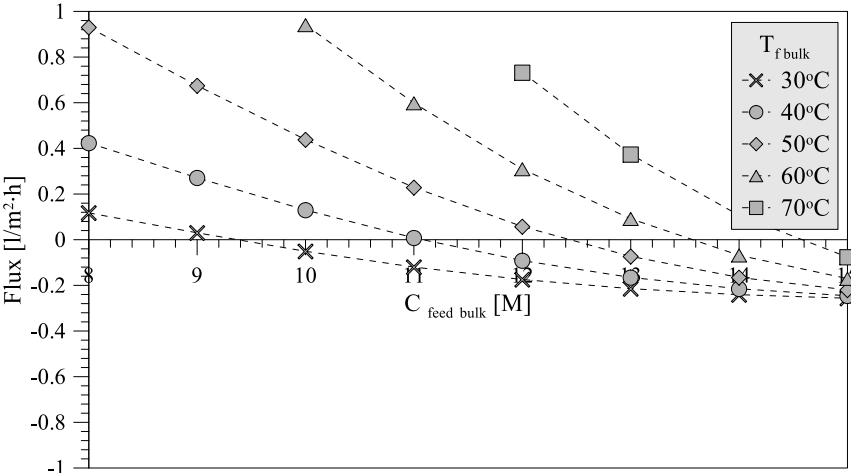


Figure 7.9: Close-up of Figure 7.8 for evaluation of negative flux.

### 7.3.3 VACUUM MEMBRANE DISTILLATION

Vacuum membrane distillation is often able to exceed the fluxes obtained in DCMD [30], although with an associated increase in energy consumptions. Experiments on VMD have been carried out by using single LiCl salt solutions starting from 8M and have been shown in Figure 7.10. Decline in trans-membrane flux is also observed in VMD configuration, but the flux is higher with respect to DCMD and OMD. The observed decrease in flux with concentration can be attributed to corresponding decrease in activity coefficient and therefore feed vapor pressure as indicated by Eq. 4.3 (Chapter 4). High concentration achievable in VMD can be attributed to heat and mass transport phenomena taking place which is different from DCMD. Contrary to DCMD, there is no cold stream in contact with membrane on permeate side. Thus thermal polarization is less, ensuring high temperature at membrane interface and, therefore, high driving force. Furthermore, the application of vacuum inside the membrane pores allows maintaining the least resistance to transporting vapors at any feed temperature. As a result, LiCl concentrations above 14M are achievable in VMD configuration and this configuration is able to realize LiCl recovery. Removal of ions due to LiCl precipitation results in constant flux near LiCl crystallization.

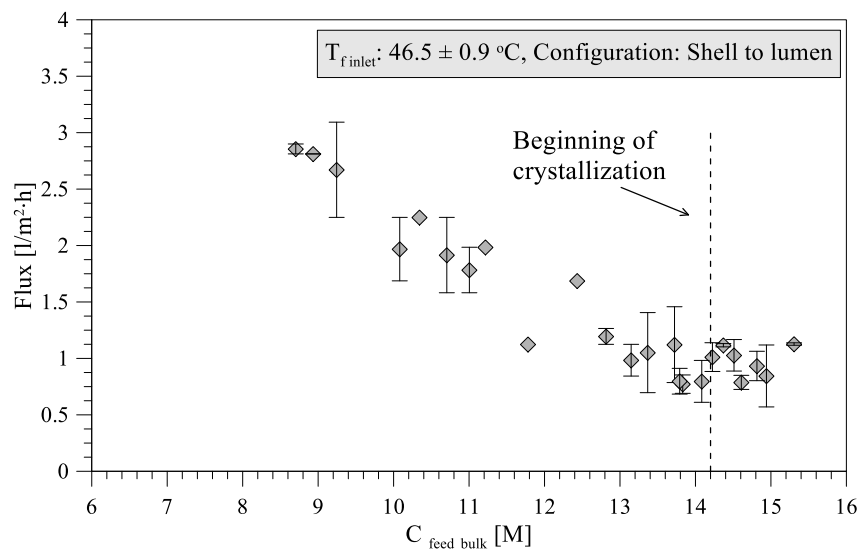


Figure 7.10: Flux for VMD with single solute lithium chloride solution starting from 8M. Configuration: Feed in shell side and vacuum on lumen side.

Comparison of DCMD, OMD and VMD in terms of flux with respect to feed vapor pressure (Figure 7.11) further illustrates the difference between the configurations. The point where flux becomes positive is related to the vapor pressure of permeate and the slope of the curve depends on membrane characteristics and temperature polarization coefficient (TPC). TPC is higher in VMD due to no cold stream on permeate side. In VMD only a slight positive feed vapor pressure has to be applied to ensure a positive flux. In OMD and DCMD, the applied vapor pressure has to be much higher and for this reason only VMD is cable of reaching LiCl saturation



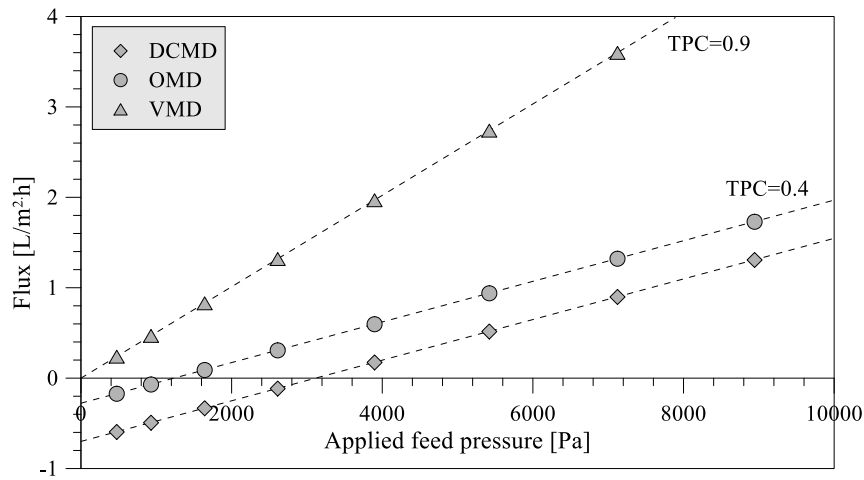


Figure 7.11: Theoretical evaluation of flux vs vapor pressure of feed solution for DCMD, VMD and OMD.

### 7.3.4 CHARACTERIZATION OF CRYSTALLIZES PRODUCT

Lithium chloride crystallizes in several forms including the anhydrous form, monohydrate, dihydrate, trihydrate and pentahydrate. Relating to the phase diagram of LiCl-H<sub>2</sub>O, the monohydrate form is precipitating in the temperature range used in MCr (30-60°C).

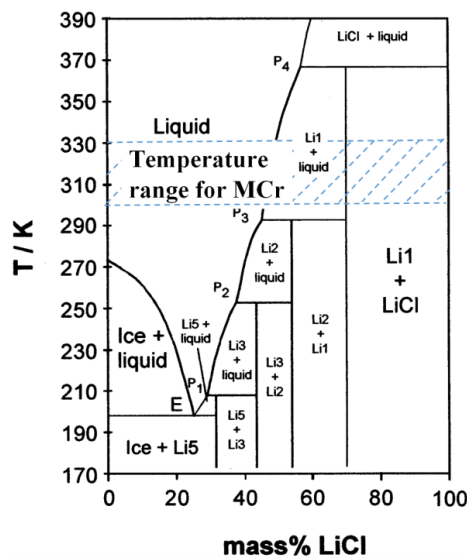


Figure 7.12: Phase diagram of LiCl-H<sub>2</sub>O. (Lix: LiCl·xH<sub>2</sub>O) [25].

In current study, preliminary results on LiCl crystallization have been obtained. At the time, the crystals appeared in the feed tank, they have been observed through optical microscope equipped with a video camera. Two types of crystal structures have been observed. The first type observed in higher quantity is an orthorhombic structure with a very high growth rate (Figure 7.13a). The orthorhombic polymorph structure of LiCl monohydrate is also found in the study by Hönnerscheid et al. [31]. The second observed structure is cubic (Figure 7.13b). This structure is always found in a mixture with the orthorhombic structure, but seems not to be formed at high feed temperatures (~64 °C) (Figure 7.14). The preliminary results indicate that low feed temperature favors the formation of cubic structure. At the highest feed temperature of 64 °C considered in current study, the cubic crystals vanish completely. The results on tunable polymorph structure by changing operative conditions is consistent with previous studies on membrane crystallization of biomolecules [32], [33]. However, in case of LiCl, the exact reason and mechanism causing the formation of different structure needs further investigation. For feed

temperatures around 38 °C, mean diameter and growth rate are ranging from 83 – 139 μm and 0.0323 – 0.824 μm/min, respectively. Crystal growth is influenced by the utilized flow rate and it appears that the mean diameter and growth rate decrease with increase in flow rate for feed temperatures of 38 °C. This indicates that the crystal growth is limited by resistance to integration of material into the crystal face instead of being controlled by the transport of materials to the face of the crystal [34].

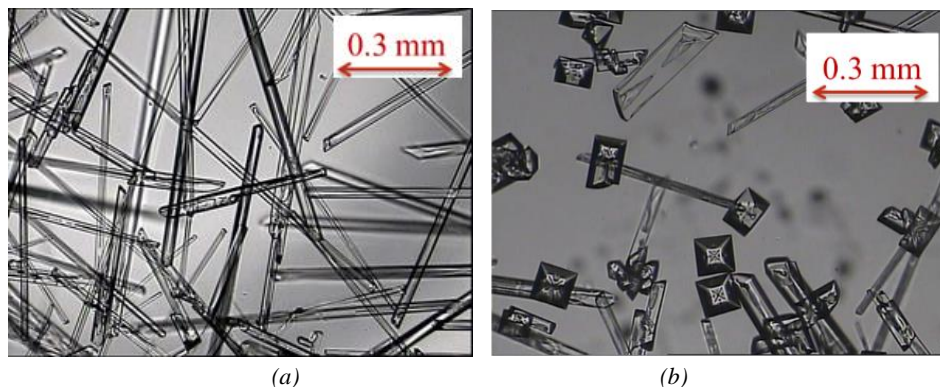


Figure 7.13: Morphology of LiCl obtained in membrane crystallization, (a) the orthorhombic polymorphic form (b) the cubic polymorphic form

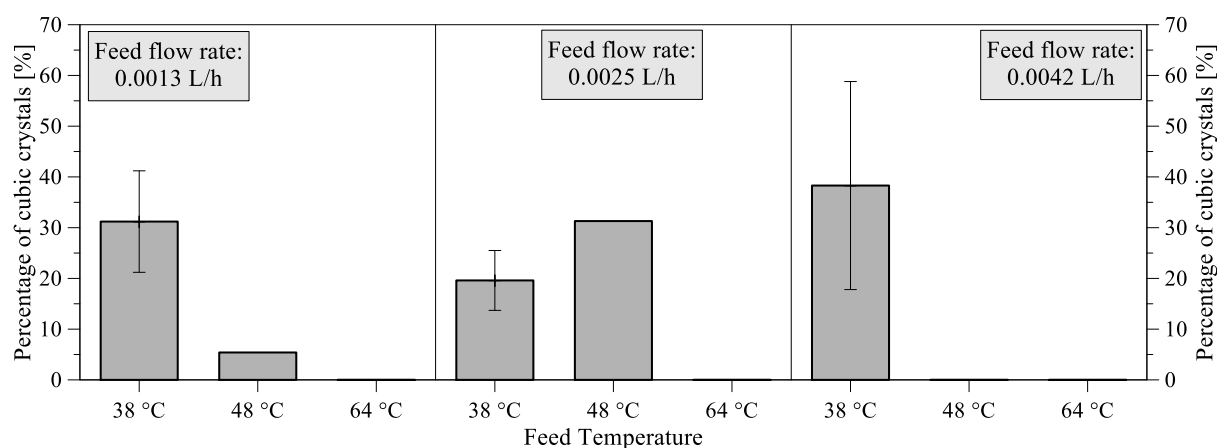


Figure 7.14: Distribution between cubic structures and orthorhombic structures at different feed temperatures and feed flow rates.

## 7.4 SUMMARY

Various configurations of membrane distillations are comparatively analyzed to simultaneously recover water and crystals from highly concentrated solutions represented here by single salt aqueous LiCl solution. Among the MD configurations investigated, DCMD and OMD are not able to concentrate the solution beyond 7 and 10 M, respectively. However, application of VMD allows treating the solution to saturation level, making the crystallization possible. Success of VMD in achieving the highest final concentration has been associated with the minimum temperature polarization and reduced resistance to vapor transport within the pore. Once formed, LiCl crystals grow in different polymorphic forms by tuning the operative conditions. The orthorhombic structures are formed under high thermal and hydrodynamic conditions, whereas the cubic structures are formed under gentle operative conditions. This study is seen as an indicator for selecting the optimal MD configuration for precipitating lithium particularly and to treat highly concentrated solutions generally. The success in lithium recovery by means of membrane technology contributes with a vision for future integrated desalination systems for water, energy and mineral production from brine. However, emphasis has now to be pointed towards recovery from mixed salt solutions to optimize the crystallization process.

## REFERENCES

- [1] F. Grosse, "Is recycling 'part of the solution'? The role of recycling in an expanding society and a world of finite resources," *S.A.P.I.EN.S [Online]*, vol. 3, 2010.
- [2] T. Prior, P. a Wäger, A. Stamp, R. Widmer, and D. Giurco, "Sustainable governance of scarce metals: the case of lithium.," *Sci. Total Environ.*, vol. 461–462, pp. 785–91, Sep. 2013.
- [3] U. Bardi, "The mineral question: how energy and technology will determine the future of mining," *Front. Energy Res.*, vol. 24, 2013.
- [4] S. H. Mohr, G. Mudd, and D. Giurco, "Lithium Resources and Production: Critical Assessment and Global Projections," *Minerals*, vol. 2, no. 4, pp. 65–84, Mar. 2012.
- [5] P. W. Gruber, P. A. Medina, G. A. Keoleian, S. E. Kesler, M. P. Everson, and T. J. Wallington, "Global Lithium Availability - A Constraint for Electric Vehicles?," *J. Ind. Ecol.*, vol. 15, pp. 760–775, 2011.
- [6] C. Grosjean, P. H. Miranda, M. Perrin, and P. Poggi, "Assessment of world lithium resources and consequences of their geographic distribution on the expected development of the electric vehicle industry," *Renew. Sustain. Energy Rev.*, vol. 16, no. 3, pp. 1735–1744, 2012.
- [7] S. E. Kesler, P. W. Gruber, P. A. Medina, G. A. Keoleian, M. P. Everson, and T. J. Wallington, "Global lithium resources : Relative importance of pegmatite , brine and other deposits," *Ore Geol. Rev.*, vol. 48, pp. 55–69, 2012.
- [8] U.S. Geological Survey, "Mineral Commodity Summaries - Lithium," 2015.
- [9] J. W. An, D. J. Kang, K. T. Tran, M. J. Kim, T. Lim, and T. Tran, "Hydrometallurgy Recovery of lithium from Uyuni salar brine," *Hydrometallurgy*, vol. 117–118, pp. 64–70, 2012.
- [10] A. Umeno, Y. Miyai, N. Takagi, R. Chitrakar, K. Sakane, and K. Ooi, "Preparation and Adsorptive Properties of Membrane-Type Adsorbents for Lithium Recovery from Seawater," *Ind. Eng. Chem. Res.*, vol. 41, no. 17, pp. 4281–4287, 2002.
- [11] K.-S. Chung, J.-C. Lee, W.-K. Kim, S. B. Kim, and K. Y. Cho, "Inorganic adsorbent containing polymeric membrane reservoir for the recovery of lithium from seawater," *J. Memb. Sci.*, vol. 325, pp. 503–508, 2008.
- [12] Y. Han, H. Kim, and J. Park, "Millimeter-sized spherical ion-sieve foams with hierarchical pore structure for recovery of lithium from seawater," *Chem. Eng. J.*, vol. 210, pp. 482–489, 2012.
- [13] J.-A. Kim, M. Kong, J.-H. Kim, K.-S. Chung, C.-Y. Eom, and H.-O. Yoon, "Identification of marine bacteria affecting lithium adsorbents in seawater," *Env. Geochem Heal.*, vol. 35, pp. 311–315, 2013.
- [14] J. Song, X.-M. Li, Y. Zhang, Y. Yin, B. Zhao, C. Li, D. Kong, and T. He, "Hydrophilic nanoporous ion-exchange membranes as a stabilizing barrier for liquid–liquid membrane extraction of lithium ions," *J. Memb. Sci.*, vol. 471, pp. 372–380, Dec. 2014.
- [15] A. K. Shukla and T. P. Kumar, "Lithium Economy: Will It Get the Electric Traction?," *J. Phys. Chem. Lett.*, 2013.
- [16] Z. K. Nagy and R. D. Braatz, "Advances and New Directions in Crystallization Control," *Annu. Rev. Chem. Biomol. Eng.*, vol. 3, pp. 55–75, 2012.
- [17] E. Curcio, A. Criscuoli, and E. Drioli, "Membrane Crystallizers," *Ind. Eng. Chem. Res.*, vol. 40, pp. 2679–2684, 2001.
- [18] G. Di Profio, E. Curcio, and E. Drioli, "A Review on membrane crystallization," *Chem. Today*, vol. 27, pp. 27–31, 2009.
- [19] E. Drioli, G. Di Profio, and E. Curcio, "Progress in membrane crystallization," *Curr. Opin. Chem. Eng.*, vol. 1, no. 2, pp. 178–182, May 2012.
- [20] E. Drioli, A. Ali, and F. Macedonio, "Membrane distillation : Recent developments and perspectives," *Desalination*, vol. 356, pp. 56–84, 2015.

- [21] F. Edwie and T.-S. Chung, "Development of simultaneous membrane distillation–crystallization (SMDC) technology for treatment of saturated brine," *Chem. Eng. Sci.*, vol. 98, pp. 160–172, Jul. 2013.
- [22] S. Meng, Y. Ye, J. Mansouri, and V. Chen, "Crystallization behavior of salts during membrane distillation with hydrophobic and superhydrophobic capillary membranes," *J. Memb. Sci.*, vol. 473, pp. 165–176, Jan. 2015.
- [23] C. M. Tun, A. G. Fane, J. T. Matheickal, and R. Sheikholeslami, "Membrane distillation crystallization of concentrated salts—flux and crystal formation," *J. Memb. Sci.*, vol. 257, no. 1–2, pp. 144–155, Jul. 2005.
- [24] F. Macedonio, C. A. Quist-Jensen, O. Al-Harbi, H. Alromaih, S. a. Al-Jlil, F. Al Shabouna, and E. Drioli, "Thermodynamic modeling of brine and its use in membrane crystallizer," *Desalination*, vol. 323, pp. 83–92, Aug. 2013.
- [25] C. Monnin, M. Dubois, N. Papaiconomou, and J. Simonin, "Thermodynamics of the LiCl + H<sub>2</sub>O System," *J. Chem. Eng. Data*, vol. 47, pp. 1331–1336, 2002.
- [26] A. Ali, F. Macedonio, E. Drioli, S. Aljlil, and O. A. Alharbi, "Experimental and theoretical evaluation of temperature polarization phenomenon in direct contact membrane distillation," *Chem. Eng. Res. Des.*, vol. 91, no. 10, pp. 1966–1977, Oct. 2013.
- [27] L. Martínez-Díez and M. I. Vázquez-González, "Temperature and concentration polarization in membrane distillation of aqueous salt solutions," *J. Memb. Sci.*, vol. 156, pp. 265–273, 1999.
- [28] D. L. Parkhurst and C. A. . Appelo, "Description of Input and Examples for PHREEQC Version 3 — A Computer Program for Speciation , Batch-Reaction, One-Dimensional Transport, and Inverse Geochemical Calculations," in *U.S. Geological Survey Techniques and Methods, book 6*, 2013.
- [29] K. S. Pitzer and J. J. Kim, "Thermodynamics of Electrolytes. IV. Activity and Osmotic Coefficients for Mixed Electrolytes," *Journal of the American Chemical Society*, vol. 96:18, pp. 5701–5707, 1974.
- [30] E. Drioli, a. Ali, S. Simone, F. Macedonio, S. a. AL-Jlil, F. S. Al Shabonah, H. S. Al-Romaih, O. Al-Harbi, a. Figoli, and a. Criscuoli, "Novel PVDF hollow fiber membranes for vacuum and direct contact membrane distillation applications," *Sep. Purif. Technol.*, vol. 115, pp. 27–38, Aug. 2013.
- [31] A. Hönnerscheid, J. Nuss, C. Mühle, and M. Jansen, "Crystal Structure of the Monohydrates of Lithium Chloride and Lithium Bromide," *Zeitschrift für Anorg. und Allg. Chemie*, vol. 629, pp. 312–316, 2003.
- [32] G. Di Profio, S. Tucci, E. Curcio, and E. Drioli, "Controlling Polymorphism with Membrane-Based Crystallizers : Application to Form I and II of Paracetamol," *Chem. Mater.*, vol. 19, pp. 2386–2388, 2007.
- [33] G. Di Profio, E. Curcio, and E. Drioli, "Supersaturation Control and Heterogeneous Nucleation in Membrane Crystallizers : Facts and Perspectives," *Ind. Eng. Chem. Res.*, pp. 11878–11889, 2010.
- [34] F. Macedonio and E. Drioli, "Hydrophobic membranes for salts recovery from desalination plants," *Desalin. Water Treat.*, vol. 18, pp. 224–234, 2010.



---

## CHAPTER 8:

# TREATMENT OF AGRO FOOD

---

### 8.1 INTRODUCTION

Food processing at industrial scale is imperative to sustain or improve food security together with high food quality and economic feasibility for industry and end-user market. Important factors regarding food processing, in general, includes; food safety, nutritional value, sensory effect, health benefits, convenience and minimal seasonal change [1]. Nevertheless, food industry also needs to avoid the adverse impact of the processing through appropriate treatment. Membrane processes, in the framework of gentle food processing are highlighted as important participant in the industry, particular within liquid processing but also for waste handling [2]. Membrane operations, depending on the process can be used as separation and concentrations units at low energy requirements and reduced damage of product quality due to no or less thermal treatment [3]. Traditional processes such as microfiltration (MF), ultrafiltration (UF), nanofiltration (NF) and reverse osmosis (RO) have been widely used for cold sterilization, clarification, drying, thickening, fractionating etc. mainly in liquid processing [3]. Moreover, membrane units including pervaporation (PV) and electrodialysis (ED) have also been utilized for dealcoholization, recovery of e.g. lactic and citric acid [3]. Today, membranes are used in several industries with some examples as in milk (cheese), beer/wine and juice treatment. Different types of juice is handled by UF for clarification and helps to improve stability of the juice without reduced quality [2]. RO can be used for concentration up to maximum 30-40 ° brix from initial concentration [2]. However, higher concentration is difficult to reach by RO, thus other novel membrane operations such as osmotic membrane distillation (OMD) or membrane distillation (MD) can replace the conventional membrane processes.

In particular, OMD has been utilized for juice concentration, in which the isothermal process ensures a viable preservation of valuable compounds in the juice. However, suitable draw agents are crucial for this process and a continuous re-concentration is needed to maintain process performance. Therefore, the emergence of membrane distillation in other fields have encourage the use of this process in the treatment of juices for the reason of avoiding the use of draw solution and producing a high quality fresh water permeate stream which can directly be utilized other places in the industry for e.g. cleaning. The difference between OMD and MD is the difference in driving force which for OMD is a concentration gradient whereas MD is a temperature gradient. In the field of desalination, MD is in general used at temperatures ranging from 40 to 80 °C, which is below conventional distillation. The low temperatures ensure reduced energy requirements, thus making the process more sustainable. However, in the juice treatment the high temperatures can destroy the essential components in the juice. Nevertheless, MD can be used also at very low temperatures ranging from 25-40 °C, suitable for food processing. Fouling constrains is an additional factor impacting food processing. In particular, fouling in pressure driven membrane operations are more prominent, thus a realization of OMD or MD can also minimize fouling making longer duration treatment and high concentrations a possibility. An additional advantage of MD is the possibility of treating solutions at high concentrations. For this reason MD is a great opportunity for realizing significant volume reduction and very high concentrations of nutrients in the final product in which the compounds eventually can be recovered. These advantages are followed by low energy cost and low footprints in the logic of process intensification process.

In this study, clarified orange juice has been treated with direct contact membrane distillation (DCMD) and membrane crystallization (MCr) to reduce the mass of the juice without losing its quality and eventually recover components from the juice.

## 8.2 MATERIALS AND METHODS

Oranges from Calabria have been processed of a total weight of 129.4 kg. Firstly, the oranges have been washed and hereafter pressed by the use of an electrical household squeezer. The oranges have been handled according to general standards for pectin removal, prevention of expiring of juice, storing etc. The complete flow sheet of the process can be found in Figure 8.1.

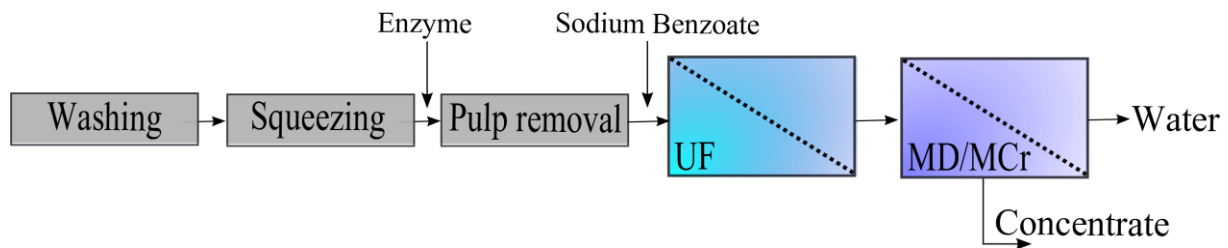


Figure 8.1: Flow sheet of orange juice processing.

### 8.2.1 CLARIFICATION OF ORANGE JUICE

A lab-scale ultrafiltration unit with feed capacity of 50 l equipped with a polysulfone membrane with the characteristics shown in Table 8.1 has been used in the clarification of the juice.

Table 8.1: Ultrafiltration membrane characteristics.

Material	Polysulfone
MWCO	400 kDa
Area	1.2 m <sup>2</sup>

The clarification process has been conducted in four batches at the operative condition shown in Table 8.2. The plant and membrane have been cleaned every day with tapped water and one time with enzyme solution overnight.

Table 8.2: Operative conditions in ultrafiltration experiments.

Transmembrane pressure	0.75 bar
Temperature range	22.5-25.5 °C
Flow rate	~827 l/h

The amount of suspended solids has been determined in ultrafiltration feed and retentate by centrifugation of the juice.

## 8.2.2 MD AND MCr EXPERIMENTAL SETUP

The potential of using membrane distillation for the concentration of clarified UF juice has been investigated. Moreover, attempt on using membrane crystallization for the recovery of components in the juice has been carried out. A lab-scale membrane distillation plant with feed capacity of 7 l, equipped with two polypropylene membranes from Microdyn-Nadir (Described in Chapter 5) have been utilized in the concentration of the orange juice. Initially the experiments have been divided into four tests using the same operative conditions (Table 8.3). The performance of membrane distillation is highly aligned with temperature difference between feed and permeate side, thus increase in temperature gradient increases the trans-membrane flux. However, the temperature of the juice is also considered to sustain the favorable components in the juice. For this reason the temperature of the juice is kept below 30 °C.

Table 8.3: Operative conditions in membrane distillation experiments.

Feed flow rate	200 l/h
Feed temperature	23-25 °C
Permeate flow rate	100 l/h
Permeate temperature	~ 17 °C
External temperature control on feed tank	25 °C

## 8.3 RESULTS AND DISCUSSION

### 8.3.1 CLARIFICATION OF ORANGE JUICE

The total weight of juice as feed entering into the ultrafiltration plant is 57.9 kg and the permeate leaving the plant is 46.3 kg. The permeate flux is illustrated in Figure 8.2. The reason for the decline in flux is the increase in concentration together with increased fouling of the membrane.

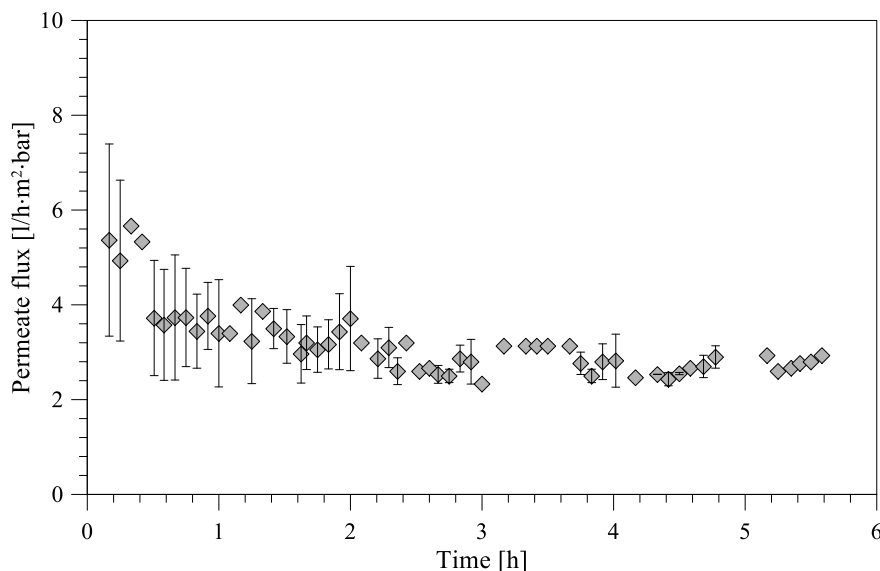


Figure 8.2: Permeability of ultrafiltration experiments.

The amount of suspended solids in different stages of the process is reported in Table 8.4. Images before and after centrifugation is illustrated in Figure 8.3 and Figure 8.4 for UF feed and UF retentate, respectively. The content of suspended solids in the retentate has increased more than a factor of 3 realizing the importance of ultrafiltration to avoid fouling in the later processes.



Table 8.4: Determination of suspended solids.

	UF feed [w/w%]	UF retentate [w/w%]
Sample 1	6.751	20.02
Sample 2	6.239	20.98
Average	6.495	20.50

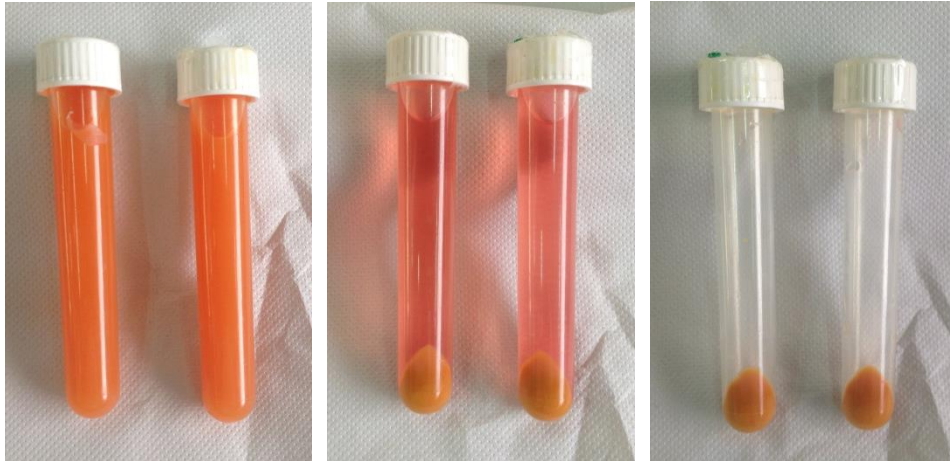


Figure 8.3: Images of UF feed before and after centrifugation.

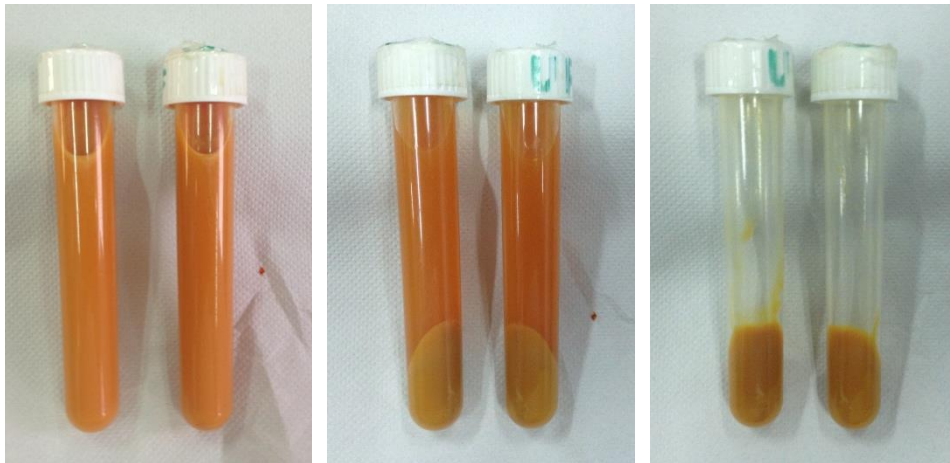


Figure 8.4: Images of UF retentate before and after centrifugation.

## 8.4 MEMBRANE DISTILLATION

The performance of membrane distillation is illustrated as the trans-membrane flux (Figure 8.5). Temperature difference is estimated on the basis of natural log mean temperature difference (Eq. 8.1). Concentration of orange juice by means of MD has been performed around 8 hours a day, where after the plant has been emptied and slightly cleaned with distilled water. The fluctuation of flux in some tests is caused by this cleaning together with the obtainment of steady temperature gradient.

$$\Delta T_{\ln} = \frac{(T_{feed,in} - T_{distillate,out}) - (T_{feed,out} - T_{distillate,in})}{\ln \left( \frac{T_{feed,in} - T_{distillate,out}}{T_{feed,out} - T_{distillate,in}} \right)} \quad (Eq. 8.1)$$

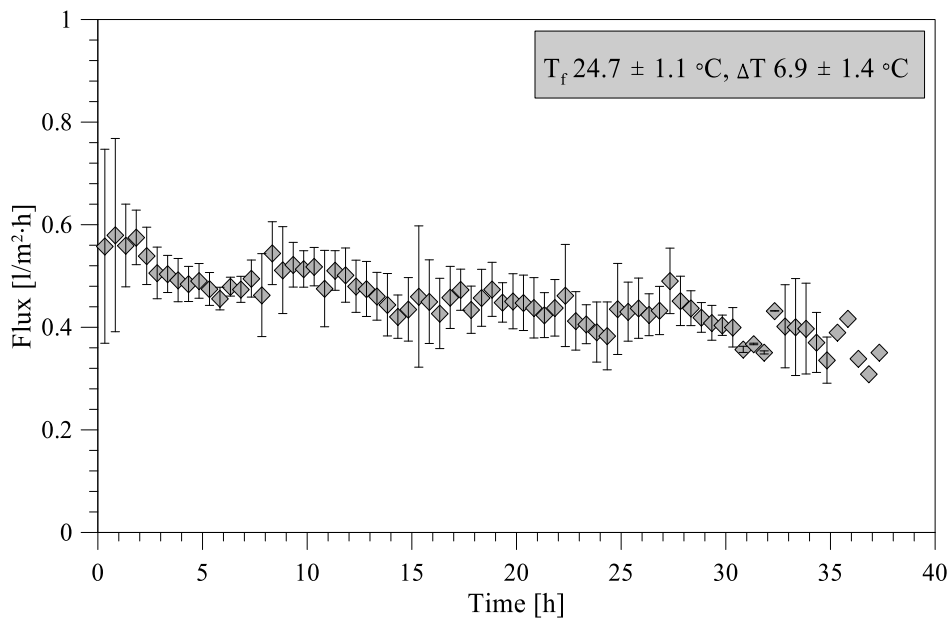


Figure 8.5: Average flux with standard deviation for membrane distillation experiments.

Neglecting the start-up of the process, the standard deviation is low for the tests, resulting in reproducible MD process. Moreover, a slightly decrease is observed of the average flux which can be due to different reasons: (i) The temperature difference decreases in same extend as the flux; (ii) the concentration is increasing and hereby reducing the driving force; (iii) the membrane has been fouled. Regarding the potential of fouling the membrane has been slightly cleaned every day in order to minimize the fouling potential. The flux might be relatively low compared to the pressure driven membrane processes due to a driving force less than 10 °C. However, it corresponds to results obtained in other studies using osmotic membrane distillation [4], [5].

Concentration of juice is measured as the content of sugar and termed brix degree (Eq. 8.2). Brix degrees have been measured regularly with a handhold refractometer. In the MD tests the concentration is increasing from around 9 to just below 24 °brix (Figure 8.6).

$$^{\circ} \text{Brix} = \frac{\text{mass sucrose [g]}}{100 \text{ g solution}} \quad (Eq. 8.2)$$

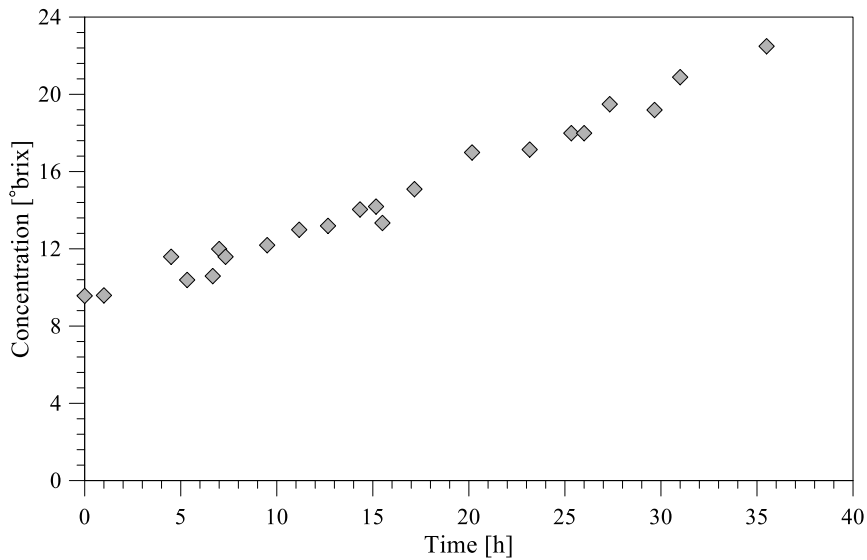


Figure 8.6: Concentration (° Brix) of membrane distillation experiments.

## 8.5 MEMBRANE CRYSTALLIZATION

In the previous cycle a concentration of only 24 °Brix has been obtained, thus the juice has been concentrated further in this cycle. The experiment has been conducted with the same operative conditions as the MD tests (Table 8.3). The performance of the membrane crystallization experiments is illustrated in Figure 8.7. The reason for the fluctuation of trans-membrane flux is the start-up process where the temperature difference has not reach steady state and the slightly cleaning with distilled water. The trans-membrane flux decreases to almost zero at the end even the driving force have been maintained.

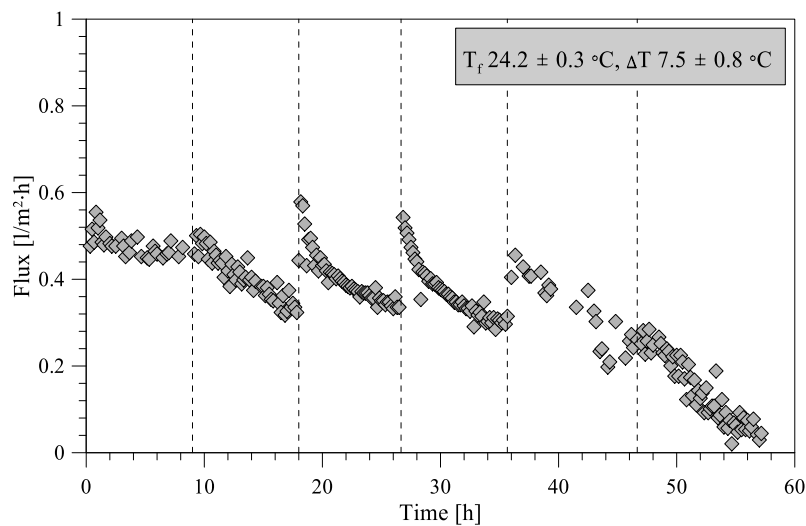


Figure 8.7: Trans-membrane flux for membrane crystallization experiment. The broken lines indicate one day experimentation.

The membrane has been characterized with distillate water before and after juice treatment (Figure 8.8), and no flux reduction has been observed. This indicates that permanent fouling phenomena is negligible and therefore, the rapid decrease in flux is associated to the highly increase in sugar content (Figure 8.9) and viscosity (Figure 8.10). The final achievable concentration is 65.4 ° Brix. This high concentration is much more from what can be obtained by pressure driven membrane operations and is comparable for what can be obtained by osmotic membrane distillation [4]–[6]. In order to solve the problem of

viscosity and the low flux, better pumps and redesign of modules and membranes might be necessary. Membrane and module development for juice treatment would be different from treating inorganic solutions. Membrane characteristics such as thickness and pore size, in juice treatment, should be optimized for temperature difference of 10-20 °C. The pressure drop and furthermore, the diffusion of vapor from bulk to membrane surface is different, due to higher viscosity. In fact, it is estimated for concentrations above 50° Brix, that it is no longer the resistance of the membrane that control the process and that a more permeable membrane will no longer improve the flux. Instead it is the resistances in the bulk which control mass transfer [7]. The higher viscosity set, moreover, also some restrictions on the mechanical strength of the membrane fibers (i.e. to avoid collapse of fibers).

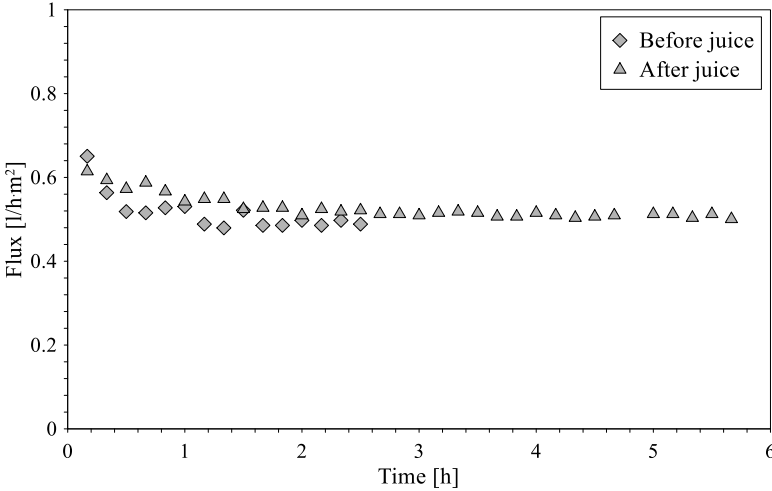


Figure 8.8: Distillate water flux before and after juice treatment. .

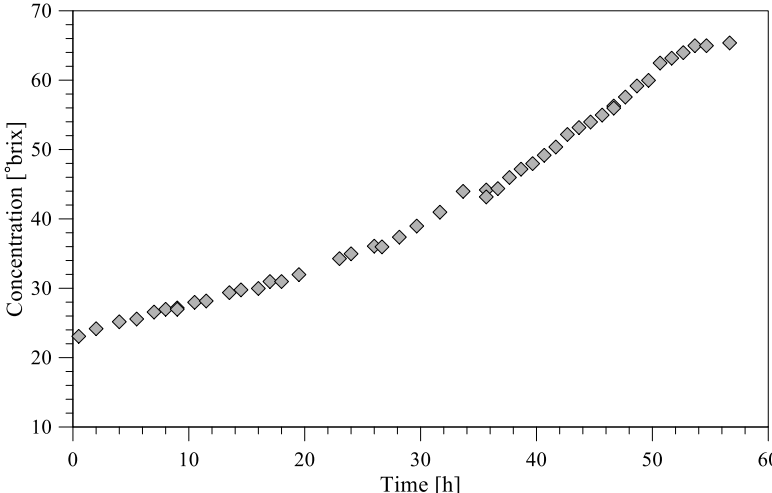


Figure 8.9: Concentration (° Brix) of membrane crystallization experiment.

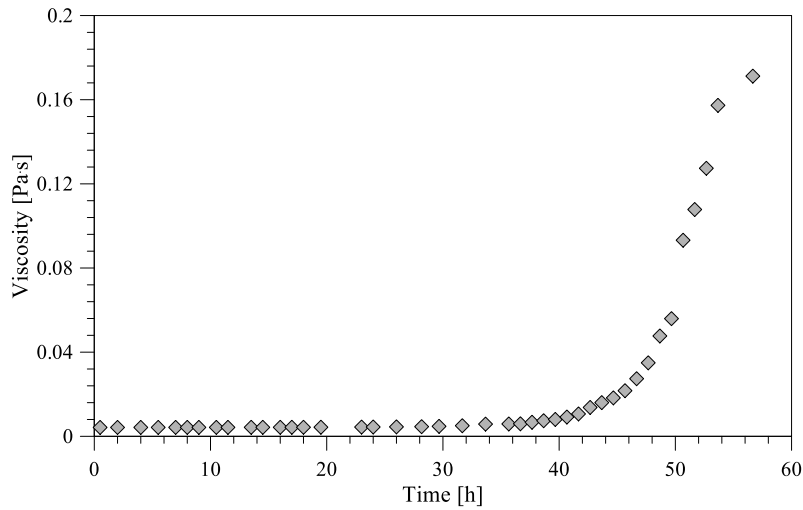


Figure 8.10: Viscosity of membrane crystallization experiment.

In Figure 8.11, a summary of the total antioxidant activity (TAA) evaluation in samples coming from the UF/MD/MCr treatment is reported. Retentate samples coming from MD (and also from the following MCr) have been diluted to the same Total Soluble Solids (TSS) concentration of the UF permeate (9°Brix) before the analysis, in order to allow the direct comparison between the different values. During the concentration by MD, the TAA of the juice has remained almost constant and equal to the UF permeate, proving that the flavonoids, polyphenols and organic acids present in the clarified orange juice have been recovered and concentrated through the MD. The same trend has been observed for the MCr process.

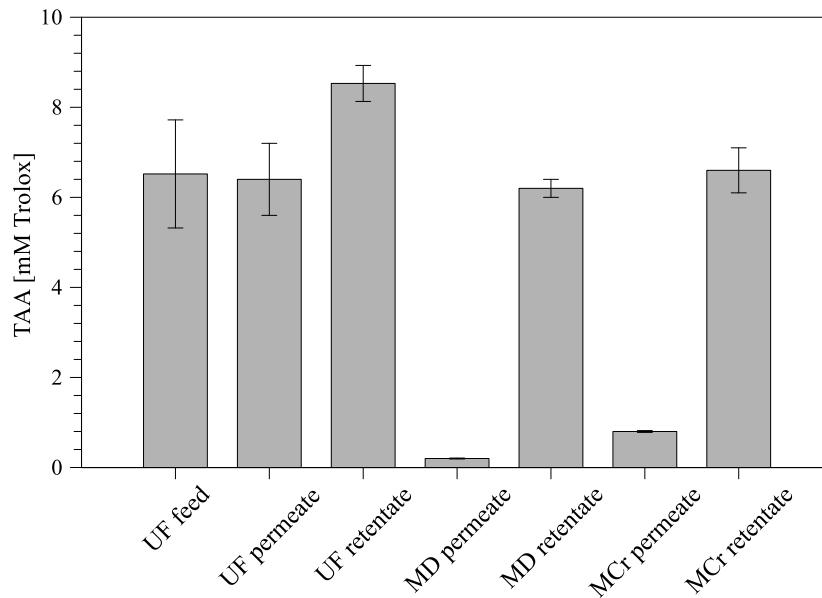


Figure 8.11: Analytical evaluations on samples of orange juice coming from the different steps of the UF/MD/MCr treatment

A juice sample has been withdrawn from the feed tank at 65 ° Brix and is observed through optical microscope in order to verify crystal nucleation and growth. Small crystals have been detected with different crystal habit (Images shown in Figure 8.12). The precipitation could be sugars, ascorbic acid or flavonoids (hesperidin and narirutin) [8]. Analyses are in progress to identify the nature of recovered crystals.

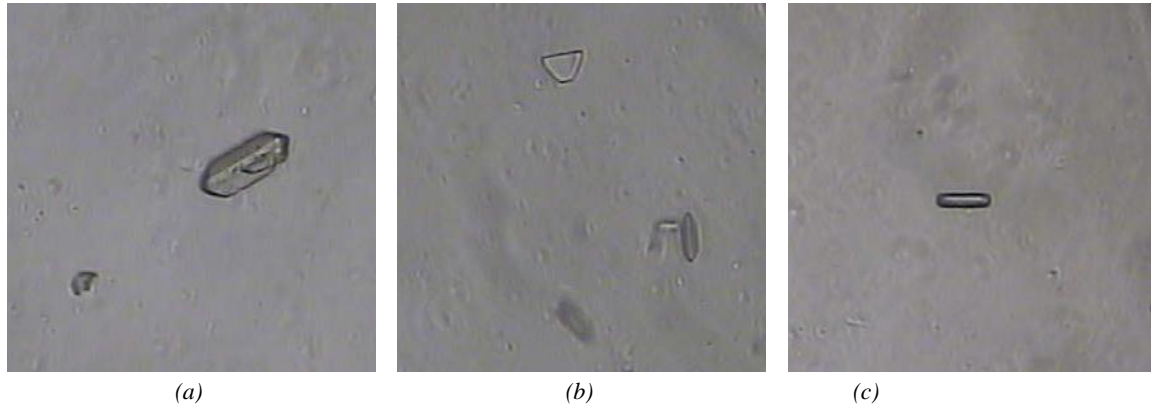


Figure 8.12: Crystal images obtained by optical microscope.

The observed crystals have also been preliminary characterized in terms of crystal size distribution (CSD) (Figure 8.13). The first sample has the most uniform crystal product, where it is slightly increasing for the later withdraw samples. Nevertheless, the crystals exhibit a narrow CSD curve indication the gentle procedure of MCr.

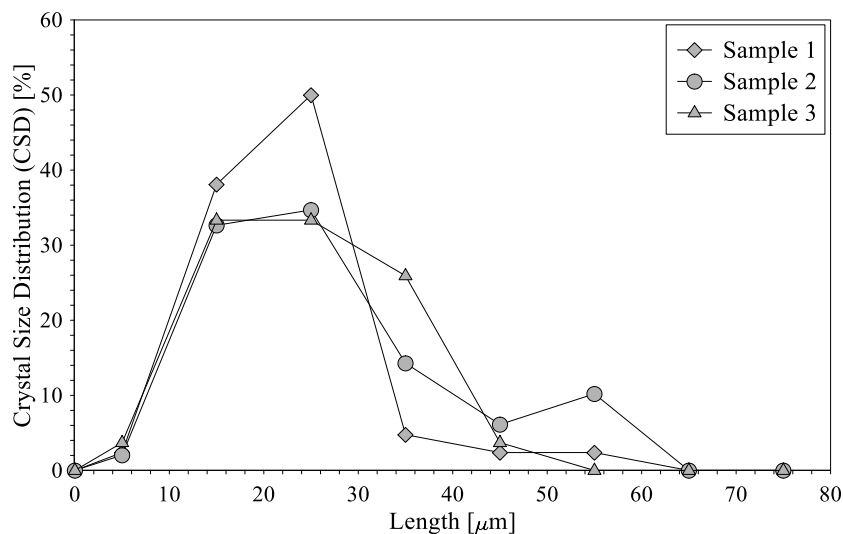


Figure 8.13: Crystal size distribution of the crystal produced by MCr.

## 8.6 EVALUATION OF NEW METRICS

In the same logic as described in Chapter 1 new metrics are a way to measure the impact of sustainability of the process. In the particular case of orange juice, one aim of the treatment is to minimize the volume of the juice in order to make it easier for storage and transportation meanwhile without destroying any of the important compounds in the juice. The TAA analysis described previous in this chapter shows that treatment by MD and MCr preserve the antioxidants in the juice even it has been treated for more than 90h. In Figure 8.14 mass reduction for each process has been illustrated. UF is contributing with the highest mass reduction. Nevertheless, MD and MCr are able to reduce the mass from 64 % to 90 %. The high quality of juice after UF/MD/MCr and high mass reduction show the interest of the membrane

based process considering the eventual transportation and storage. Another positive aspect of MD and MCr treatment is that these processes are not creating any waste stream. The low amount of antioxidants in the permeate streams indicates that no or less wetting occurs, meaning that permeate, which is a good quality water stream, can be used elsewhere in industry or reused as cleaning water.

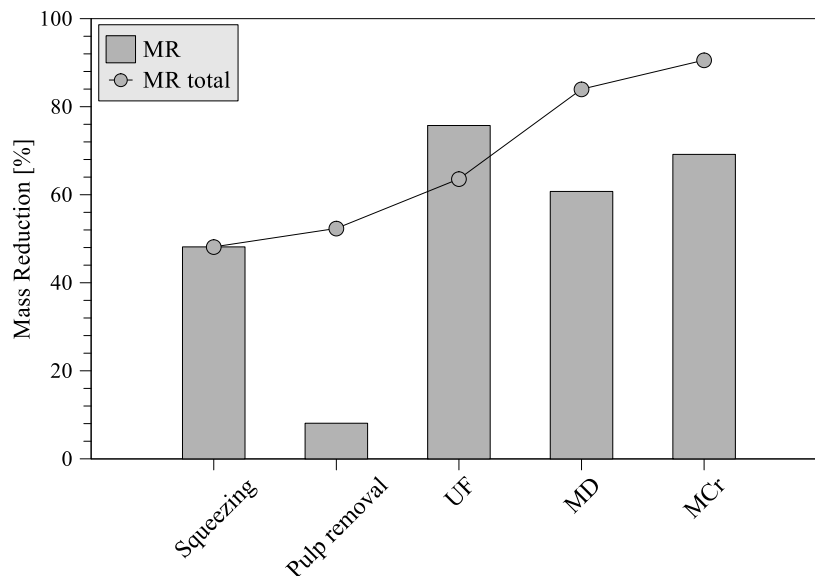


Figure 8.14: Mass reduction of the different treatment stages of juice processing

## 8.7 SUMMARY

Orange juice has been treated with MD and MCr until elevated concentrations (~65 °Brix). The MD/MCr process is able to maintain the quality of the juice. In this study crystals have been observed in the high concentrated fruit juice, which could be flavonoids or other essential components. These components still need to be separated/recovered from the liquid phase and further characterized. The problems caused by viscosity increase need to be solved in order to continue the concentration. However, mass reduction of more than 90 % with respect to initial weight of oranges has been obtained. The juice has been treated for more than 90 hours of operation, a concentration from 9 – 65 °Brix has been achieved and only slightly cleaning with distillate water has been carried out and still no fouling has been permanent present on the membrane surface, thus MD and MCr are potential candidates for concentration and component recovery of juice. Moreover, the advantage compared to OMD is that it is not necessary to re-concentrate the draw solution making MD and MCr more competitive.

## REFERENCES

- [1] M. Van Boekel, V. Fogliano, N. Pellegrini, C. Stanton, G. Scholz, S. Lalljie, V. Somoza, D. Knorr, P. R. Jasti, and G. Eisenbrand, "A review on the beneficial aspects of food processing," *Mol. Nutr. Food Res.*, vol. 54, pp. 1215–1247, 2010.
- [2] R. Skelton, "Membrane filtration applications in the food industry," *Filtration + Sep.*, pp. 28–30, 2000.
- [3] F. P. Cuperus and H. H. Nijhuis, "Applications of," vol. 4, no. September, pp. 277–282, 1993.
- [4] A. Cassano, "Clarification and concentration of citrus and carrot juices by integrated membrane processes," *Journal of Food Engineering* vol. 57, pp. 153–163, 2003.

- [5] V. D. Alves and I. M. Coelho, "Orange juice concentration by osmotic evaporation and membrane distillation : A comparative study," *Journal of Food Engineering*, vol. 74, pp. 125–133, 2006.
- [6] A. Cassano and E. Drioli, "Concentration of clarified kiwifruit juice by osmotic distillation," *Journal of Food Engineering* vol. 79, pp. 1397–1404, 2007.
- [7] M. Gryta, "Osmotic MD and other membrane distillation variants," *Journal of Membrane Science*, vol. 246, no. February 2004, pp. 145–156, 2005.
- [8] A. Cassano, M. Marchio, and E. Drioli, "Clarification of blood orange juice by ultrafiltration: analyses of operating parameters, membrane fouling and juice quality," *Desalination*, vol. 212, pp. 15–27, Jun. 2007.





---

## CHAPTER 9:

# CONCLUSION AND FUTURE PERSPECTIVES

---

High water stress, increasing energy consumptions and mineral depletion are already critical issues. Membrane process engineering is one of the disciplines involved in the technological innovations necessary to face these problems. Traditional membrane separation operations (e.g., MF, UF, NF, RO), widely used in many different applications, can today be combined with new membrane systems (such as membrane crystallization) for the design of integrated membrane processes with aim to obtain higher water production, lower energy consumption and minerals recovery. Membrane crystallization is a new process, but it continues to grow and mature and is today a very promising technology.

The results achieved in this Ph.D. work on MCr show some of the many possible applications such as desalination, wastewater, treatment of solutions with LiCl concentrations above 14M and agro food. Initially, in this work, lab-made PVDF membranes have been evaluated. As expected, the structure of the membrane influences its performance, but it is also found that the performance, of some membranes, changes at high concentrations. Membranes with finger-like structure have higher probability for wetting and therefore, are not able to be used in MCr applications. On the other hand, the optimal membranes, found in this study, have been membranes with symmetric sponge layer structure. Thickness reduction appears to be better choice to increase membrane performance than increasing pore size. However, thin membranes can cause more heat losses in practical applications and therefore, this have to be taken into account in commercial modules. Recently, membrane development has improved greatly, though a gap between development and fully commercialization still exist. New super-hydrophobic membrane materials with targeted membrane features, dual-layer membranes, improved membrane stability, optimal membrane lengths and operative conditions are some of the aspects being studied today. In particular, the increasing interest of membrane distillation can also accelerate the implementation of membrane crystallizers. However, the major lack of commercial available membranes put some restriction to the treatment by MCr. For example, to make membrane crystallization more interesting from industrial point of view, MCr needs to perform well with commercial membranes. Though, commercial membranes have very good stability, they might, at the same time, not work well enough with respect to trans-membrane flux. Therefore, it is crucial for right MCr membranes to be commercially available. This perspective might be fulfilled in near future, due to the accelerated progress in membrane development for MD applications.

In this study,  $\text{Na}_2\text{SO}_4$  and NaCl have also been recovered from wastewater and produced water, respectively. It is shown, that MCr is cable to maintain a stable performance, despite the complex solutions and moreover, produce high quality streams of water and salts. In case of  $\text{Na}_2\text{SO}_4$ , the solution has also been treated by nanofiltration prior to MD/MCr. However, here the trans-membrane flux has not been stable and more impurities have been detected in the produced crystals due to the higher amount of bivalent ions. Nanofiltration speeds up the time to reach saturation, but at the same time, it does not produce high quality pure water like MD and MCr. Due to the mentioned reasons, it is recommended to treat wastewater directly with MD and MCr. Crystallization of NaCl from produced water is also characterized by having high quality crystals from water recovery factors of 33%. In this study, overall water recovery factor of 37% has been achieved. However, it is possible to increase salt and water recovery, taking into account a relative stable flux and no wetting of the membrane. Nevertheless, it is necessary to introduce a continuous crystal recovery system to avoid crystal accumulation in the MCr plant and on membrane surface. Crystal recovery system might also make the salt production more

efficient. In this study, salt and water production with respect to membrane surface area is found to be 0.32 kg/(m<sup>2</sup>h) and 0.56 kg/(m<sup>2</sup>h) for salt and water, respectively. These values have been obtained utilizing commercial membranes, thus new and improved membranes are again an important factor for improving the production rate. Moreover, salt and water production can also be improved easily by increasing feed temperature. In fact, in the carried out study, only positive aspects of increasing temperature has been observed, such as higher flux and improved crystal quality in terms of higher mean diameter and growth rate, more narrow size distribution and more crystals in the samples that have perfect cubic structure.

Testing of lab-made membranes, crystallization of MgSO<sub>4</sub>·7H<sub>2</sub>O, NaCl and Na<sub>2</sub>SO<sub>4</sub> have all been carried out utilizing direct-contact membrane distillation, which is the most simple of all the MD configurations. To study the aspiring objective of zero-liquid discharge in desalination, lithium recovery from single salt solution has also been investigated. However, using similar conditions as in the previous experiments (i.e. DCMD, feed temperatures and flow rates) recovery of LiCl has not been possible. Membrane distillation is reported to be less influenced by concentration (as also observed in this work), however, this is only true until specific concentrations. LiCl is very soluble in water and in order to reach saturation, concentrations above 14M are required. DCMD is only able to achieve a concentration of around 7M LiCl (T<sub>feed</sub>: 51.6°C, commercial PP membrane). The reason is a significant reduction in water activity, which is proportional to the driving force. To overcome the decrease in vapor pressure, feed temperature must be increased further. However, the increase in feed temperature increases further the solubility of LiCl and achievement of supersaturation remains an unachievable task. Thus, the recovery of lithium by means of DCMD configuration is impractical by using PP membrane considered in this study. Instead of increasing the vapor pressure of the feed solution, another possibility is to decrease the vapor pressure on permeate side. This can be obtained by introducing a salt solution on permeate side, i.e. draw solution. This process is normally denoted osmotic membrane distillation (OMD), when it is carried out under isothermal conditions. In this study DCMD and OMD have been combined by introducing temperature and concentration gradient. This type of configuration has been able to increase the highest achievable concentration to around 10M. However, it is still far from saturation of LiCl. Therefore, vacuum membrane distillation has been introduced in order to remove the effect of osmotic phenomena. VMD allows treating the solution to saturation level, making the crystallization possible. Success of VMD in achieving the highest final concentration has been associated with the minimum temperature polarization and reduced resistance to vapor transport within the pore. Another interesting outcome is that LiCl crystals grow in different polymorphic forms, which can be tuned by operative conditions. Orthorhombic structures are formed under high thermal and hydrodynamic conditions, whereas the cubic structures are formed under gentle operative conditions. The achieved results indicate that DCMD can be used until a particular concentration; however, moving towards higher concentrations and towards compounds which are more soluble, VMD is required. It is believed that the obtained results, although preliminary, can be a guideline for future integrated desalination systems for water, energy and mineral production from brine. However, emphasis has now to be pointed towards recovery from mixed salt solutions to optimize the crystallization process.

Until this part, MCr has only been utilized for inorganic solutions such as desalination brine and wastewater solutions. Nevertheless, the last chapter in this thesis shows the potential of MD and MCr in the treatment of agro food. First oranges have been squeezed and treated by ultrafiltration to remove suspended solids, which can also cause as fouling matter in MD/MCr if not removed. MD/MCr has shown stable performance throughout more than 90 h of experimental duration. Each day the membrane has only been slightly cleaned with water and still no fouling has been permanently present on the membrane surface. MD and MCr have been able to concentrate the orange juice from 9 – 65 °Brix and

have been able to maintain the quality of the juice. Some compounds have been observed in the juice through optical microscope but these compounds still need to be separated and characterized. Currently, it has not been possible to increase the concentration further due to very high viscosity. However, the mass from initial oranges has been reduced with more than 90%, which highlights easier storage and transportation. Focus has now to be given to characterization of the crystallized product in order to identify the prospective of MCr in the treatment of agro food.

In general, MCr have been able to treat, with success, various kinds of feed streams to their saturation level. Different obstacles, in terms of membrane wetting, scaling and decrease in vapor pressure, had to be overcome for the successful application of MCr. Nevertheless, wetting and scaling have been avoided by choosing operative conditions below liquid entry pressure and a gentle flux, which positively helps in avoiding scaling. Recovery of LiCl, although only a single salt solution, has been the most difficult salt to crystallize. However, change in configuration from DCMD to VMD solved the problem of osmotic phenomena and showed good results, though the results are still very preliminary. The perspective of lithium crystallization is to recover it from RO brine. In this logic very high concentration factors have to be obtained before this can be realized and yet, lithium has to be recovered from mixed solutions. Although, it seems as a very difficult objective, it has to be pointed out that some of the largest desalination projects are seeking the recovery of minerals and metals from RO brine. It might also become of even more significant interest in near future due to rapidly changing scenario of conventional resources of raw material and recent development in separation and purification technologies. The mining industry, which normally produces the required minerals, is facing problems of risk of mineral depletion, water shortages and high energy requirements. In particular, the outlook of water shortage in future has made water in mining a hot topic and has constrained the mining industry to look towards alternative water resources and water production methods to meet their increasing demands. Therefore, it is very interesting to combine water production with mineral recovery to solve, partly, the problems of mineral depletion and water shortage and in this regard membrane crystallizers can play an important role in future perspectives.



---

# PUBLICATIONS AND COMMUNICATIONS

---

## ARTICLES IN JOURNALS

### Published or accepted:

1. L. Giorno, **C.A. Quist-Jensen**, E. Drioli, *Molecular Weight Cut-Off*, Entry for Encyclopedia on Membranes, Springer. Accepted
2. A. Ali, **C.A. Quist-Jensen**, F. Macedonio\*, E. Drioli, *Application of membrane crystallization for minerals recovery from produced water*. Membranes 5(4) (2015), 772-792, doi:10.3390/membranes5040772
3. E. Drioli\*, A. Ali, F. Macedonio, **C.A. Quist-Jensen**, *Minerals, energy and water from the sea: a new strategy for Zero Liquid Discharge in desalination*, JSM Environ Sci Ecol 3(2) (2015), 1018.
4. **C.A. Quist-Jensen**, F. Macedonio\*, E. Drioli, *Membrane technology for water production in agriculture: Desalination and wastewater reuse*, Desalination 364 (2015), 17-32.
5. **C.A. Quist-Jensen**, F. Macedonio, E. Drioli\*, *Membrane crystallization for salts recovery from brine – An experimental and theoretical analysis*, Desalination and water treatment (2015), DOI: 10.1080/19443994.2015.1030110. In Press
6. F. Macedonio\*, **C.A. Quist-Jensen**, O. Al-Harbi, H. Alromaih, S.A. Al-Jlil, F. Al Shabouna, E. Drioli, *Thermodynamic modeling of brine and its use in membrane crystallizer*, Desalination 323 (2013), 83-92.

### Submitted:

1. **C.A. Quist-Jensen**, F. Macedonio\*, C. Conidi, A. Cassano, S.A. Al-Jlil, O. Al-Harbi, E. Drioli, *Direct contact membrane distillation for the concentration of clarified orange juice*. Submitted to Journal of Food Engineering.
2. **C.A. Quist-Jensen\***, A. Ali, S. Mondal, F. Macedonio, E. Drioli, *A study of Membrane Crystallization for lithium recovery from high concentrated aqueous solutions*, Submitted to Journal of Membrane Science.
3. E. Drioli\*, F. Macedonio, A. Ali, **C.A. Quist-Jensen**, *Membrane technology for innovative process engineering*, Submitted to Journal of The Maharaha Sayajirao University of Baroda (ISSN 0025-0422).

### In preparation:

1. A. Ali\*, **C.A. Quist-Jensen**, F. Macedonio, E. Drioli, *Effect of module length on performance of membrane distillation process*, in preparation.

### Full papers in conference proceedings

1. F. Macedonio, **C.A. Quist-Jensen**, E. Drioli\*, *Raw materials recovery from seawater for zero liquid discharge*, Proceedings of IDA World Congress on Desalination and Water Reuse (2015).

2. E. Drioli\*, F. Macedonio, **C.A. Quist-Jensen**, *Membrane Crystallization for metals recovery from waste liquid streams*, Proceedings of 4th International Congress on water management in Mining, Gecamin (2014).

## CONFERENCE PROCEEDINGS (ORAL)

1. E. Drioli\*, F. Macedonio, **C. A. Quist-Jensen**, *Membrane Engineering for water purification and reuse in mining industry*, Presented at the 8<sup>th</sup> Sino/US joint conference of chemical engineering, October 12/16, 2015 in Shanghai, China.
2. **C.A. Quist-Jensen\***, A. Ali, H. Kim, F. Macedonio, E. Drioli, *Membrane crystallization for water production and salt recovery from produced water*, Presented at ECCE 10 + ECAP 3 + EPIC 5, September 27-October 2, 2015 in Nice, France.
3. A. Ali\*, **C.A. Quist-Jensen**, A. Figoli, F. Macedonio, E. Drioli, *Relating membrane characteristics in membrane distillation*, Presented at Euromembrane, September 6-10, 2015 in Aachen, Germany.
4. F. Macedonio, **C.A. Quist-Jensen**, E. Drioli\*, *Raw materials recovery from seawater for zero liquid discharge*, Presented at IDA World Congress on Desalination and Water Reuse, August 30-September 4, 2015 in San Diego, USA.
5. E. Drioli\*, **C. A. Quist-Jensen**, F. Macedonio, *Fluoropolymers Potentialities In The Re-Design Of Unit Operations In Process Engineering*, Presented at 21<sup>st</sup> ISFC & ISoFT'15, August 24-28, 2015 in Como, Italy.
6. A. Ali\*, **C.A. Quist-Jensen**, F. Macedonio, E. Drioli, *Optimization of Module Length and Membrane Thickness for Membrane Distillation*, Presented at 2<sup>nd</sup> International Workshop on Membrane Distillation and Innovating Membrane Operations in Desalination and Water Reuse, July 1-4, 2015 in Ravello, Italy.
7. **C.A. Quist-Jensen\***, F. Macedonio, E. Drioli, *Progress in membrane crystallization for zero liquid discharge in desalination*, Presented at 248th American Chemical Society National Meeting & Exposition, August 10 -14, 2014 in San Francisco, USA.
8. E. Drioli\*, F. Macedonio, **C.A. Quist-Jensen**, *Membrane Crystallization for metals recovery from waste liquid streams*, Presented at Water in Mining 2014, May 28-30, 2014 in Santiago, Chile.
9. E. Drioli\*, F. Macedonio, A. Ali, **C. A. Quist-Jensen**, *Nanostructured membranes for ZLD in desalination and water reuse*, Presented at IWA symposium on environmental nanotechnology, April 24-27, 2013 in Nanjing, China.

## CONFERENCE PROCEEDINGS (POSTER)

1. F. Macedonio, **C. A. Quist-Jensen\***, E. Drioli, *Water and Minerals extraction from seawaters with advances integrated membrane systems*, Presented at ECCE 10 + ECAP 3 + EPIC 5, September 27-October 2, 2015 in Nice, France.
2. **C.A. Quist-Jensen\***, A. Ali, S. Mondal, F. Macedonio, E. Drioli, *Membrane crystallization for minerals recovery from brine*. Presented at 2<sup>nd</sup> International Workshop on Membrane Distillation and Innovating Membrane Operations in Desalination and Water Reuse, July 1-4 2015 in Ravello, Italy. **Selected for Best Poster Presentation**
3. F. Macedonio\*, **C.A. Quist-Jensen**, C. Conidi, A. Cassano, E. Drioli, *Direct contact membrane distillation for the concentration of clarified orange*. Presented at 2<sup>nd</sup> International Workshop on Membrane Distillation and Innovating Membrane Operations in Desalination and Water Reuse, July 1-4 2015 in Ravello, Italy.

4. **C.A. Quist-Jensen\***, F. Macedonio, E. Drioli, *Perspectives of membrane based desalination – Water production and mineral recovery*. Presented at 31st European Membrane Summer School 2014, September 28th – October 3rd 2014 in Cetraro, Italy.
5. **C.A. Quist-Jensen\*** F. Macedonio, E. Drioli, *Thermodynamic modeling of RO brine for approaching zero-liquid discharge in desalination*. Presented at Advances in Science and Engineering for Brackish Water and Seawater Desalination II, September 30th – October 3rd 2013 in Cetraro, Italy
6. **C.A. Quist-Jensen\***, F. Macedonio, S. Simone, A. Figoli, E. Drioli, *Effect of membrane characteristics on performance in membrane distillation and crystallization*. Presented at 30th European Membrane Summer School 2013, July 22nd – 26th 2013 in Essen, Germany.

## **PARTICIPATION IN SCHOOLS AND CONFERENCES**

1. ECCE 10 + ECAP 3 + EPIC 5, September 27-October 2, 2015 in Nice, France.
2. 2<sup>nd</sup> International Workshop on Membrane Distillation and Innovating Membrane Operations in Desalination and Water Reuse, July 1-4 2015 in Ravello, Italy
3. 31<sup>st</sup> European Membrane Summer School 2014, September 28th – October 3rd 2014 in Cetraro, Italy
4. 248th American Chemical Society National Meeting & Exposition, August 10 -14, 2014 in San Francisco, USA
5. Advances in Science and Engineering for Brackish Water and Seawater Desalination II, September 30th – October 3rd 2013 in Cetraro, Italy
6. 30th European Membrane Summer School 2013, July 22nd – 26th 2013 in Essen, Germany.